2019

Wheat streak mosaic virus alters the transcriptome of its vector, wheat curl mite (*Aceria tosichella Keifer*), to enhance mite development and population expansion

Adarsh K. Gupta
University of Nebraska-Lincoln, adarsh.bio@gmail.com

Erin D. Scully
USDA, Agricultural Research Service, erin.scully@ars.usda.gov

Nathan A. Palmer
USDA, Agricultural Research Service, nathan.palmer@ars.usda.gov

Scott M. Geib
USDA, Agricultural Research Service, scott.geib@ars.usda.gov

Gautam Sarath
USDA, Agricultural Research Service, Gautam.sarath@ars.usda.gov

See next page for additional authors

JOURNAL OF GENERAL VIROLOGY

RESEARCH ARTICLE

Gupta *et al.*, *Journal of General Virology* 2019;100:889–910

DOI 10.1099/jgv.0.001256

MICROBIOLOGY SOCIETY

Wheat streak mosaic virus alters the transcriptome of its vector, wheat curl mite (*Aceria tosichella* Keifer), to enhance mite development and population expansion

Adarsh K. Gupta,[1] Erin D. Scully,[2] Nathan A. Palmer,[3] Scott M. Geib,[4] Gautam Sarath,[3,5] Gary L. Hein[6] and Satyanarayana Tatineni[1,3,*]

Abstract

Wheat streak mosaic virus (WSMV; genus *Tritimovirus*; family *Potyviridae*) is an economically important wheat virus that is transmitted by the wheat curl mite (WCM; *Aceria tosichella* Keifer) in a persistent manner. Virus–vector coevolution may potentially influence vector gene expression to prolong viral association and thus increase virus transmission efficiency and spread. To understand the transcriptomic responses of WCM to WSMV, RNA sequencing was performed to assemble and analyse transcriptomes of WSMV viruliferous and aviruliferous mites. Among 7291 *de novo*-assembled unigenes, 1020 were differentially expressed between viruliferous and aviruliferous WCMs using edgeR at a false discovery rate $\leq$0.05. Differentially expressed unigenes were enriched for 108 gene ontology terms, with the majority of the unigenes showing downregulation in viruliferous mites in comparison to only a few unigenes that were upregulated. Protein family and metabolic pathway enrichment analyses revealed that most downregulated unigenes encoded enzymes and proteins linked to stress response, immunity and development. Mechanistically, these predicted changes in mite physiology induced by viral association could be suggestive of pathways needed for promoting virus–vector interactions. Overall, our data suggest that transcriptional changes in viruliferous mites facilitate prolonged viral association and alter WCM development to expedite population expansion, both of which could enhance viral transmission.

INTRODUCTION

The wheat curl mite (WCM; *Aceria tosichella* Keifer; family *Eriophyidae*) causes damage to wheat plants by feeding on leaf sap, which ultimately results in dehydration and the formation of characteristic leaf curling. Cumulatively, the loss of sap and leaf surface area due to curling hamper the photosynthetic ability of the plant. However, the most detrimental effect of WCM infestation is its ability to transmit several wheat viruses, including *Wheat streak mosaic tritimovirus* (WSMV) [1], *High Plains wheat mosaic emaravirus* [2], *Brome streak mosaic rymovirus* [3] and *Triticum mosaic poacevirus* [4]. Two distinct genotypes of WCM, type 1 and type 2, have been identified in the USA [5]. Both mite genotypes often occur as mixed populations within wheat fields; however, these genotypes vary in their ability to transmit wheat viruses [6–8].

Among WCM-transmitted viruses, WSMV is the most economically important virus in the Great Plains of the USA [9, 10]. Although WSMV on average causes 3–5 % annual yield loss in wheat [11], yield losses of as high as 100 % have been observed in infected winter wheat [12]. WSMV is the type species of the genus *Tritimovirus* in the family *Potyviridae* [13]. The 9384-nucleotide single-stranded, positive-sense genomic RNA of WSMV is encapsidated in flexuous filamentous virions of 690–700×11–15 nm. WSMV genomic RNA contains a single large open reading frame (ORF) encoding a polyprotein of ~350 kDa that is processed into at least 10 mature proteins by 3 virus-encoded proteinases: P1, HC-Pro and NIa-Pro [13]. WCMs efficiently transmit

Received 12 December 2018; Accepted 14 March 2019; Published 24 April 2019

Author affiliations: [1]Department of Plant Pathology, University of Nebraska-Lincoln, Lincoln, NE 68583, USA; [2]Center for Grain and Animal Health Research, Stored Product Insect and Entomology Research Unit, United States Department of Agriculture-Agricultural Research Services (USDA-ARS), Manhattan, KS 66502, USA; [3]Wheat, Sorghum, and Forage Research Unit, USDA-ARS, Lincoln, NE 68583, USA; [4]Daniel K. Inouye US Pacific Basin Agricultural Research Center, USDA-ARS, Hilo, HI 96720, USA; [5]Department of Agronomy and Horticulture, University of Nebraska-Lincoln, Lincoln, NE 68583, USA; [6]Department of Entomology, University of Nebraska-Lincoln, Lincoln, NE 68583, USA.

***Correspondence:** Satyanarayana Tatineni, satya.tatineni@ars.usda.gov

Keywords: Wheat curl mites; *Wheat streak mosaic virus*; transcriptome; differential gene expression; population expansion; behavioral changes.

The NCBI BioProject PRJNA489675 contains all raw reads of wheat curl mite transcriptome data. SRR7796148, SRR7796152 and SRR7796153 contain reads derived from viruliferous mites, and SRR7796149, SRR7796150 and SRR7796151 contain reads derived from aviruliferous control mite samples.

Four supplementary tables and one supplementary figure are available with the online version of this article.

001256

WSMV at transmission rates of approximately 50 and 100 % with single and 5 to 10 viruliferous mites per test plant, respectively [1, 8]. HC-Pro and coat protein (CP) are required for WCM transmission of WSMV [14–16]. The mode of WCM transmission of WSMV appears to be persistent and circulative, as virus-like particles and inclusion bodies have been found in the digestive tracts of viruliferous mites [17, 18]. Juveniles acquire the virus while feeding on infected wheat and mites remain viruliferous through moulting [17, 19, 20].

The plant cell wall and cuticle offer primary lines of defence against biotic and abiotic factors, including viruses. To circumvent these physical barriers, many plant viruses have evolved precise vector-specific interactions with herbivorous insects [21]. In some cases, viruses are capable of manipulating vector behaviour and physiology to enable more efficient viral transmission and spread, a phenomenon termed 'adaptive manipulation' [22]. These behavioural changes can be quite dramatic and include enhanced feeding and increased preference of viruliferous vectors for noninfected host [22–25]. In addition to behavioural modifications, viruses have evolved mechanisms to facilitate acquisition, retention and, occasionally, replication in vectors, often governed by signature motifs in the viral proteome. Often, these molecular determinants facilitate specific interactions with receptors of the vector [26]. In some cases, initial binding of viruses with vector receptors triggers transcriptional responses that directly alter the behaviour of vectors [27].

Studying virus–vector interactions is particularly important because vector-borne plant viruses cause severe economic damage to crops, and vectors can turn an apparently non-significant disease into an epidemic by enhancing virus transmission. Understanding how viruses modulate the metabolism of the vector can provide important information on the biology of these complex interactions and potentially lead to development of improved strategies for integrated pest management. Although virus–vector interactions can be queried using different methodologies, high-throughput RNA sequencing has become a powerful tool to study the global transcriptomic response of vectors influenced by viruses. A number of studies comparing aviruliferous and viruliferous arthropod vectors have been conducted in recent years and have provided insights into how viruses interact with vectors. For example, in viruliferous *Graminella nigrifrons* (black-faced leafhopper), which transmits *Maize chlorotic dwarf waikavirus* and *Maize fine streak rhabdovirus*, viral acquisition was associated with higher expression of genes related to energy production and innate immunity pathways and significant downregulation of peptidoglycan recognition genes [28, 29]. Similarly, viruliferous *Frankliniella occidentalis* (western flower thrips), which transmits *Tomato spotted wilt virus*, showed elevated expression levels of genes associated with insecticide resistance and immune response pathways [30, 31]. *Southern rice black-streaked dwarf fijivirus*, which is transmitted by *Sogatella furcifera* (white-backed plant-hopper), induced higher stress responses in vectors as compared to aviruliferous insects [32], whereas the acquisition of *Pea enation mosaic luteovirus* was associated with the upregulation of genes involved in transcytosis in the vector, *Acyrthosiphon pisum* (pea aphid) [33]. Additionally, acquisition of *Tomato yellow leaf curl China begamovirus* was associated with the downregulation of genes linked to immune responses and autophagy in whiteflies [34].

The microscopic nature (~200 µm) of WCMs and the lack of adequate genomic and transcriptomic resources for this important vector have hampered research to discern the impact of virus acquisition on vector physiology and delineate the virus–vector dynamics in this economically important pathosystem. In this study, high-throughput RNA sequencing and complementary bioinformatic analyses were used to assemble the *de novo* transcriptome of the WCM and evaluate the transcriptomic signatures of WCMs upon acquisition of WSMV.

METHODS

Preparation of WSMV viruliferous and aviruliferous control WCMs

Type 2 mites reared on the WCM-susceptible wheat cultivar Settler CL (NH03614 CL) grown in caged pots maintained at the University of Nebraska-Lincoln [5] were used for this study. Single seeds of wheat cultivar Settler CL were sown in 4 cm diameter cone-tainers (Stuewe and Sons, Inc., Tangent, OR, USA) filled with standard steam-sterilized greenhouse soil. The cone-tainers were covered with plastic tubular cages of 60 cm in height with two circular air vents of 6 cm diameter and the top was guarded by Nitex Bolting cloth (BioQuip Products, Inc. Compton, CA, USA). The cone-tainers were maintained in a growth chamber at 25 ±2 °C with 16 h light. Wheat seedlings were infested with a single type 2 WCM at the two-leaf stage using an eyelash attached to a wooden dowel. The successful transfer of each mite was confirmed via observation under a stereo microscope. At 21 days post-infestation, curled top leaves were microscopically observed to confirm the establishment of mite infestations. WCMs from these plants were used to infest WSMV-infected and buffer-inoculated wheat seedlings (see below).

Wheat cv. Settler CL was sown in two sets of five 15 cm diameter pots filled with standard greenhouse soil. Both sets of pots were maintained in separate growth chambers at 25±2 °C with 16 h light. Wheat seedlings at the two-leaf stage were thinned to 15 seedlings per pot. Wheat seedlings in one set of pots designated for viruliferous mites were mechanically inoculated with freshly prepared crude sap from wheat leaves infected with *in vitro* transcripts of WSMV isolate Sidney 81 at a 1 : 20 dilution in 20 mM sodium phosphate buffer, pH 7.0 (inoculation buffer) [35]. The second set of wheat seedlings were inoculated with inoculation buffer as a control. At 4 days post-inoculation, both sets of plants were infested with WCMs by placing 1 cm-long pieces of infested leaves from the source plants

between the leaf bases of the virus- and buffer-inoculated plants. Three independent infestations of viruliferous and aviruliferous mites were prepared to generate three biological replicates to be used for RNA-seq and RT-qPCR studies.

Mites were collected separately from infected (viruliferous) and uninfected control plants (aviruliferous) at 28 days after infestation. Infested plants were processed in batches of five to six plants, which were cut into 5 cm-long pieces and vortexed in 30 ml of phosphate-buffered saline (PBS) with 0.2 % polysorbate 20. Mites were filtered from the washings using a cell strainer with a pore size of 40 µm (EASYstrainer Cell Sieves) and were transferred into a clean Petri dish. WCMs were inspected visually under a stereo light microscope and selectively aspirated using a micropipette to separate the mites from any contaminating plant debris. The mites were snap frozen in liquid nitrogen in 200 µl aliquots in PBS and stored at −80 °C until further processing for RNA extraction.

RNA extraction and Illumina sequencing

Total RNA (rRNA+mRNA) was extracted from three biological replicates each of frozen viruliferous and aviruliferous mites by pulverizing the samples in liquid nitrogen using a mortar and pestle and adding 1 ml of TriPure isolation reagent (Sigma-Aldrich, St Louis, MO, USA). RNA was processed following the manufacturer's directions and treated with RT enhancer to eliminate genomic DNA contamination. The quantity and integrity of each RNA sample were validated on an Agilent 2100 Bioanalyzer (Agilent Technologies, Santa Clara, CA, USA) (data not shown). The total RNA (~1.0 µg) from each sample was subjected to mRNA enrichment using oligo dT magnetic beads and subsequently each RNA sample was prepared for reverse transcription and sequencing using the TruSeq Stranded mRNA Library Preparation Kit (Illumina, Inc., San Diego, CA, USA) per the manufacturer's instructions. The six barcoded libraries were combined into a single library pool and sequenced on an Illumina HiSeq 2500 platform to a depth of approximately 40 million 2×50 bp paired-end reads (40 Gb) per sample at the University of Minnesota Genomics Center (Minneapolis, MN, USA). All raw reads were submitted to the NCBI Sequence Read Archive under BioProject PRJNA489675. SRR7796148, SRR7796152 and SRR7796153 contain reads derived from viruliferous mites, and SRR7796149, SRR7796150 and SRR7796151 contain reads derived from aviruliferous control mite samples.

De novo transcriptome assembly, filtering and annotation

Reads from all biological replicates from both treatments were quality-checked using the program FastQC (https://www.bioinformatics.babraham.ac.uk/projects/fastqc/) and pooled together to build a *de novo* transcriptome assembly with Trinity (version 2.0.6) [36]. Reads were normalized *in silico* prior to assembly to a maximum coverage of 50× to reduce the frequency of erroneous kmers in reads used to build the assembly [37], and the normalized reads were used for assembly with the following parameters: min_kmer_cov 1, min_contig_length 200, and SS_lib_type RF for strand specificity. All other parameters were set to default. Transcriptome assemblies are inherently noisy and often contain multiple allelic variants derived from the same parent unigenes, which is caused by pooling multiple unrelated individuals together to obtain sufficient levels of RNA for extraction and library preparation. Additionally, they can also contain fusion transcripts and/or misassembled transcripts [38, 39]. In order to reduce the abundance of these spurious transcripts and unigenes in the assembly, it was filtered to retain only high-quality transcripts containing full-length or near full-length coding regions. To accomplish this, several steps were undertaken. First, all reads were mapped back to the assembly using Bowtie2 [40] with the align_and_estimate_abundance.pl script packaged with Trinity and abundance was computed on per isoform and per unigene levels using RSEM [41]. Next, coding regions were predicted using Transdecoder (https://github.com/TransDecoder/TransDecoder/). Default parameters were used with the addition of HMMER (version 3.0) [42] to identify Pfam-A domains and facilitate the detection of ORFs. Additionally, transcripts derived from potential microbial contaminates were identified by BLASTP and BLASTN comparisons (version 2.4.0+) to the non-redundant protein and nucleotide databases (NR and NT; downloaded 17 February 2018). The top five matches with *e*-values ≤1e-5 were retained for each transcript and used for taxonomic classification with MEGAN [43]. Because lower-quality and misassembled transcripts are usually low in abundance, we removed transcripts and unigenes with TPM values below 0.5 and transcripts that represented less than 5 % of the abundance of the dominant isoform of each unigene from the assembly. Transcripts and unigenes that did not have BLASTP or BLASTN matches to arthropod-derived sequences in the nucleotide database (nt; downloaded 17 February 2018) were also removed from the assembly.

Functional annotations of protein-coding unigenes were performed using Trinotate (https://trinotate.github.io/). In brief, the top BLASTP and BLASTX matches to the UniProtKB/Swiss-Prot 2018_02 database (downloaded 17 February 2018) for each protein coding unigene were retrieved, Pfam-A domains were identified using HMMER (version 3.0) [42], transmembrane domains were identified using TMHMM [44], and signal peptides were identified using signalP [45]. GO, eggNOG and KEGG [46] terms were retrieved from the Trinotate.sqlite database using the top BLASTP matches to the Swiss-Prot/Uniprot database as queries. Transcripts were screened for any remaining adapter sequence using BLASTN searches against the UniVec database (downloaded on 15 May 2018) and fully annotated transcripts were submitted to the NCBI's Transcriptome Shotgun Assembly (TSA) database (accession number GGYP00000000). The programs Transvestigator [47] and Annie [48] were used to facilitate NCBI submission of the annotated transcripts. Other supporting information, such as Trinotate annotations and predicted protein translations for all unigenes

Table 1. Summary of Trinity *de novo* assembly of read mapping and contig read counts for wheat curl mite

Before length-filtering	No. of bases	29.96 Mb
	No. of transcripts	26989
	No. of unigenes	25678
	Contig N50 (bp)	1857
	Median contig length (bp)	656
After length-filtering*	No. of bases	15.87 Mb
	No. of transcripts	7785
	No. of unigenes	7291
	Contig N50 (bp)	2644
	Median contig length (bp)	1718

*Transcripts with lengths less than 200 bp (minimum cutoff), transcripts putatively derived from microbial taxa and transcripts with transcripts per million (TPM) values below 0.5 were removed from the assembly prior to differential expression analysis.

(including the unfiltered unigene set), can be found at https://data.nal.usda.gov/dataset/de-novo-transcriptome-assembly-and-annotations-wheat-curl-mite-aceria-tosichella.

Differential expression analysis

To compare global unigene expression patterns between viruliferous and aviruliferous mites, reads from each of the three biological replicates from the two treatments were separately mapped back to the filtered transcriptome assembly using Bowtie2 [40], and transcript abundances were determined using RSEM [41]. Differential expression analysis between transcriptomes from viruliferous and aviruliferous mites was performed at the unigene level using EdgeR [49]. Read counts were normalized using the trimmed mean of M-values (TMM) approach and transcripts with counts $\leq$10 across at least four samples were removed. Transcripts with $\log_2$-fold changes $\geq$0.5 and FDR-corrected *P*-values $\leq$0.05 were defined as differentially expressed. A $\log_2$-fold change of 0.5 was chosen because even small fold changes in expression levels can have biological and phenotypic significance and FDR is well controlled by EdgeR when $\log_2$-fold change thresholds >0.3 and FDR $\leq$0.05 are used [50].

Table 2. Annotation metrics for unigenes from the filtered wheat curl mite transcriptome assembly. Values indicate numbers of unigenes

	No. of unigenes
BLASTX matches to Sprot/Uniprot	6749
BLASTP matches to Sprot/Uniprot	6798
Pfam domains	6592
Signal peptides	516
Transmembrane domains	1691
Gene ontology (GO) assignments	5019
KEGG assignments	5412
BLASTP matches to NR	7788
Matches to hypothetical proteins (NR)	1204
Full-length ORFs	5636
5′ partial ORFs	1530
3′ partial ORFs	622

Table 3. MEGAN taxonomy classification for highest scoring BLASTP matches of protein-coding unigenes from filtered wheat curl mite transcriptome assembly against the non-redundant protein database

Order	No. of unigenes
Anura	99
Coleoptera	407
Diplostraca	381
Diptera	878
Echinoida	92
Enteropneusta	141
Hemiptera	258
Hymenoptera	836
Ixodida	1010
Neoptera	289
Phthiraptera	229
Rhabditida	160
Other	3011
Could not be classified to order	26

GO enrichment analyses for up- and downregulated genes in viruliferous mites were performed using GoSeq [51]. Basal terms for all GO assignments were retrieved using the extract_GO_assignments_from_Trinotate_xls.pl script included in the Trinotate package. For both up- and downregulated genes, the entire list of transcripts/unigenes tested for differential expression was used as a reference to determine enrichment. All genes were weighted by gene length and enriched terms were identified using the Wallenius approximation ('pwf' option) with Benjamini–Hochberg adjusted *P*-values $\leq$0.05.

KEGG and Pfam enrichment analysis

Pfam, KO and KEGG pathway enrichment analyses for up- and downregulated genes were performed using the GeneOverlap package in R, which calculates enrichment significance using Fisher's exact test on individual gene sets [52], and the Trinotate Pfam and KO annotations [53]. Benjamini–Hochberg adjustment was used on the resulting *P*-values to correct for multiple testing [54].

Assessment of transcriptome completeness and comparison to other mite transcriptomes

To assess the completeness of the transcriptome, Benchmarking Using Single Copy Orthologs (BUSCO) analysis [55] was performed using the Arthropod odb9 orthologue set available at https://busco.ezlab.org/datasets/arthropoda_odb9.tar.gz and representation of core metabolic pathways was validated using the KEGG pathway assignments computed in the previous section. Further, comparisons were made to the genomes and transcriptomes of other mites, focusing primarily on phytophagous species belonging to the same superorder as WCM (Acariformes). Because

protein-coding sequences were not available for the mite species found in TSA, transcriptomes from the raw sequence read archive reads were reassembled and reannotated using Trinity and Trinotate as described above for WCM. TBLASTN searches were performed using predicted protein coding sequences derived from the fully annotated *T. urticae* genome assembly [56] as queries against the three mite transcriptome assemblies [*P. ulmi* [57], *P. citri* [58] and *A. tosichella* (this study)] to identify homologous coding regions that may have been missed by Trinotate. To facilitate comparisons, orthology assignments were computed using bidirectional BLASTP searches and the program OrthoFinder (2.1.2) [59] to identify unigenes that were conserved among these mites, unigenes that were unique to *A. tosichella* and unigenes whose copy number may be expanded in *A. tosichella* relative to the other mite species. To ensure that transcript isoforms derived from the same unigene did not contribute to copy number inflation, only the most highly expressed isoform per unigene from transcriptome assemblies was included in the orthology analysis.

RT-qPCR

Total RNA (1.0 µg) was treated with RT enhancer to eliminate genomic DNA contamination and was reverse-transcribed using random hexamers and AMV RT (Roche, Indianapolis, IN, USA) in a 10 µl reaction. RT-qPCR was performed on technical duplicates with cDNA prepared from the same three biological replicates of total RNA that were used for the RNA-seq experiment. SsoAdvanced SYBR Green Supermix (Bio-Rad, Hercules, CA, USA) was used per the manufacturer's instructions and analysis was performed using the Bio-Rad CFX Connect Real-Time PCR System. The primers used for RT-qPCR are listed in Table S1 (available in the online version of this article) with the transcript identifier, annotation of templates along with orientation and corresponding nucleotides. The amplification conditions used for qPCR were 95 °C for 2 min, followed by 40 cycles of 95 °C for 10 s, 50 °C for 30 s and 72 °C for 1 min. No template and no RT reactions were included as negative controls. The relative expression levels of WCM unigenes in viruliferous and aviruliferous mites were calculated with the ΔΔCt method [60] using actin and glucose-6-phosphate dehydrogenase as references for normalization.

RESULTS

WCM transcriptome assembly and annotation

To study the transcriptomic response of WCMs exposed to WSMV, RNA-seq analysis was performed on three biological replicates of mites fed on WSMV-infected and buffer-inoculated wheat plants. A total of approximately 270 million 2×50 bp paired reads totalling over 27 Gb were generated from the 6 transcriptomic libraries with an average coverage of approximately 45.7 million reads (4.6 Gb) per library. Few PCR duplicates were identified in the raw reads (<0.3 %) and the average PHRED quality scores (Illumina 1.9) exceeded 32 along the entire lengths of the forward and reverse read. Approximately 14.5 million high-quality normalized read pairs (~1.5 Gb) were used to generate the *de novo* transcriptome assembly, which led to the initial assembly of 26 989 transcripts derived from 25 678 unigenes (Table 1); although the reads were not quality-filtered prior to assembly, 99.9 % of the raw reads matched the consensus sequence for each transcript, indicating that the raw data used to build the assemblies were of extremely high quality. From this initial assembly, the majority of the transcripts had matches to proteins derived from metazoa; however, approximately 2800 unigenes had the highest scoring

Table 4. Summary of RNA-seq-derived raw reads and mapped sequences from *Wheat streak mosaic virus* (WSMV) viruliferous and control wheat curl mites (WCMs)

Sample description[a]	No. of raw reads	No. of reads mapped to the transcriptome assembly in proper pairs	% of reads mapped in proper pairs	% of reads mapped to other genomes		
				Wheat	WSMV	Fungus
Aviruliferous WCMs-1	46 848 229	26 045 552	55.60	0.14	0	1.08
Aviruliferous WCMs-2	43 317 338	24 217 625	55.91	0.12	0	1.09
Aviruliferous WCMs-3	45 938 305	24 974 195	54.36	0.2	0	0.25
Mean	45 367 957	25 079 124	55.29	0.15	0	0.81
Viruliferous WCMs-1	41 971 907	21 188 142	50.48	0.12	7.49	0.34
Viruliferous WCMs-2	43 694 956	23 160 099	53.00	0.1	4.46	0.23
Viruliferous WCMs-3	48 296 451	25 506 536	52.81	0.09	3.81	0.25
Mean	45 038 641	23 284 926	52.10	0.11	5.25	0.27

a, 1–3 represent RNA from biological replicates prepared from three independent experiments. Aviruliferous WCMs and viruliferous WCMs represent wheat curl mites reared on buffer-inoculated and WSMV-infected wheat plants, respectively.

BLASTP matches to fungal taxa, while 44 and 3 unigenes had matches to bacteria and archaea, respectively. Overall, the majority of the unigenes (~2500) derived from microbes had the highest scoring BLASTP matches to the fungal class Sordariomycetes, with the majority of these unigenes having matches to the Nectriaceae (*Fusarium*, *Gibberella* and *Nectria*). A small percentage of reads (<1 %) were derived from fungi in both the aviruliferous and viruliferous mites (Table 4). In addition, approximately 29 % of the unigenes (4651) that coded for putative proteins showed no significant matches to any annotated GenBank protein sequence, suggesting significant divergence from previously annotated proteins. Although many of these proteins could represent erroneous protein predictions, 404 of these proteins (8.7 %) had predicted Pfam domains, 1049 had predicted transmembrane domains (22.6 %) and 964 had predicted signal peptides (20.7 %), suggesting that at least some of these unigenes encode functional proteins.

After filtering to remove non-coding sequences, low-abundance transcripts with transcripts per million (TPM) values $\leq$0.5 and sequences derived from microbes, 7785 transcripts derived from 7291 unigenes remained. The contig N50 was 2644 nt, the median contig length was 1718 nt and the total assembly length was approximately 15.9 Mb (GC content: 46.07 %) (Table 1). When only the longest isoform per unigene was considered, the contig N50 decreased slightly to 2626 nt, median contig length remained approximately the same at 1709 nt, and total assembly length decreased to approximately 15.87 Mb (Table 1). Of the 7291 unigenes that coded for proteins, 6749 had BLASTX matches to the Swiss-Prot/UniProt database, 6798 had BLASTP matches to the Swiss-Prot/UniProt database, approximately 7700 had BLASTP matches to NR, 6592 had PfamA domains, 516 had predicted signal peptides and 1691 had predicted transmembrane domains (Table 2). The vast majority of the unigenes identified had the highest scoring BLASTP matches to proteins derived from phylum Arthropoda (~70.1 % of the protein-coding unigenes). Because few genomic resources exist for taxa derived from the subclass Acari, which includes mites, the most abundant BLASTP matches to the NR database were actually to proteins derived from the class Insecta (~46.1 % of the protein coding unigenes), with Arachnida representing the class with the second most frequent matches (~15.5 %, of which most matched to members of the subclass Acari). This finding indicates that the nucleotide and amino acid sequences derived from the WCM transcriptome are divergent from potential orthologues and homologues from other mite species represented in the NR database. At finer taxonomic resolutions, the highest scoring BLASTP matches were broadly distributed over more than 50 different orders; however, the most frequent orders observed included Ixodida, Diptera and Hymenoptera (Table 3).

Additionally, one unigene that was approximately 6160 nt in length and corresponded to the WSMV polyprotein was

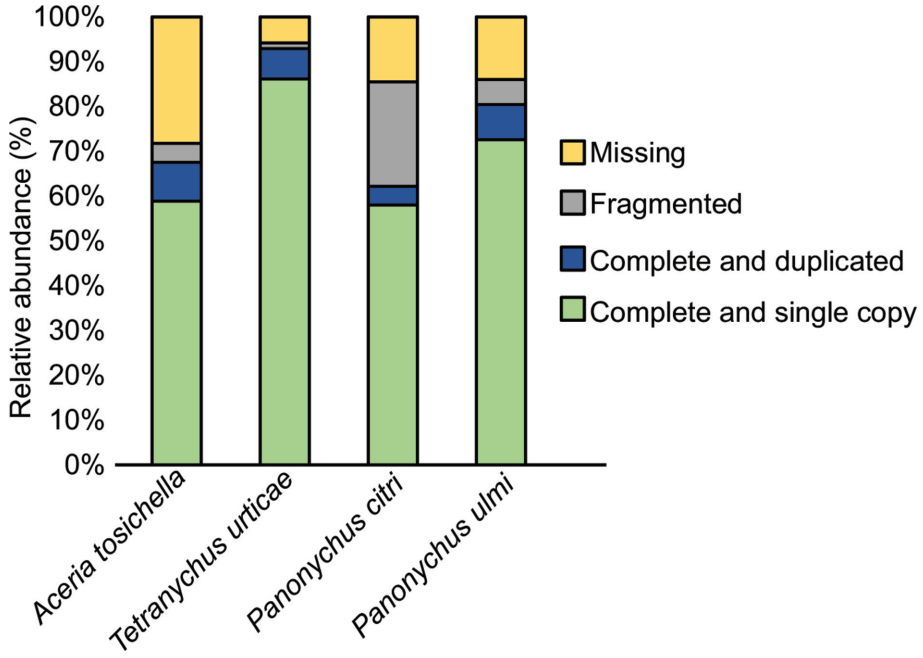

Fig. 1. Benchmarking Universal Single-Copy orthologs (BUSCO) analysis of WCM transcriptome and transcriptomes and genomes of other mites belonging to the superorder Acariformes. One isoform from each WCM unigene was searched against the arthropoda odb 9 database. WCM results were compared to results from protein-coding unigenes derived from the *Panonychus citri* [97] and *Panonychus ulmi* [95] transcriptome assemblies and protein-coding genes derived from the *Tetranychus urticae* [96] genome assembly.

Table 5. Top 30 enriched orthogroups in the wheat curl mite compared to other mite genomes and transcriptomes

Orthogroup	Annotation	Representative unigene	*P. ulmi*	*P. citri*	WCM	*T. urticae*
OG0000243	C2H2-type zinc finger	TR1204|c0_g1	1	2	4	3
OG0000200	Troponin	TR133|c0_g1	1	2	6	2
OG0000246	Cyclophilin-type peptidyl-prolyl cis-trans isomerase/CLD	TR2015|c0_g1	3	1	4	2
OG0000186	Ion transport protein	TR2139|c0_g1	1	3	4	3
OG0000178	DEAD/DEAH box helicase	TR2337|c0_g1	2	2	4	3
OG0000072	Cathepsin propeptide inhibitor domain (I29)	TR254|c0_g1	1	0	15	0
OG0000009	ABC transporter	TR3201|c1_g1	5	10	18	9
OG0000202	Trypsin	TR3233|c0_g1	0	2	6	3
OG0000137	RyR domain	TR3639|c0_g1	2	3	6	1
OG0000173	Hypothetical	TR3639|c3_g1	1	3	5	2
OG0000149	Cytochrome P450	TR3694|c0_g1	0	4	5	3
OG0000073	Zinc carboxypeptidase	TR3749|c0_g1	1	2	9	4
OG0000066	Fatty acid desaturase	TR3970|c1_g1	5	2	6	3
OG0000195	Tropomyosin	TR4510|c0_g1	2	2	5	2
OG0000097	Eukaryotic elongation factor 1 beta central acidic region	TR479|c0_g1	3	1	8	2
OG0000067	Acyltransferase family	TR4951|c0_g1	2	3	7	4
OG0000099	Hypothetical	TR4951|c4_g1	3	4	6	1
OG0000059	Aldo/keto reductase family	TR5435|c0_g1	4	2	7	4
OG0000114	C2 domain	TR5758|c0_g1	2	3	5	3
OG0000227	RasGEF N-terminal motif	TR5959|c12_g2	1	3	5	1
OG0000171	Adenylate and guanylate cyclase catalytic domain	TR5974|c21_g1	3	2	4	2
OG0000237	Hypothetical	TR5991|c32_g1	1	2	6	1
OG0000140	VWA N-terminal	TR6023|c1_g1	3	2	5	2
OG0000110	Hypothetical	TR6040|c11_g1	2	2	5	4
OG0000179	Protein kinase domain	TR6042|c0_g1	2	1	6	2
OG0000235	C2 domain	TR6044|c16_g1	3	1	4	2
OG0000241	Pyruvate phosphate dikinase, PEP/pyruvate-binding domain	TR6118|c0_g1	3	1	5	1
OG0000098	Hypothetical	TR6144|c0_g1	2	4	7	1
OG0000182	Phorbol esters/diacylglycerol-binding domain (C1 domain)	TR6149|c11_g1	2	2	4	3
OG0000068	Low-density lipoprotein receptor repeat class B	TR6207|c9_g2	4	3	8	1

All-versus-all BLASTP searches in combination with the program OrthoFinder were used to identify gene families whose copy number was potentially expanded in WCM compared to other mites. The transcriptomes for *P. ulmi* and *P. citri* were assembled and annotated as described in the Methods section, and the proteome of *T. urticae* was downloaded from NCBI. Single isoforms for each gene or unigene were used in the all-versus-all BLASTP searches to ensure that different isoforms did not contribute to any copy number inflations.

recovered from the assembly. BLASTP and BLASTN matches were 100 and 99 % identical to the WSMV Sidney 81 strain (GenBank: AF057533.1), respectively, and the nucleotide sequence for the unigene aligned with positions 3225 to 9384 of its closest match. A small percentage of reads from each of the libraries derived from viruliferous WCMs also mapped to the WSMV transcriptome, confirming that the virus had been successfully transmitted to the mites (Table 4). No reads from the control libraries mapped to WSMV and only a small percentage of reads in all samples mapped to the wheat genome (*Triticum aestivum* v2.2, phytozome.jgi.doe.gov) (Table 4).

Overview of WCM transcriptome annotations and orthology analysis

Overall, the recovery of Benchmarking Universal Single-Copy Orthologs (BUSCOs) from the WCM was similar to recovery of BUSCOs from the transcriptomes and genomes of other phytophagous mites, suggesting that the transcriptome assembly represents a fairly complete reconstruction relative to other mites. Approximately 59 % of the arthropod BUSCOs were identified as complete and single copy, 8.6 % were identified as complete and duplicated, and 28.2 % were identified as missing (Fig. 1). The percentages of recovered and missing BUSCOs may seem low and high, respectively, especially in comparison to metrics that are typically reported for insect genomes and transcriptomes. However, these values are similar to the number of BUSCOs recovered from transcriptomes of two mites belonging to the genus *Panonychus* (58 % complete/single copy and 14.5 % missing in *P. citri*, and 72.6 % complete/single copy and 14.0 % missing in *Panonychus ulmi*). Additionally, 5.8 % of arthropod BUSCOs were missing from the genome assembly of two-spotted spider mite (*Tetranychus urticae*) (Fig. 1). This

suggests that it may be difficult to obtain a complete gene space inventory from a transcriptome assembly in some mite species or that the BUSCO arthropod database might not perform well with species of Arachnida. Additionally, the percentage of complete and duplicated BUSCOs was lower in the filtered assembly compared to the raw transcriptome assembly (8.6 vs 11.6 %, respectively) and the recovery of complete and single copy BUSCOs and fragmented BUSCOs did not differ (data not shown). This finding indicates that removing low-abundance transcripts and isoforms from the data potentially improved our assembly by removing duplications caused by allelic variation in the sequence data.

Orthology analyses among the 4 different mite species revealed the presence of over 3000 different orthologue groups that included representative proteins from all 4 mites, and of these 903 consisted exclusively of single-copy orthologues. Approximately 500 different orthogroups contained higher numbers of assigned unigenes in the WCM compared to other mite transcriptomes and genomes, which is potentially indicative of copy number expansion in this species (Table 5). The majority of these unigenes encoded proteins such as trypsin, CYP450, ABC transporters, aldo-keto reductases (AKRs), catalases, cuticular proteins, glutathione S-transferases (GSTs), juvenile hormone-binding proteins (JHBPs), heat-shock proteins (HSPs), leucine-rich repeat proteins (LRRs), sugar transporters, chemoreceptors and insulinases, which tend to be amplified in taxon-specific manners in the genomes of many other arthropod species. Notably, proteins containing cathepsin propeptide inhibitor domains (I29) were uniquely expanded in the transcriptome of the WCM compared to the other 3 mites, and were assigned to an orthogroup containing 16 of the copies found in the WCM compared to 1 copy found in *P. citri* and no copies found in the other 2 mites (Table 5). Other notable expansions included orthogroups of ABC transporters (18 unigenes in the WCM compared to <10 copies in the other mites), zinc carboxypeptidases (9 unigenes in the WCM compared to <5 copies in the other mites), lipoproteins (8 unigenes in the WCM compared to $\leq$5 copies in the other mites), sodium channel proteins (7 unigenes in the WCM compared to $\leq$4 copies in the other mites) and conserved hypothetical proteins (6 unigenes in the WCM compared to $\leq$4 copies in the other mites) (Table 5). Although these expansions are of potential importance for the biology of the WCM, genome assembly will be required to validate the expansion of these paralogues observed in the transcriptome assembly.

In general, unigenes encoding proteins involved in signalling, structural proteins, proteinases and immunity were among the most abundant protein families observed in the WCM transcriptome (Fig. 2). Specifically, protein kinases were the most abundant Pfams, followed by WD domains, trypsins, homeobox proteins, immunoglobulins, ubiquitin-conjugating enzymes, RNA-recognition motifs, DEAD/DEAH box helicases and cuticle proteins (Fig. 2). Unigenes encoding trypsins (86 unigenes) were the most common types of proteinases identified in the assembly, followed by papain family cysteine proteinases (27) and aspartyl

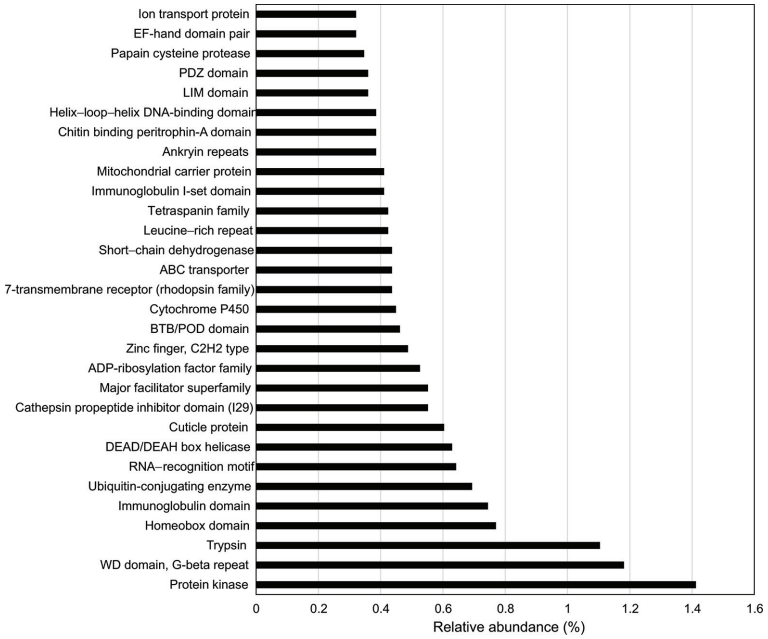

Fig. 2. Relative abundances of the most dominant Pfam domains in the wheat curl mite transcriptome assembly. Pfam annotations were retrieved using Trinotate as described in the Methods section. Occurrences of Pfam domains were counted only once for each protein and abundance was expressed relative to the total number of proteins in the transcriptome that had detectable Pfam domains.

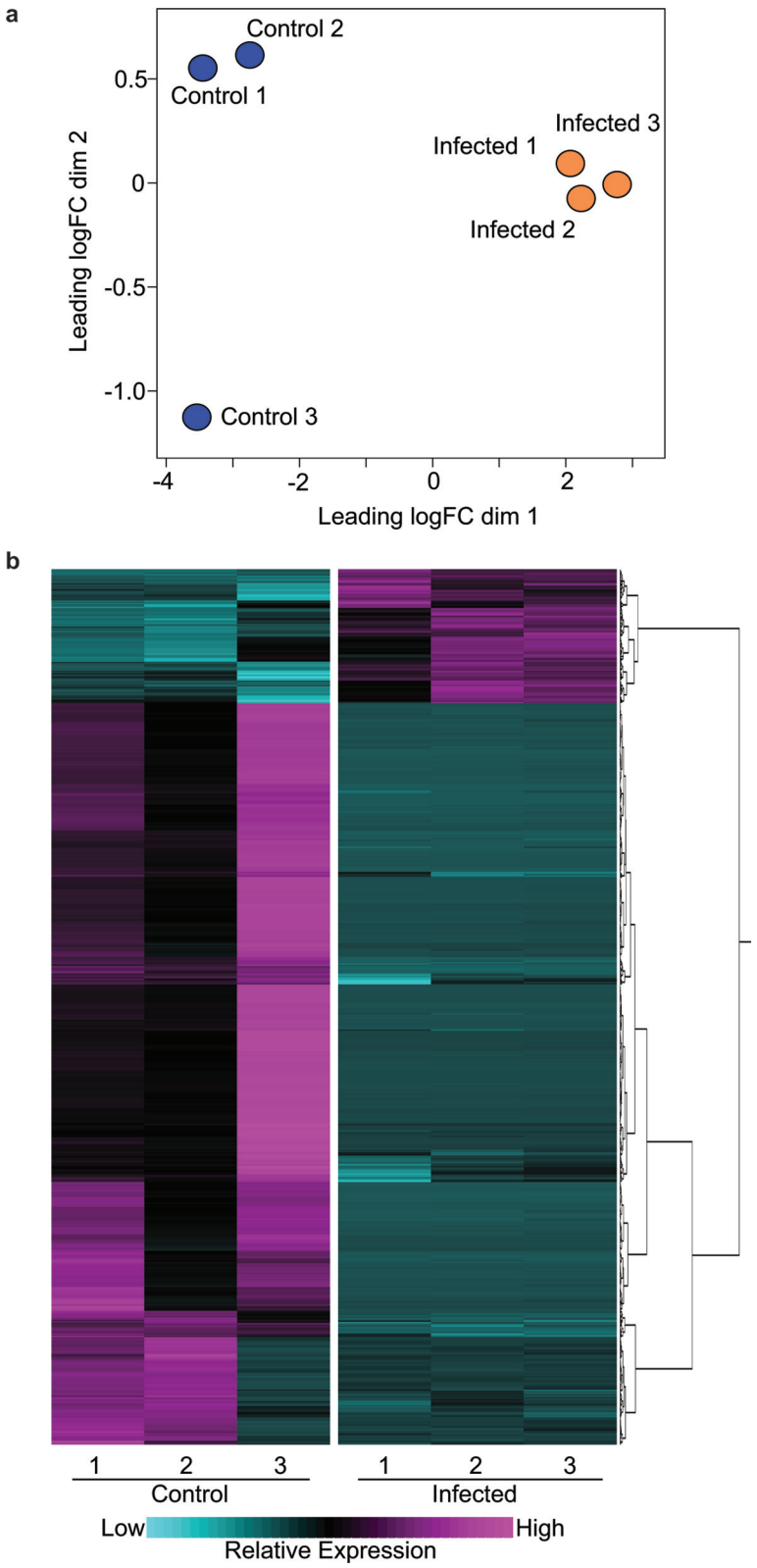

Fig. 3. Differentially expressed genes in *Wheat streak mosaic virus* viruliferous wheat curl mites. (a) Non-metric multidimensional scaling (NMDS) analysis of the expression profiles of viruliferous and aviruliferous WCMs. The NMDS analysis was based on Euclidean dissimilarities between the sample pairs and was performed using the plotMDS function in edgeR. Aviruliferous control samples are shown in blue and viruliferous samples are shown in orange. (b) Heatmap and clustering analysis of differentially expressed unigenes

identified in viruliferous WCMs. Differentially expressed unigenes were identified using edgeR with an FDR cutoff of $\leq$0.05 and a $\log_2$FC of $\geq$0.5, the heatmap was prepared using JMP (v12) and clustering was performed using Ward's method. The colour key depicts the magnitude of the expression levels for each unigene ranging, from very low expression (cyan) through very high expression (magenta) to moderate expression (black).

proteases (15). Other protein families linked to immunity and stress response that were found in the assembly included cytochrome P450s (35 unigenes), short-chain dehydrogenases (34), LRRs (33), lipases (21), GSTs (15), peroxidases (15), GMC oxidoreductases (8), carboxylesterases (7) and UDP-glucuronosyltransferases (UGTs; 2). Similar to other phloem-feeding arthropod taxa, unigenes encoding enzymes capable of degrading plant cell walls were not particularly abundant; however, one unigene predicted to encode a glycoside hydrolase (GH) family 45 $\beta-1,4$-endoglucanase was identified. Additional unigenes encoding GH family proteins included GH 18 chitinases (10), GH 1 β-glucosidases (6), GH 15 phosphorylase kinases (glycogen breakdown; 2), GH 31 lysosomal α-glucosidases (4), GH 30 glucosylceramidases (5), GH 38 lysosomal α-glucosidases (2) and GH 47 α-mannosidase-like proteins involved in degrading misfolded glycoproteins (5). A unigene encoding a pectin acetylesterase also was identified, which could be important for digesting homogalacturonan polysaccharides found in plant primary cell walls.

Influence of WSMV on WCM transcriptome

Overall, a total of 1020 differentially expressed genes were detected in WSMV viruliferous mites relative to the aviruliferous control mites at a false discovery rate (FDR)-corrected *P*-value of 0.05 and a $\log_2$-fold change of 0.5 (Fig. S1). The number of reads mapped to the reference assembly did not differ among the viruliferous and aviruliferous mites, which ranged from 50–52 % and 54–55 % of the raw reads, respectively (Table 4). Of these, 155 unigenes were upregulated in viruliferous mites relative to the controls and 865 were downregulated (Fig. 3a, b). Additionally, the two treatments were clearly separable from one another via non-metric multidimensional scaling, and correlation values among the three biological replicates within each treatment were $\geq$0.95 (Fig. 3a), suggesting consistent responses among replicates within each treatment. The downregulated unigenes were associated with the enrichment of 112 different gene ontology terms, of which 85, 111 and 16 were assigned to the biological processes (BP), molecular function (MF) and cellular component (CC) parent categories, respectively (Fig. 4a; Tables 6 and S2). BP gene ontology (GO) terms were mostly related to purine nucleoside metabolic processes, hydrogen ion transmembrane transport, glycosyl compound metabolic processes, translational elongation, energy coupled proton transport and oxidation-reduction, while CC was enriched for terms related to ribosomes and MF was enriched for the structural constituents of ribosomes, hydrolase activity, peptidase activity, magnesium chelatase activity and ligase activity (Fig. 4a; Tables 6 and S2). Among the upregulated unigenes, two MF terms showed enrichment, including structural constituents of cuticle and iron ion binding (Table 7, Fig. 4a). Although not significantly enriched, several terms were highly represented among upregulated unigenes, including steroid metabolic process (4 out of 15 annotated unigenes) and fatty-acyl-CoA (alcohol-forming) activity (4 out of 12 annotated unigenes) (Table S2).

Pfam, Kyoto Encyclopedia of Genes and Genomes (KEGG) orthology (KO) and KEGG pathway enrichment analyses of differentially expressed unigenes provided some additional insights into the impacts of viral acquisition on the WCM transcriptome. Overall, a total of 115 different Pfam domains were associated with 1020 differentially expressed unigenes detected in this study. Over 40 Pfam domains (~35 %) were enriched among unigenes that were downregulated in response to WSMV and only one Pfam domain was enriched among upregulated unigenes (Table 8; Fig. 4b). Enriched Pfam domains from unigenes that were downregulated in viruliferous mites included aldo-keto reductases (AKRs), α-amylases, insect cuticle proteins (22 downregulated unigenes), GSTs, trypsin, cathepsin propeptide inhibitor domain I29 proteins, HSPs, JHBPs, lipocalins, ferritins and ubiquitins (Table 8). Among upregulated unigenes, enriched Pfam domains also included insect cuticle proteins (10 upregulated unigenes) (Fig. 3b). Although not enriched, other prominent Pfam domains included CYP450s, male sterility proteins, animal haem peroxidases, HSP20s and lipases (Table S3; Fig. 4b), most of which were associated with the downregulated unigenes. Overall, Pfam enrichments and pathway analyses suggest that WSMV influenced the development, reproduction, apoptosis, immunity, oxidative stress, and digestive and metabolic processes of WCM.

KO analysis showed an enrichment of 34 different terms among unigenes that were downregulated in viruliferous WCMs, which included myosin heavy chain; aldehyde reductase; apolipoprotein D and lipocalin family protein; cathepsins L, B and D; elongation factor 1-α; HSP 70; transmembrane serine protease; and glutathione peroxidase (Table 9; Fig. 5a). No significantly enriched KO terms were found in upregulated unigenes; however, high numbers of unigenes were assigned to terms related to CYP450s, dystonin and calcium/calmodulin-dependent protein kinases were upregulated (Fig. 5a). Several KEGG pathways were enriched among differentially expressed unigenes, including 22 that were enriched in downregulated unigenes (Table 10; Fig. 5b). These pathways were mostly related to ribosome, oxidative phosphorylation, apoptosis, glutathione metabolism, metabolism of xenobiotics by CYP450, translation, innate immunity, galactose metabolism and the pentose phosphate pathway (Table 10; Fig. 5b). Although not significantly enriched, several unigenes encoding proteins involved in steroid hormone biosynthesis were upregulated (Fig. 5b).

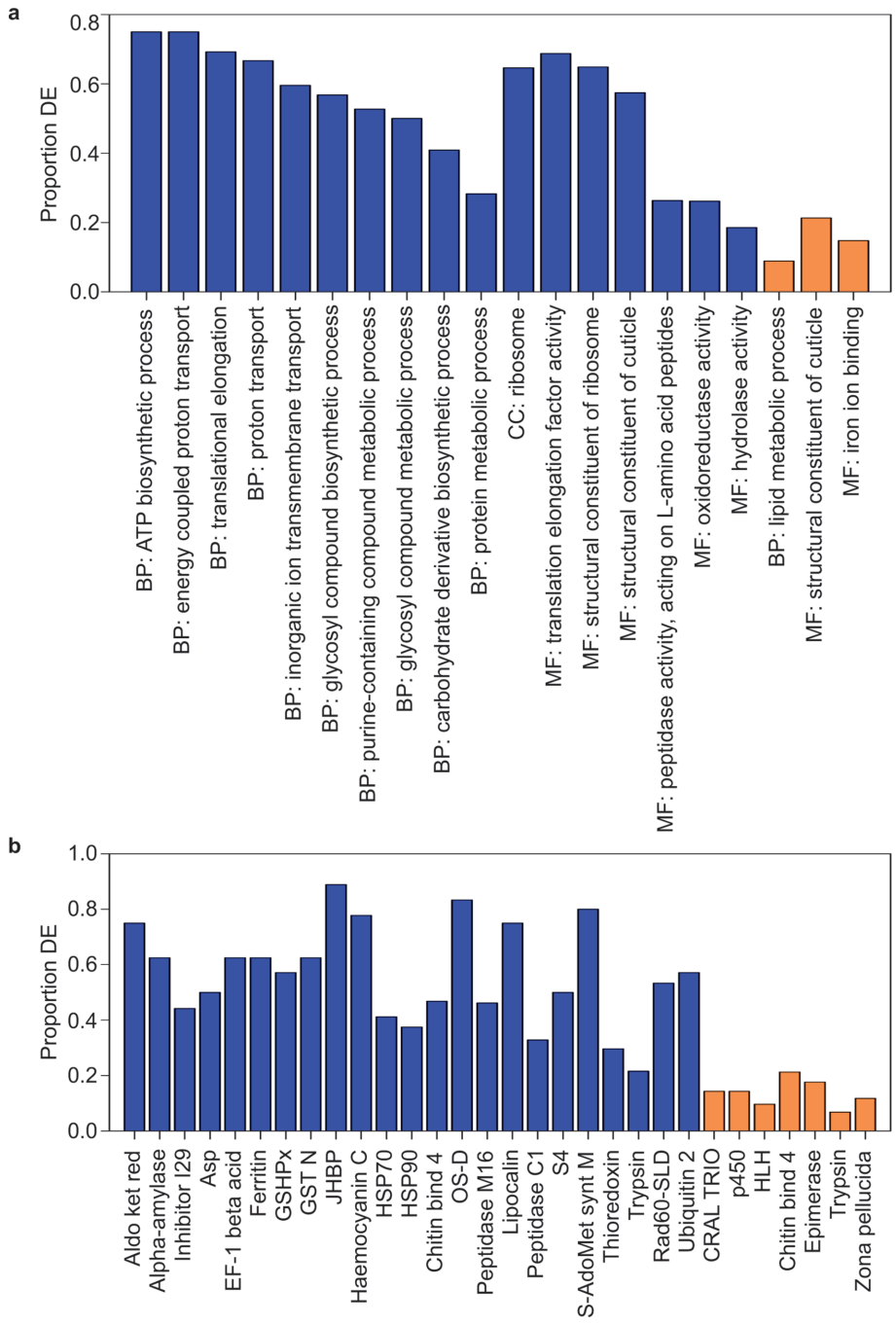

Fig. 4. Select enriched gene ontology (GO) terms and Pfam domains in differentially expressed wheat curl mite unigenes under the influence of *Wheat streak mosaic virus*. (a) Graphical representation of select significantly enriched (FDR <0.05) GO categories in differentially expressed unigenes after WSMV acquisition. (b) Graphical representation of select significantly enriched (*P*-value<0.05) Pfam domains in differentially expressed unigenes. In both (a) and (b), the bars depict the percentage of unigenes assigned to each category that were downregulated (blue) and upregulated (orange) in viruliferous mites relative to the total number of unigenes in the transcriptome.

Additional influences of WSMV on unigenes linked to stress response, development and digestion

Overall, the strongest transcriptional impacts on WCMs that had acquired WSMV were to unigenes encoding ribosomal proteins, the majority of which were downregulated in viruliferous mites. In addition to those unigenes, other unigenes related to translation, protein biosynthesis and processing, folding and transport were downregulated

Table 6. Top 20 enriched gene ontology (GO) terms observed in unigenes that were downregulated in *Wheat streak mosaic virus*-viruliferous wheat curl mites

Term	Ontology	No. of downregulated unigenes	No. of assigned unigenes	FDR corrected *P*-value	Description
GO:0008152	BP	469	1962	4.30E-14	Metabolic process
GO:0005198	MF	173	287	7.66E-14	Structural molecule activity
GO:0003735	MF	146	225	3.12E-13	Structural constituent of ribosome
GO:0005840	CC	146	226	3.49E-13	Ribosome
GO:0006412	BP	139	216	1.29E-12	Translation
GO:0030529	CC	146	240	1.43E-11	Intracellular ribonucleoprotein complex
GO:0043228	CC	146	253	5.29E-11	Non-membrane-bounded organelle
GO:0043232	CC	146	253	5.29E-11	Intracellular non-membrane-bounded organelle
GO:0044444	CC	193	405	1.64E-10	Cytoplasmic part
GO:1901576	BP	197	479	4.26E-10	Organic substance biosynthetic process
GO:0034645	BP	158	322	8.86E-10	Cellular macromolecule biosynthetic process
GO:0071704	BP	374	1550	8.86E-10	Organic substance metabolic process
GO:0009058	BP	202	524	2.03E-09	Biosynthetic process
GO:0044249	BP	191	463	2.36E-09	Cellular biosynthetic process
GO:0044238	BP	352	1473	1.31E-08	Primary metabolic process
GO:0032991	CC	210	534	1.86E-08	Macromolecular complex
GO:0009059	BP	158	347	3.76E-08	Macromolecule biosynthetic process
GO:0019538	BP	241	853	1.27E-05	Protein metabolic process
GO:0072521	BP	39	74	0.000214	Purine-containing compound metabolic process

GoSeq was used to identify enriched GO terms among the downregulated unigenes. All genes were weighted by length and enrichment was determined using an FDR-corrected *P*-value of 0.05. BP, biological processes; MF, molecular function; CC, cellular complex. All GO enrichment results can be found in Table S2.

in viruliferous mites, including unigenes encoding proteins of the following pathways: RNA transport via the nuclear export complex, translation initiation elongation factor proteins, protein processing in the endoplasmic reticulum, ubiquitin-mediated proteolysis, and protein digestion and absorption (Table S4). These data suggest that the majority of unigenes encoding enzymes and structural proteins involved in protein biosynthesis were downregulated in viruliferous mites. In tandem, unigenes encoding the majority of enzymes linked to the citric acid cycle (12) and pyruvate metabolism (10) were downregulated, along with unigenes linked to oxidative phosphorylation (62), glycolysis (18) and the pentose phosphate pathway (10) (Table S4), suggesting that energy production was likely reduced in viruliferous mites. Downregulated unigenes derived from other KEGG pathways included those linked to lysosome (42 unigenes), the cell cycle (4), starch and sucrose metabolism (8), regulation of actin cytoskeleton (8), glutathione metabolism (17), calcium signalling (14), peroxisome (10), fatty acid degradation (5), fatty acid elongation (2) and endocytosis (8) (Table S4). Few pathways were impacted with upregulated unigenes; however, three unigenes encoding enzymes involved in the synthesis of glycosphingolipids were upregulated in viruliferous mites, along with two unigenes encoding GNS1/SUR4 proteins (Table S4). GNS1/SUR4 enzymes can produce precursors for sphingolipid biosynthesis.

Acquisition of WSMV was associated with a large-scale downregulation of unigenes encoding enzymes and proteins

Table 7. Enriched gene ontology (GO) terms observed in unigenes that were upregulated in *Wheat streak mosaic virus* viruliferous wheat curl mites

Term	Ontology	No. of downregulated unigenes	No. of assigned unigenes	FDR corrected *P*-value	Description
GO:0042302	MF	10	47	1.94E-06	Structural constituent of cuticle
GO:0005506	MF	9	61	0.001677	Iron ion binding
GO:0020037	MF	8	60	0.00963	Heme binding
GO:0046906	MF	8	60	0.00963	Tetrapyrrole binding
GO:0006629	BP	11	124	0.012473	Lipid metabolic process

GoSeq was used to identify enriched GO terms among the downregulated unigenes. All genes were weighted by length and enrichment was determined using an FDR-corrected *P*-value of 0.05. BP, biological processes; MF, molecular function.

Table 8. Enriched Pfam domains in downregulated unigenes

Accession	PFAM_name	PFAM description	Total no. of unigenes	Total no. of downregulated unigenes	FDR
PF00379.18	Chitin_bind_4	Insect cuticle protein	47	22	3.93E-06
PF08246.7	Inhibitor_I29	Cathepsin propeptide inhibitor domain (I29)	43	19	6.73E-05
PF06585.6	JHBP	Haemolymph juvenile hormone-binding protein (JHBP)	9	8	8.99E-05
PF00061.18	Lipocalin	Lipocalin/cytosolic fatty acid-binding protein family	12	9	0.000128
PF00248.16	Aldo_ket_red	Aldo/keto reductase family	12	9	0.000128
PF02798.15	GST_N	Glutathione S-transferase, N-terminal domain	16	10	0.00022
PF00467.24	KOW	KOW motif	16	10	0.00022
PF00112.18	Peptidase_C1	Papain family cysteine protease	67	22	0.000559
PF03723.9	Hemocyanin_C	Haemocyanin, ig-like domain	9	7	0.00065
PF00240.18	Ubiquitin	Ubiquitin family	24	11	0.002232
PF00736.14	EF1_GNE	EF-1 guanine nucleotide exchange domain	8	6	0.002803
PF14560.1	Ubiquitin_2	Ubiquitin-like domain	14	8	0.002803
PF03392.8	OS-D	Insect pheromone-binding family, A10/OS-D	6	5	0.004589
PF11976.3	Rad60-SLD	Ubiquitin-2-like Rad60 SUMO-like	15	8	0.004589
PF05193.16	Peptidase_M16_C	Peptidase M16 inactive domain	12	7	0.005549
PF00026.18	Asp	Eukaryotic aspartyl protease	16	8	0.007471
PF00372.14	Hemocyanin_M	Haemocyanin, copper-containing domain	7	5	0.011572
PF01849.13	NAC	NAC domain	7	5	0.011572
PF00578.16	AhpC-TSA	AhpC/TSA family	14	7	0.015625
PF03953.12	Tubulin_C	Tubulin C-terminal domain	11	6	0.017497
PF00213.13	OSCP	ATP synthase delta (OSCP) subunit	5	4	0.017497
PF02772.11	S-AdoMet_synt_M	S-adenosylmethionine synthetase, central domain	5	4	0.017497
PF00956.13	NAP	Nucleosome assembly protein (NAP)	5	4	0.017497
PF00128.19	Alpha-amylase	Alpha amylase, catalytic domain	8	5	0.018002
PF00210.19	Ferritin	Ferritin-like domain	8	5	0.018002
PF10587.4	EF-1_beta_acid	Eukaryotic elongation factor 1 beta central acidic region	8	5	0.018002
PF00012.15	HSP70	Hsp70 protein	17	7	0.038901
PF13881.1	Rad60-SLD_2	Ubiquitin-2 like Rad60 SUMO-like	13	6	0.038901
PF00675.15	Peptidase_M16	Insulinase (peptidase family M16)	13	6	0.038901
PF00464.14	SHMT	Serine hydroxymethyltransferase	6	4	0.038901

Only one enriched term was associated with the upregulated unigenes (PF00379.18 insect cuticle protein; *P*-value=5.77E-7).

linked to immunity and stress responses, including several proteins involved in canonical detoxification reactions (Table S4). These included proteins containing AhpC/TSA domains (7 unigenes), which can act as antioxidants, aldehyde dehydrogenases (2), antifungal peptide (1), aspartyl proteases (8), catalases (2), CYP450s (4), superoxide dismutases (2), glutaredoxins (2), glutathione peroxidases (4), immunoglobulin domain protein (1), LRRs (1), lipases (5), lipocalins (9), papain cysteine proteinases (22) and thioredoxins (8). In contrast, only a handful of unigenes encoding stress-responsive proteins were upregulated, which included carboxylesterase (1), CYP450s (5), carbonic anhydrase (1), HSP20s (2), immunoglobulin domain protein (1), lipases (3), animal haem peroxidases (3) and trypsins (6) (Table S4). The expression levels of several unigenes encoding enzymes related to digestion and nutrient acquisition were affected in viruliferous mites. Downregulated unigenes encoding proteins involved in these processes were annotated as ABC transporters (2), α-amylase (5), ferritin-like proteins involved in iron storage (5), major facilitator superfamily transporters (4), melibiase (1) and uricase (1) (Table S4). As was the case with unigenes linked to stress response, fewer unigenes associated with digestion and nutrient acquisition were upregulated in viruliferous mites. Such unigenes included amino acid permease (1) and major facilitator superfamily transporter (1). Additionally, some of the most strongly upregulated unigenes in WSMV-exposed mites included unigenes encoding CYP450s, cuticle proteins, dual oxidase maturation factors and a putative defence protein (Fig. 6). In contrast, some of the most strongly downregulated unigenes included those encoding apolipoprotein, trypsin, lysosomal aspartic protease, trypsins, JHBPs, cathepsins, cytochrome C oxidase and GSTs (Fig. 6).

Validation of differential expression by RT-qPCR

Differential expression of five each of up- and downregulated unigenes identified through RNA-seq were validated. RT-qPCR reactions were performed on the same pools of RNA samples that were used for the RNA-seq study. Log_2 fold change values ($\Delta\Delta$Cq, viruliferous–aviruliferous)

Table 9. Enriched KEGG orthology (KO) terms in downregulated unigenes

Term	Description	FDR
K17751	MYH6_7; myosin heavy chain 6/7	0.00046
K00011	AKR1B; aldehyde reductase [EC:1.1.1.21]	0.00046
K03098	APOD; apolipoprotein D and lipocalin family protein	0.00105
K04097	HPGDS; prostaglandin-H2 D-isomerase/glutathione transferase [EC:5.3.99.2 2.5.1.18]	0.00105
K01365	CTSL; cathepsin L [EC:3.4.22.15]	0.00227
K17732	PMPCB, MAS1; mitochondrial-processing peptidase subunit beta [EC:3.4.24.64]	0.00227
K02132	ATPeF1A, ATP5A1, ATP1; F-type H+-transporting ATPase subunit alpha	0.00227
K02898	RP-L26e, RPL26; large subunit ribosomal protein L26e	0.00227
K02973	RP-S23e, RPS23; small subunit ribosomal protein S23e	0.00227
K02989	RP-S5e, RPS5; small subunit ribosomal protein S5e	0.00227
K01379	CTSD; cathepsin D [EC:3.4.23.5]	0.0037
K13247	CRYL1; L-gulonate 3-dehydrogenase [EC:1.1.1.45]	0.00594
K03231	EEF1A; elongation factor 1-alpha	0.0073
K05863	SLC25A4S, ANT; solute carrier family 25 (mitochondrial adenine nucleotide translocator), member 4/5/6/31	0.0073
K14753	RACK1; guanine nucleotide-binding protein subunit beta-2-like 1 protein	0.0073
K00789	metK; S-adenosylmethionine synthetase [EC:2.5.1.6]	0.0073
K02137	ATPeF0O, ATP5O, ATP5; F-type H+-transporting ATPase subunit O	0.0073
K02889	RP-L21e, RPL21; large subunit ribosomal protein L21e	0.0073
K02920	RP-L36e, RPL36; large subunit ribosomal protein L36e	0.0073
K02934	RP-L6e, RPL6; large subunit ribosomal protein L6e	0.0073
K02966	RP-S19e, RPS19; small subunit ribosomal protein S19e	0.0073
K03283	HSPA1_8; heat shock 70 kDa protein 1/8	0.00741
K00615	E2.2.1.1, tktA, tktB; transketolase [EC:2.2.1.1]	0.00741
K07374	TUBA; tubulin alpha	0.01429
K09640	TMPRSS9; transmembrane protease serine 9 [EC:3.4.21.-]	0.01429
K00600	glyA, SHMT; glycine hydroxymethyltransferase [EC:2.1.2.1]	0.01429
K01363	CTSB; cathepsin B [EC:3.4.22.1]	0.01429
K02896	RP-L24e, RPL24; large subunit ribosomal protein L24e	0.01429
K09580	PDIA1, P4HB; protein disulfide isomerase A1 [EC:5.3.4.1]	0.01429
K00432	gpx; glutathione peroxidase [EC:1.11.1.9]	0.02907
K03257	EIF4A; translation initiation factor 4A	0.02928
K01623	ALDO; fructose bisphosphate aldolase, class I [EC:4.1.2.13]	0.02928
K02865	RP-L10Ae, RPL10A; large subunit ribosomal protein L10Ae	0.02928
K02998	RP-SAe, RPSA; small subunit ribosomal protein SAe	0.02928

No enriched terms with FDR <0.05 were identified in the upregulated unigenes.

calculated from relative expression determined by RT-qPCR were plotted along with Pearson's correlation between the RNA-seq expression values and the RT-qPCR ΔCq values for each sample (Fig. 7). With the exception of data derived from the unigene encoding the ryanodine receptor, the RT-qPCR and RNA-seq data were highly correlated.

DISCUSSION

Viruses can modulate a variety of biochemical pathways and behaviours to promote vector colonization and prolong association with vectors. This phenomenon, termed adaptive manipulation, often results in rapid vector population expansions and provide viruses with obvious selective advantages [22–25, 61–63]. To study the impact of WSMV on the WCM, we generated a *de novo*-assembled transcriptome of WCM and profiled global changes in gene expression that occurred after the acquisition of WSMV. A majority of unigenes were downregulated in viruliferous mites, with only a few unigenes being upregulated (Table S4). Protein family and metabolic pathway enrichment analyses revealed that the majority of downregulated unigenes coded for enzymes and proteins linked to stress response, immunity and development (such as JHBP), HSPs, GSTs, trypsins, aspartyl proteases, cuticle proteins and cathepsin propeptide inhibitors. Overall, the downregulation of these unigenes may inhibit WCM immune response to prolong viral association and/or alter WCM development to expedite population expansion, both of which could enhance viral transmission or vector spread, or both.

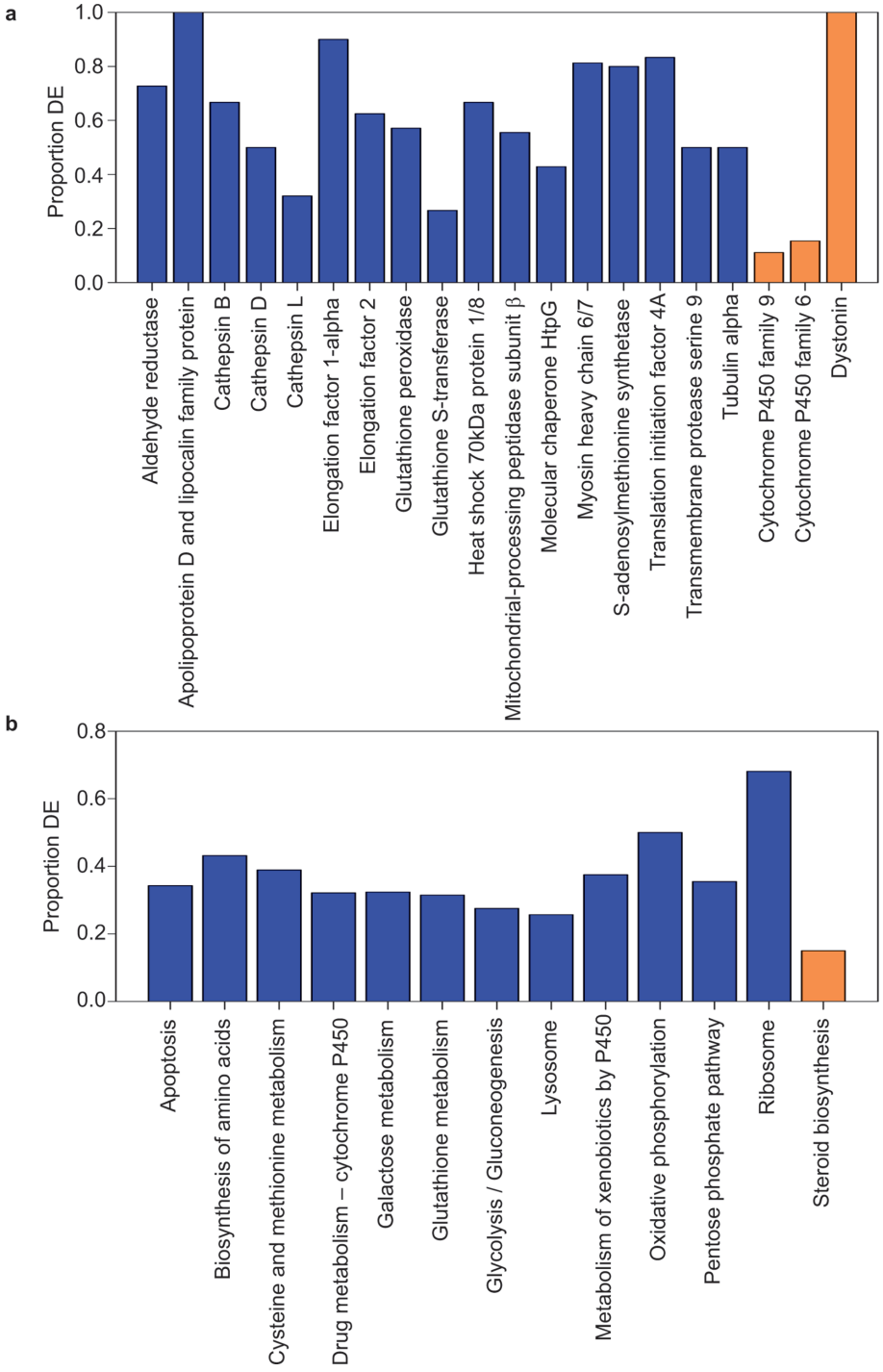

Fig. 5. Select enriched KEGG orthology (KO) terms and KEGG pathways in differentially expressed wheat curl mite unigenes under the influence of *Wheat streak mosaic virus*. (a) Graphical representation of select significantly enriched (*P*-value <0.05) KO categories in differentially expressed unigenes after WSMV acquisition. (b) Graphical representation of select significantly enriched (*P*-value <0.05) KEGG pathways in differentially expressed unigenes after WSMV acquisition. In both (a) and (b), the bars depict the percentage of unigenes assigned to each category that were downregulated (blue) and upregulated (orange) in viruliferous mites relative to the total number of unigenes in the transcriptome.

Table 10. Enriched KEGG pathways in downregulated unigenes

Pathway	FDR
Ribosome	0.0000
Oxidative phosphorylation	0.0000
Biosynthesis of amino acids	0.0000
Carbon metabolism	0.0000
Apoptosis	0.0000
Phagosome	0.0000
Methane metabolism	0.0001
Lysosome	0.0001
Pentose and glucuronate interconversions	0.0001
Glutathione metabolism	0.0002
Fructose and mannose metabolism	0.0010
Metabolism of xenobiotics by cytochrome P450	0.0014
Cysteine and methionine metabolism	0.0019
Glyoxylate and dicarboxylate metabolism	0.0020
Arachidonic acid metabolism	0.0020
Drug metabolism – cytochrome P450	0.0045
Glycine, serine and threonine metabolism	0.0059
Glycolysis/gluconeogenesis	0.0084
Galactose metabolism	0.0086
PPAR signalling pathway	0.0116
Autophagy – animal	0.0165
Pentose phosphate pathway	0.0165

Pfams associated with ribosomal proteins were removed from the table. No enriched terms with FDR <0.05 were identified in the upregulated unigenes.

Development and reproduction

The expression levels for unigenes coding for enzymes linked to development and reproduction were extensively impacted on by the acquisition of WSMV, including many with potential roles in hormone biosynthesis, binding and metabolism. Arthropod development, moulting and sexual maturity are tightly regulated by several hormonal molecules, including ecdysteroids [64]. In this study, the downregulation of unigenes associated with steroid biosynthesis pathway, such as hydroxyl-delta-5-steroid dehydrogenase and cholesteryl ester hydrolase (one upregulated and one downregulated), could be linked to reduced synthesis of ecdysteroids, suggesting that infection with WSMV may alter the ecdysis and reproductive maturity of WCMs. Signalling is the next most important step downstream to hormonal biogenesis. The normal activity of ecdysteroids is mediated by juvenile hormone (JH), which is involved in maintaining the larval stage and also has roles in regulating metamorphosis and reproduction [65, 66]. JHBP is the first and the most important signal transmitter of JH [67] and also protects JH against haemocoelic esterase-mediated hydrolysis [68]. More than 99.8 % of JH exists as JH–JHBP complexes in the haemolymph [69]. Thus, the downregulation of eight unigenes encoding JHBP may result in JH depletion, which may expedite development [70], resulting in precocious sexual maturity and promoting population expansion, which was previously observed in WSMV-exposed mites [71, 72].

Also related to growth and development, a majority of unigenes encoding cuticular proteins, which provide structural stability to the epicuticle and cuticle of the chitinous exoskeleton [73], were downregulated in viruliferous mites, although a smaller number of these unigenes were upregulated. The large degree of differential expression in unigenes encoding these proteins suggests that cuticle formation and chitin metabolism were likely affected in viruliferous mites. Supporting this hypothesis, a unigene encoding GH 18 chitinase was downregulated in viruliferous mites. Additionally, lysosomal cysteine proteases called cathepsins can be involved in hydrolyzing cuticle proteins and are often linked with arthropod developmental events, including moulting and eclosion [74]. In this study, 19 unigenes encoding cathepsin inhibitors, which can suppress or delay cathepsin enzyme activity during earlier life stages [75], were exclusively downregulated in viruliferous mites, and this downregulation may expedite WCM development under the influence of WSMV.

Behaviour and signalling

Behavioural manipulation of the vector is another mechanism by which viruses can facilitate transmission [24]. In WCM, unigenes encoding numerous components of signalling pathways and components of the nervous system showed differential expression in viruliferous WCMs. For example, acetylcholinesterase (AChE) is one of the highly conserved carboxylesterases involved in terminating nerve impulses by rapidly hydrolyzing acetylcholine (ACh) in neural synapses [76]. The upregulation of a unigene encoding AChE suggests that neurotransmission may be altered in WCM under the influence of WSMV. Related to neuronal activity, a unigene encoding a ryanodine receptor was upregulated. These receptors can play pivotal roles in intracellular calcium flux between the cytosol and endoplasmic reticulum of myocytes and neurons [77] and may similarly alter neural activity in WCMs. Other unigenes encoding proteins related to cell signalling were downregulated, including unigenes encoding components of the MAPK, sphingolipid, TOL and IMD, and Rap1 signalling pathways. While the differential expression of unigenes encoding proteins associated with these pathways could have a variety of effects on the physiology of WCMs, it is possible that these expression changes could alter the behaviour of viruliferous mites, as many of these genes have been linked to increased locomotion, spermatophore acquisition and altered oviposition behaviours in other studies [78, 79].

Nutrition

Many unigenes related to digestion, nutrient uptake and storage were downregulated in viruliferous WCMs. For example, many unigenes associated with the degradation of fatty acids were downregulated in viruliferous mites. Lipids are known to play critical roles in energy homeostasis, membrane integrity and signalling [80], and the

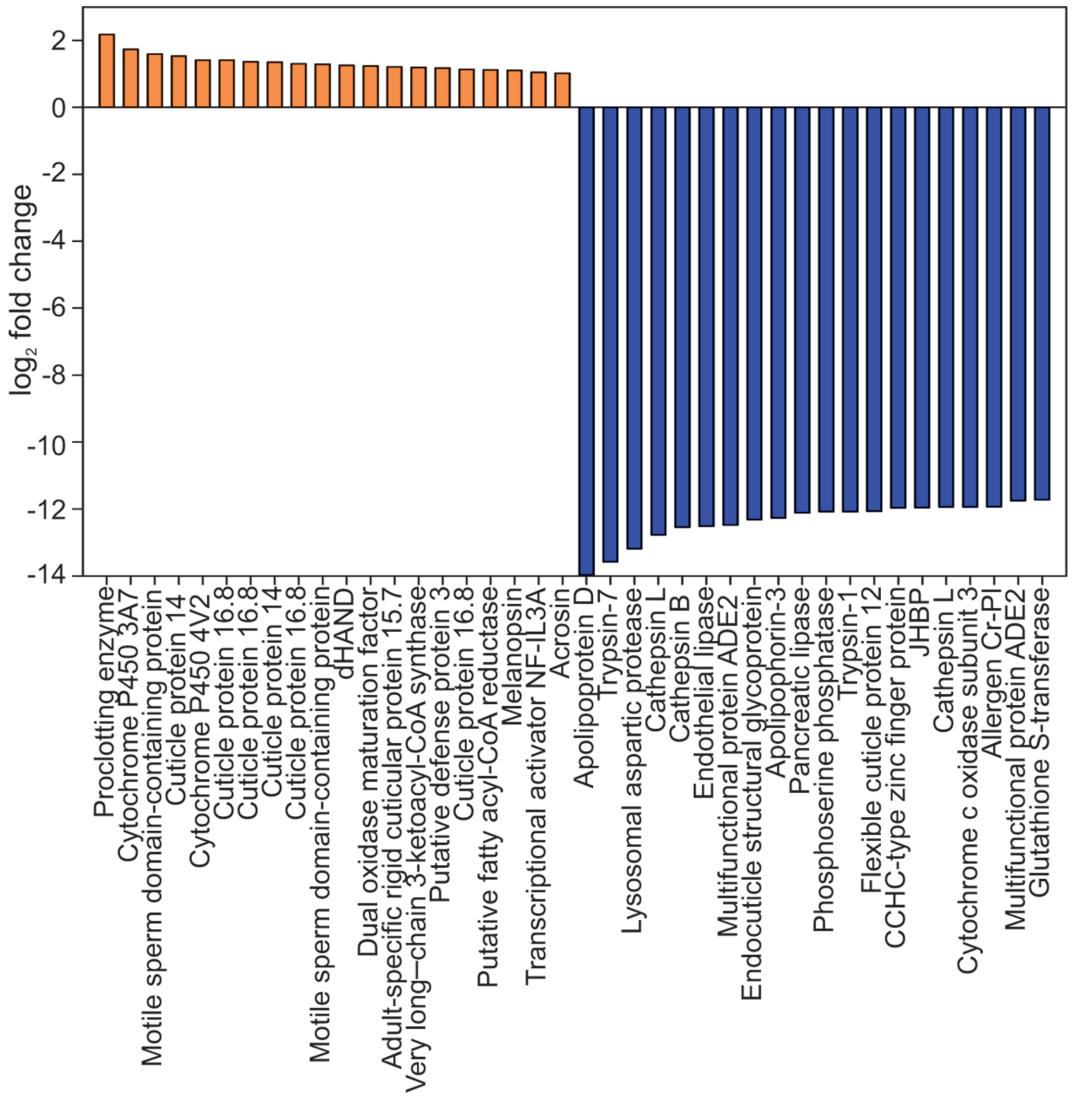

Fig. 6. Top 20 up- and downregulated unigenes in viruliferous wheat curl mites. The bars depict the $\log_2$ fold changes in upregulated (orange) and downregulated (blue) unigenes.

downregulation of unigenes linked to lipid and fatty acid degradation may support increased rate of growth and potentially the increased demand for signal-transducing lipoproteins due to the upregulation of several signalling pathways in viruliferous mites, as discussed in the previous section. Unigenes encoding proteins that bind and sequester minerals and other nutrients were also affected in viruliferous WCMs. For example, several unigenes encoding ferritin (involved in iron uptake, transport and storage [81]), calsequestrin domains (involved in the binding and release of calcium ions [82]) and lipocalin proteins (involved in transportation of lipids, vitamins and building up energy reserves in fat bodies [83]) were all downregulated in viruliferous mites. Likewise, a unigene encoding a perilipin protein, which safeguards lipid droplets in *Drosophila* fat bodies [84], was downregulated in WSMV viruliferous mites, suggesting that virus acquisition could change fat storage and/or more broadly influence energy metabolism in WCMs. The broad downregulation of unigenes associated with nutrition, glycolysis, gluconeogenesis and the citric acid cycle suggests that energy production could be significantly altered in WSMV viruliferous WCMs. Plausibly, resources were redirected for other processes, such as development, and were not available for anabolism or storage.

Ubiquitination

The acquisition of WSMV was associated with lower expression levels of unigenes encoding enzymes and proteins related to apoptosis and ubiquitination. Ubiquitins are regulatory proteins that are covalently attached post-translationally to damaged, overexpressed and misfolded proteins targeted for degradation via proteasomes [85, 86]. As an

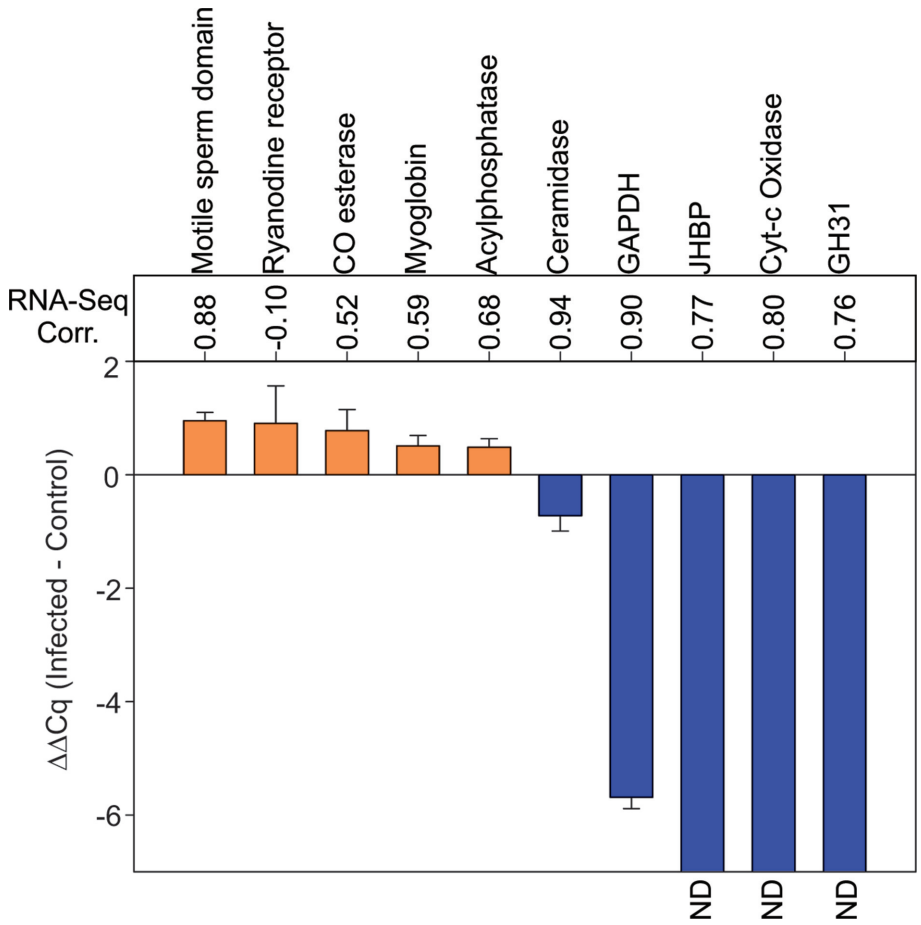

Fig. 7. Reverse-transcription real-time PCR (RT-qPCR) validation of selected wheat curl mite unigenes. Five each of up- and downregulated unigenes observed in the viruliferous mites detected in the RNA-seq analysis were validated using RT-qPCR. Technical duplicates of the same three biological replicates of viruliferous (infected) and control mites that were used in the RNA-seq analysis were used for RT-qPCR validation. The ΔΔCt method was used with actin and G6PDH as internal reference genes. ND indicates that expression was not detected in viruliferous mite samples. The bars represent standard error. Pearson's correlations between the RT-qPCR and RNA-seq data were also calculated for each unigene.

additional factor, unigenes encoding translocons and secY translocases, and membrane proteins, which typically maintain ER–cytosol traffic [87], were downregulated in viruliferous mites. Overall, many other unigenes encoding enzymes related to protein biosynthesis were downregulated in viruliferous WCMs, consistent with lowered rates of ubiquitination and protein degradation by 26S proteasomes. In other virus–vector systems, ubiquitination, proteolysis and protein biosynthesis are common targets of viral manipulation that can result in enhanced viral nucleoprotein accumulation and titre [88]. Supporting this hypothesis, other factors that could be linked to viral replication and virus–vector associations were observed in viruliferous WCMs. For example, a unigene encoding serpin (serine protease inhibitor) was highly downregulated in viruliferous WCMs, which may promote activity of the WSMV P1 serine protease, required for posttranslational polyprotein processing during viral infection [89, 90].

Immunity and stress response

Overall, the majority of differentially expressed unigenes that encode proteins related to stress response and immunity were downregulated in viruliferous WCMs. For example, several unigenes encoding apolipophorin-III (apoLp-III) were downregulated. In addition to its role in lipid transport, apoLp-III can act as a pattern recognition protein that can bind to pathogen-associated molecular patterns (PAMPs) to induce innate immunity in other systems [91]. Additionally, insect cells often overexpress apoLp-III during programmed cell death [92]. Four unigenes encoding Reeler domain proteins were also differentially expressed in viruliferous WCMs (three downregulated and one upregulated) as compared to aviruliferous WCMs. Reeler domain proteins have also been linked to defence responses and can possess nonspecific affinity towards haemocytes and PAMPs, resulting in nodulation, which is one of the most important arthropod immune responses [93, 94]. Other unigenes, such

as one encoding cupins and one encoding an LRR, were downregulated, indicative of modulated defence response in viruliferous mites. In addition, the majority of the proteolytic enzymes currently identifiable in the WCM transcriptome were extensively downregulated in viruliferous WCM. WSMV viruliferous mites also showed greater downregulation of unigenes encoding CYP450s, although five copies showed upregulation. In addition to roles in stress response and detoxification, CYP450s have been shown to play roles in membrane synthesis, cuticular biosynthesis and hormone metabolism [95, 96]. Although the downregulation of CYP450s in viruliferous mites was consistent with the overall downregulation of stress-related transcripts observed after viral acquisition, it is possible that some of these CYP450 unigenes were associated with other metabolic processes, such as cuticular and/or membrane synthesis. Overall, the downregulation of unigenes encoding canonical proteins and enzymes linked to immunity and stress responses suggests that viral acquisition potentially modulates innate immune responses in WCMs.

Oxidative stress

A single unigene encoding dual oxidase maturation factor (DUOX) was upregulated in WSMV viruliferous WCMs. DUOX is an NADPH-oxidative transmembrane enzyme that is involved in reactive oxygen species (ROS) generation and has previously been shown to be involved in antimicrobial defence mechanisms [97]. In tandem, the coordinated downregulation of unigenes that encode ROS-mitigating enzymes in viruliferous WCMs, such as superoxide dismutase, peroxiredoxin, and glutathione peroxidases, uricase [98], thioredoxin-like domain-containing proteins, alkyl hydroperoxidases and catalases, is suggestive of greater oxidative stress after viral acquisition in this system. In addition, 11 unigenes encoding GSTs were extensively downregulated in viruliferous mites, which also can serve as inhibitors of oxidative stress. This finding is in contrast to the findings of previous studies on *Bombyx mori* [99], where infections with *B. mori* nuclear polyhedrosis virus (*Bm*NPV) and *B. mori* densonucleosis virus (*Bm*DNV) were associated with an upregulation of GSTs. Why the responses of GSTs differ in the WCM-WSMV and *B. mori*-virus systems is not known; however, both *Bm*NPV and *Bm*DNV are pathogens to their hosts, whereas WSMV is not known to cause disease in WCMs. Additional factors, such as differences in the ages and nutritional statuses of the hosts used in the studies, or exposure to pesticides or other abiotic stresses, can also influence the expression levels of GSTs and could also account for the differences observed between the two studies.

Conclusions

This study represents the first transcriptome-level analysis of the WCM and contributes significantly to our understanding of the influence of WSMV on WCM biology. Transcriptomic analyses to study virus–vector interactome are essential to understand the cascade of events starting from WSMV acquisition through transmission. Comparative analyses of WCM transcriptomes from WSMV viruliferous and aviruliferous mites suggested that transcriptional changes in viruliferous mites may inhibit WCM immune response, and growth and development. The downregulation of unigenes coding for proteins and enzymes linked to stress response, detoxification and immunity could reduce innate immune responses in viruliferous mites and prolong viral association with WCMs. Furthermore, the downregulation of unigenes coding for enzymes involved in hormone biosynthesis and JHBPs may expedite WCM development to enhance population expansion, as has been previously observed [71, 72]. In addition to studying differential expression under WSMV influence, this study also provides a catalogue of annotated WCM unigenes that can facilitate functional genomics studies and may help to devise novel strategies of vector control as a component of WSMV disease management.

Funding information
This work was funded by USDA ARS CRIS (5440-21000-033-00D) and USDA-NIFA (2013-68004-20358).

Acknowledgements
USDA is an equal opportunity provider and employer. Mention of trade names or commercial products in this publication is solely for the purpose of providing specific information and does not imply recommendation or endorsement by the US Department of Agriculture.

Conflicts of interest
The authors declare that there are no conflicts of interest.

Ethical statement
This article does not contain any studies involving human participants or animals.

References

1. Slykhuis JT. *Aceria tulipae* Keifer (Acarina: Eryophydae) in relation to the spread of wheat streak mosaic. *Phytopathology* 1955;45:116–128.
2. Seifers DL, Harvey TL, Martin TJ, Jensen SG. Identification of the wheat curl mite as the vector of the high plains virus of corn and wheat. *Plant Dis* 1997;81:1161–1166.
3. Stephan D, Moeller I, Skoracka A, Ehrig F, Maiss E. Eriophyid mite transmission and host range of a Brome streak mosaic virus isolate derived from a full-length cDNA clone. *Arch Virol* 2008;153:181–185.
4. Seifers DL, Martin TJ, Harvey TL, Fellers JP, Michaud JP. Identification of the wheat curl mite as the vector of Triticum mosaic virus. *Plant Dis* 2009;93:25–29.
5. Hein GL, French R, Siriwetwiwat B, Amrine JW. Genetic characterization of North American populations of the wheat curl mite and dry bulb mite. *J Econ Entomol* 2012;105:1801–1808.
6. McMechan AJ, Tatineni S, French R, Hein GL. Differential transmission of *Triticum mosaic virus* by wheat curl mite populations collected in the Great Plains. *Plant Dis* 2014;98:806–810.
7. Seifers DL, Harvey TL, Louie R, Gordon DT, Martin TJ. Differential transmission of isolates of the High Plains virus by different sources of wheat curl mites. *Plant Dis* 2002;86:138–142.
8. Wosula EN, McMechan AJ, Oliveira-Hofman C, Wegulo SN, Hein GL. Differential transmission of two isolates of *Wheat streak mosaic virus* by five wheat curl mite populations. *Plant Dis* 2016;100:154–158.
9. Brakke MK. Virus disease in wheat. In: Heyne EG (editor). *Wheat and Wheat Improvement*, 2nd ed. Madison, WI: American Society of Agronomy, Crop Science Society of America, Soil Science Society of America; 1987. pp. 585–603.

10. Burrows M, Franc G, Rush C, Blunt T, Ito D *et al.* Occurrence of viruses in wheat in the Great Plains region, 2008. *Plant Health Progress* 2009;10:14.
11. Appel J, DeWolf E, Todd T, Bockus W. Preliminary 2015 Kansas wheat disease loss estimates. *Kansas Cooperative PlantDisease Survey Report* . 2015 https://agriculture.ks.gov/docs/default-source/pp-disease-reports-2012/2015-ks-wheat-disease-loss-estimates4ec4d4002e6262e1aa5bff0000620720.pdf?sfvrsn=0.
12. Wegulo SN, Hein GL, Klein RN, French R. *Managing Wheat Streak Mosaic*. Univ. Neb. Lincoln Ext.; EC 1871; 2008.
13. Stenger DC, Hall JS, Choi IR, French R. Phylogenetic relationships within the family *Potyviridae*: wheat streak mosaic virus and brome streak mosaic virus are not members of the genus *Rymovirus*. *Phytopathology* 1998;88:782–787.
14. Stenger DC, Hein GL, Gildow FE, Horken KM, French R. Plant virus HC-Pro is a determinant of eriophyid mite transmission. *J Virol* 2005;79:9054–9061.
15. Stenger DC, Hein GL, French R. Nested deletion analysis of *Wheat streak mosaic virus* HC-Pro: Mapping of domains affecting polyprotein processing and eriophyid mite transmission. *Virology* 2006; 350:465–474.
16. Tatineni S, McMechan AJ, Hein GL. Wheat streak mosaic virus coat protein is a determinant for vector transmission by the wheat curl mite. *Virology* 2018;514:42–49.
17. Paliwal YC. Relationship of Wheat streak mosaic and Barley stripe mosaic viruses to vector and nonvector eriophyid mites. *Arch Virol* 1980;63:123–132.
18. Tatineni S, Hein GL. Genetics and mechanisms underlying transmission of Wheat streak mosaic virus by the wheat curl mite. *Curr Opin Virol* 2018;33:47–54.
19. Orlob GB. Feeding and transmission characteristics of *Aceria tulipae* Keifer as vector of Wheat streak mosaic virus). *J Phytopathol* 1966;55:218–238.
20. Takahashi Y, Orlob GB. Distribution of Wheat streak mosaic virus-like particles in *Aceria tulipae*. *Virology* 1969;38:230–240.
21. Whitfield AE, Falk BW, Rotenberg D. Insect vector-mediated transmission of plant viruses. *Virology* 2015;479-480:278–289.
22. Jeger MJ, Holt J, van den Bosch F, Madden LV. Epidemiology of insect-transmitted plant viruses: modelling disease dynamics and control interventions. *Physiol Entomol* 2004;29:291–304.
23. Fereres A, Moreno A. Behavioural aspects influencing plant virus transmission by homopteran insects. *Virus Res* 2009;141:158–168.
24. Ingwell LL, Eigenbrode SD, Bosque-Pérez NA. Plant viruses alter insect behavior to enhance their spread. *Sci Rep* 2012;2:578.
25. Stafford CA, Walker GP, Ullman DE. Infection with a plant virus modifies vector feeding behavior. *Proc Natl Acad Sci USA* 2011; 108:9350–9355.
26. Atreya PL, Lopez-Moya JJ, Chu M, Atreya CD, Pirone TP. Mutational analysis of the coat protein N-terminal amino acids involved in potyvirus transmission by aphids. *J Gen Virol* 1995;76:265–270.
27. Ng JC, Falk BW. Virus-vector interactions mediating nonpersistent and semipersistent transmission of plant viruses. *Annu Rev Phytopathol* 2006;44:183–212.
28. Cassone BJ, Wijeratne S, Michel AP, Stewart LR, Chen Y *et al.* Virus-independent and common transcriptome responses of leafhopper vectors feeding on maize infected with semi-persistently and persistent propagatively transmitted viruses. *BMC Genomics* 2014;15:133.
29. Chen Y, Cassone BJ, Bai X, Redinbaugh MG, Michel AP. Transcriptome of the plant virus vector Graminella nigrifrons, and the molecular interactions of maize fine streak rhabdovirus transmission. *PLoS One* 2012;7:e40613.
30. Schneweis DJ, Whitfield AE, Rotenberg D. Thrips developmental stage-specific transcriptome response to tomato spotted wilt virus during the virus infection cycle in *Frankliniella occidentalis*, the primary vector. *Virology* 2017;500:226–237.
31. Zhang Z, Zhang P, Li W, Zhang J, Huang F *et al.* *De novo* transcriptome sequencing in *Frankliniella occidentalis* to identify genes involved in plant virus transmission and insecticide resistance. *Genomics* 2013;101:296–305.
32. Xu D, Zhong T, Feng W, Zhou G. Tolerance and responsive gene expression of Sogatella furcifera under extreme temperature stresses are altered by its vectored plant virus. *Sci Rep* 2016;6: 31521.
33. Brault V, Tanguy S, Reinbold C, Le Trionnaire G, Arneodo J *et al.* Transcriptomic analysis of intestinal genes following acquisition of pea enation mosaic virus by the pea aphid Acyrthosiphon pisum. *J Gen Virol* 2010;91:802–808.
34. Luan JB, Li JM, Varela N, Wang YL, Li FF *et al.* Global analysis of the transcriptional response of whitefly to tomato yellow leaf curl China virus reveals the relationship of coevolved adaptations. *J Virol* 2011;85:3330–3340.
35. Choi IR, French R, Hein GL, Stenger DC. Fully biologically active *in vitro* transcripts of the eriophyid mite-transmitted Wheat streak mosaic tritimovirus. *Phytopathology* 1999;89:1182–1185.
36. Grabherr MG, Haas BJ, Yassour M, Levin JZ, Thompson DA *et al.* Full-length transcriptome assembly from RNA-Seq data without a reference genome. *Nat Biotechnol* 2011;29:644–652.
37. MacManes MD. On the optimal trimming of high-throughput mRNA sequence data. *Front Genet* 2014;5:13.
38. Góngora-Castillo E, Buell CR. Bioinformatics challenges in *de novo* transcriptome assembly using short read sequences in the absence of a reference genome sequence. *Nat Prod Rep* 2013;30: 490–500.
39. Grabherr MG, Haas BJ, Yassour M, Levin JZ, Thompson DA *et al.* Full-length transcriptome assembly from RNA-Seq data without a reference genome. *Nat Biotechnol* 2011;29:644–652.
40. Langmead B, Salzberg SL. Fast gapped-read alignment with Bowtie 2. *Nat Methods* 2012;9:357–359.
41. Li B, Dewey CN. RSEM: accurate transcript quantification from RNA-Seq data with or without a reference genome. *BMC Bioinformatics* 2011;12:323.
42. Eddy SR. Accelerated profile HMM searches. *PLoS Comput Biol* 2011;7:e1002195.
43. Huson DH, Auch AF, Qi J, Schuster SC. MEGAN analysis of metagenomic data. *Genome Res* 2007;17:377–386.
44. Krogh A, Larsson B, von Heijne G, Sonnhammer EL. Predicting transmembrane protein topology with a hidden Markov model: application to complete genomes. *J Mol Biol* 2001;305:567–580.
45. Petersen TN, Brunak S, von Heijne G, Nielsen H. SignalP 4.0: discriminating signal peptides from transmembrane regions. *Nat Methods* 2011;8:785–786.
46. Kanehisa M, Goto S, Sato Y, Furumichi M, Tanabe M. KEGG for integration and interpretation of large-scale molecular data sets. *Nucleic Acids Res* 2012;40:D109–D114.
47. Derego T, Hall B, Tate R, Geib SM. Transvestigator early release. *ZENODO* 2014.
48. Tate R, Hall B, Derego T. Annie the functional annotator-initial release. *ZENODO* 2014.
49. Robinson MD, McCarthy DJ, Smyth GK. edgeR: a Bioconductor package for differential expression analysis of digital gene expression data. *Bioinformatics* 2010;26:139–140.
50. Schurch NJ, Schofield P, Gierliński M, Cole C, Sherstnev A *et al.* How many biological replicates are needed in an RNA-seq experiment and which differential expression tool should you use? *RNA* 2016;22:839–851.
51. Young MD, Wakefield MJ, Smyth GK, Oshlack A. Gene ontology analysis for RNA-seq: accounting for selection bias. *Genome Biol* 2010;11:R14.
52. Fisher RA. On interpretation of $\chi 2$ from contingency tables, and the calculation of P. *J R Stat Soc* 1922;85:87–94.

53. **Shen L, Sinai M.** GeneOverlap: test and visualize gene overlaps. *R package version* 2013:1.16.0.
54. **Benjamini Y, Hochberg Y.** Controlling the false discovery rate: a practical and powerful approach to multiple testing. *J R Stat Soc: Series B* 1995;57:289–300.
55. **Simão FA, Waterhouse RM, Ioannidis P, Kriventseva EV, Zdobnov EM.** BUSCO: assessing genome assembly and annotation completeness with single-copy orthologs. *Bioinformatics* 2015;31: 3210–3212.
56. **Grbić M, van Leeuwen T, Clark RM, Rombauts S, Rouzé P *et al.*** The genome of *Tetranychus urticae* reveals herbivorous pest adaptations. *Nature* 2011;479:487–492.
57. **Bajda S, Dermauw W, Greenhalgh R, Nauen R, Tirry L *et al.*** Transcriptome profiling of a spirodiclofen susceptible and resistant strain of the European red mite Panonychus ulmi using strand-specific RNA-seq. *BMC Genomics* 2015;16:974.
58. **Liu B, Jiang G, Zhang Y, Li J, Li X *et al.*** Analysis of transcriptome differences between resistant and susceptible strains of the citrus red mite *Panonychus citri* (Acari: Tetranychidae). *PLoS One* 2011;6: e28516.
59. **Emms DM, Kelly S.** OrthoFinder: solving fundamental biases in whole genome comparisons dramatically improves orthogroup inference accuracy. *Genome Biol* 2015;16:157.
60. **Bustin SA, Benes V, Garson JA, Hellemans J, Huggett J *et al.*** The MIQE guidelines: minimum information for publication of quantitative real-time PCR experiments. *Clin Chem* 2009;55:611–622.
61. **Colvin J, Omongo CA, Govindappa MR, Stevenson PC, Maruthi MN *et al.*** Host-plant viral infection effects on arthropod-vector population growth, development and behaviour: management and epidemiological implications. *Adv Virus Res* 2006;67:419–452.
62. **Fereres A, Lister RM, Araya JE, Foster JE.** Development and reproduction of the english grain aphid (homoptera: aphididae) on wheat cultivars infected with barley yellow dwarf virus. *Environ Entomol* 1989;18:388–393.
63. **McKenzie CL, Shatters RG, Doostdar H, Lee SD, Inbar M *et al.*** Effect of geminivirus infection and Bemisia infestation on accumulation of pathogenesis-related proteins in tomato. *Arch Insect Biochem Physiol* 2002;49:203–214.
64. **Bownes M.** The roles of juvenile hormone, ecdysone and the ovary in the control of Drosophila vitellogenesis. *J Insect Physiol* 1989; 35:409–413.
65. **Nijhout HF.** *Insect Hormones*, vol. 267. Princeton, NJ: Princeton University Press; 1994.
66. **Riddiford LM.** Cellular and molecular actions of juvenile hormone I. General considerations and premetamorphic actions. *Adv Insect Physiol* 1994;24:213–274.
67. **Kramer KJ, Sanburg LL, Kézdy FJ, Law JH.** The juvenile hormone binding protein in the hemolymph of Manduca sexta Johannson (Lepidoptera: Sphingidae). *Proc Natl Acad Sci USA* 1974;71:493–497.
68. **de Kort CAD, Granger NA.** Regulation of JH titers: the relevance of degradative enzymes and binding proteins. *Arch Insect Biochem Physiol* 1996;33:1–26.
69. **Hidayat P, Goodman WG.** Juvenile hormone and hemolymph juvenile hormone binding protein titers and their interaction in the hemolymph of fourth stadium Manduca sexta. *Insect Biochem Mol Biol* 1994;24:709–715.
70. **Touhara K, Prestwich GD.** Juvenile hormone epoxide hydrolase. Photoaffinity labeling, purification, and characterization from tobacco hornworm eggs. *J Biol Chem* 1993;268:19604–19609.
71. **Murugan M, Sotelo Cardona P, Duraimurugan P, Whitfield AE, Schneweis D *et al.*** Wheat curl mite resistance: interactions of mite feeding with *Wheat streak mosaic virus* infection. *J Econ Entomol* 2011;104:1406–1414.
72. **Siriwetwiwat B.** Interactions between the wheat curl mite Aceria tosichella Keifer (Eriophyidae), and wheat streak mosaic virus and distribution of Wheat curl mite biotypes in the field. *Ph.D. dissertation*, University of Nebraska, Lincoln; 2006.
73. **Tellam RL, Wijffels G, Willadsen P.** Peritrophic matrix proteins. *Insect Biochem Mol Biol* 1999;29:87–101.
74. **Turk B, Turk D, Turk V.** Lysosomal cysteine proteases: more than scavengers. *Biochim Biophys Acta* 2000;1477:98–111.
75. **Liu J, Shi GP, Zhang WQ, Zhang GR, Xu WH.** Cathepsin L function in insect moulting: molecular cloning and functional analysis in cotton bollworm, *Helicoverpa armigera*. *Insect Mol Biol* 2006;15: 823–834.
76. **Perry E, Walker M, Grace J, Perry R.** Acetylcholine in mind: a neurotransmitter correlate of consciousness? *Trends Neurosci* 1999; 22:273–280.
77. **Santulli G, Marks AR.** Essential roles of intracellular calcium release channels in muscle, brain, metabolism, and aging. *Curr Mol Pharmacol* 2015;8:206–222.
78. **Ikeno T, Tanaka SI, Numata H, Goto SG.** Photoperiodic diapause under the control of circadian clock genes in an insect. *BMC Biol* 2010;8:116.
79. **Sternhcht M, Goldenberg S.** Fertilisation, sex ratio and postembryonic stages of the citrus bud mite Aceria sheldoni (Ewing) (Acarina, Eriophyidae). *Bull Entomol Res* 1971;60:391–397.
80. **Borradaile NM, Han X, Harp JD, Gale SE, Ory DS *et al.*** Disruption of endoplasmic reticulum structure and integrity in lipotoxic cell death. *J Lipid Res* 2006;47:2726–2737.
81. **Harrison PM, Arosio P.** The ferritins: molecular properties, iron storage function and cellular regulation. *Biochim Biophys Acta* 1996;1275:161–203.
82. **Wang S, Trumble WR, Liao H, Wesson CR, Dunker AK *et al.*** Crystal structure of calsequestrin from rabbit skeletal muscle sarcoplasmic reticulum. *Nat Struct Biol* 1998;5:476–483.
83. **Ruiz M, Sanchez D, Correnti C, Strong RK, Ganfornina MD.** Lipid-binding properties of human ApoD and Lazarillo-related lipocalins: functional implications for cell differentiation. *Febs J* 2013;280: 3928–3943.
84. **Beller M, Bulankina AV, Hsiao HH, Urlaub H, Jäckle H *et al.*** PERILIPIN-dependent control of lipid droplet structure and fat storage in Drosophila. *Cell Metab* 2010;12:521–532.
85. **Baumeister W, Cejka Z, Kania M, Seemüller E.** The proteasome: a macromolecular assembly designed to confine proteolysis to a nanocompartment. *Biol Chem* 1997;378:121–130.
86. **Finley D, Chau V.** Ubiquitination. *Annu Rev Cell Biol* 1991;7:25–69.
87. **Hampton RY, Sommer T.** Finding the will and the way of ERAD substrate retrotranslocation. *Curr Opin Cell Biol* 2012;24:460–466.
88. **Gorovits R, Czosnek H.** The involvement of heat shock proteins in the establishment of *Tomato Yellow Leaf Curl Virus* infection. *Front Plant Sci* 2017;8:355.
89. **Choi IR, Horken KM, Stenger DC, French R.** Mapping of the P1 proteinase cleavage site in the polyprotein of Wheat streak mosaic virus (genus Tritimovirus). *J Gen Virol* 2002;83:443–450.
90. **Young BA, Stenger DC, Qu F, Morris TJ, Tatineni S *et al.*** Tritimovirus P1 functions as a suppressor of RNA silencing and an enhancer of disease symptoms. *Virus Res* 2012;163:672–677.
91. **Niere M, Meisslitzer C, Dettloff M, Weise C, Ziegler M *et al.*** Insect immune activation by recombinant Galleria mellonella apolipophorin III. *Biochim Biophys Acta* 1999;1433:16–26.
92. **Sun D, Ziegler R, Milligan CE, Fahrbach S, Schwartz LM.** Apolipophorin III is dramatically up-regulated during the programmed death of insect skeletal muscle and neurons. *J Neurobiol* 1995;26: 119–129.
93. **Gandhe AS, John SH, Nagaraju J.** Noduler, a novel immune upregulated protein mediates nodulation response in insects. *J Immunol* 2007;179:6943–6951.
94. **Trudeau D, Washburn JO, Volkman LE.** Central role of hemocytes in Autographa californica M nucleopolyhedrovirus pathogenesis in

Heliothis virescens and Helicoverpa zea. *J Virol* 2001;75:996–1003.

95. **Qiu Y, Tittiger C, Wicker-Thomas C, Le Goff G, Young S *et al.*** An insect-specific P450 oxidative decarbonylase for cuticular hydrocarbon biosynthesis. *Proc Natl Acad Sci USA* 2012;109:14858–14863.
96. **Casida JE.** Neonicotinoid metabolism: compounds, substituents, pathways, enzymes, organisms, and relevance. *J Agric Food Chem* 2011;59:2923–2931.
97. **Kim SH, Lee WJ.** Role of DUOX in gut inflammation: lessons from Drosophila model of gut-microbiota interactions. *Front Cell Infect Microbiol* 2014;3:116.
98. **Tasaki E, Sakurai H, Nitao M, Matsuura K, Iuchi Y.** Uric acid, an important antioxidant contributing to survival in termites. *PLoS One* 2017;12:e0179426.
99. **Gui Z, Hou C, Liu T, Qin G, Li M *et al.*** Effects of insect viruses and pesticides on glutathione S-transferase activity and gene expression in Bombyx mori. *J Econ Entomol* 2009;102:1591–1598.

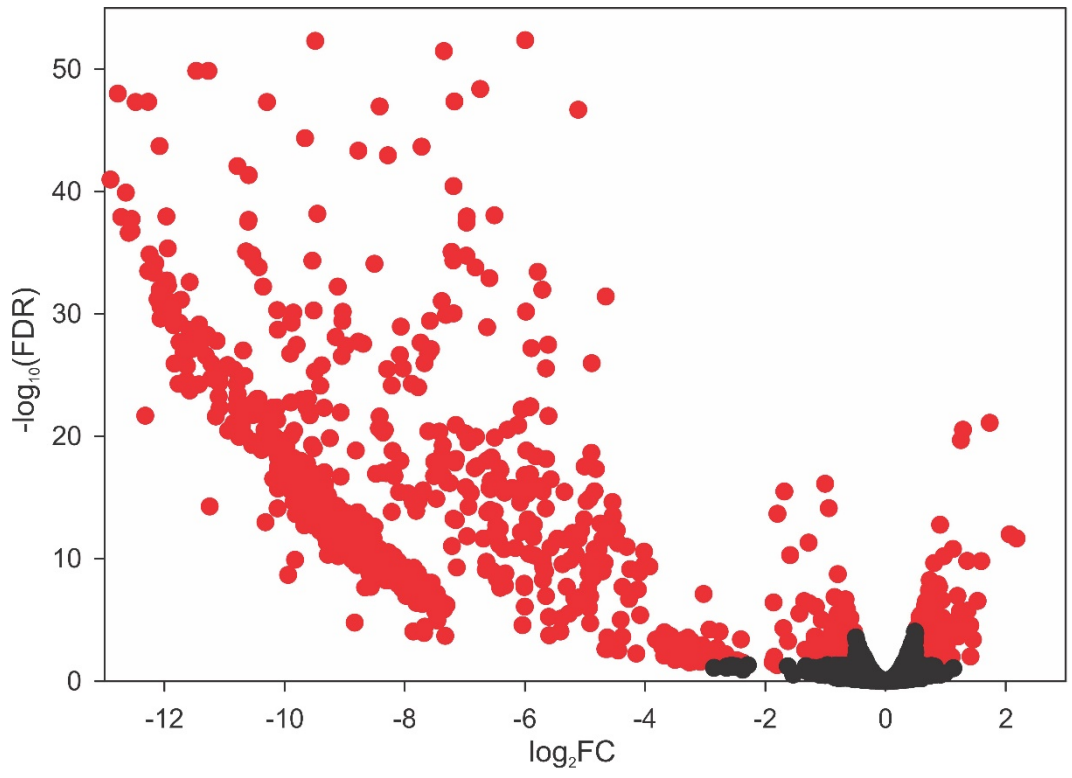

Fig. S1. Volcano plot of expressed unigenes in *Wheat streak mosaic virus* (WSMV) viruliferous and aviruliferous wheat curl mites (WCM). Differentially expressed unigenes (1,020; red) were identified with an FDR cutoff of ≤ 0.05 and a log2FC ≥ 0.5. Non-differentially expressed unigenes (6,271) are shown in black.

Table S1: Primers used for qRT-PCR of representative candidates to validate RNA-Seq analysis of wheat curl mite transcriptome in response to WSMV

Unigene ID	Gene	Primer (5' to 3') forward / reverse
TR6223|c6_g1	Actin	GCCACAACAATCACAACCC/ CGCGATTCGGATCAGCGG
TR2714|c0_g1	Glucose-6-phosphate dehydrogenase (G6I	ATGTATGTATTTGTTACATTTGG/ CCTGTTCTTTTGTTGTAAGG
TR6258|c1_g2	Glyceraldehyde 3-phosphate dehydrogena	TCCAAGATCGGAATTAACGG/ GGTAGTGAAGACACCAGTGG
TR6295|c13_g1	Ceramidase	GGCATTGCCGACATAACAGG/ GAGCATGTACTGAAAGTAACC
TR1462|c0_g1	Cyt-C Oxidase	CCCTACTGTAAAGAACAGACC/ CTTGTAATACGAATACAGAGCC
TR4699|c0_g2	Glycosyl hydrolase family 31 gene (GH31)	AGTCGCCGGGCCAGATTTGC/ TGTCGTCGATCTCGAGCTGG
TR6354|c5_g1	Juvenile Hormone Binding Protein (JHBP)	GCGGCACACACAGAAACAAACAG/ GATGTTAAGGTCCGAGAACTGC
TR5487|c1_g1	Acylphosphatase	AGCGCCCAAATCCAGGAGCC/ TTATCTTATTCTAAAGTCGC
TR6320|c2_g1	Carboxylesterase	ACATCAGCATCAGCATCATC/ TGAGAAAGGTGTATAGGTGC
TR6383|c4_g1	Cral-trio	CAACGATTGCAAAACGGGCTC/ CCGTTTCGGTTGCAACCGGC
TR6108|c11_g2	Globin-1	ATGGCTTTGAGCGAGGCCGACG/ TTGGTGACCACGAACAAGG
TR4132|c0_g1	Ryanodie receptor	CGGTGGAGGGGCCACTGGTCC/ GCGAGCTTGACCGTTCCAAAGG

Table S2: GO Enrichment Results

GOs Enriched in Downregulated DEGs						GOs enriched in Upregulated DEGs					
category	ontology	numDEInCa	numInCat	FDR	term	category	ontology	numDEInCa	numInCat	FDR	term
GO:0006754	BP	18	24	0.0209443	ATP biosynthetic process	GO:0042302	MF	10	47	1.94E-06	structural constituent of cuticle
GO:0015991	BP	10	19	0.053052	ATP hydrolysis coupled proton transport	GO:0005506	MF	9	61	0.0016772	iron ion binding
GO:0046034	BP	22	31	0.0054352	ATP metabolic process	GO:0020037	MF	8	60	0.00963	heme binding
GO:0015986	BP	18	24	0.0209443	ATP synthesis coupled proton transport	GO:0046906	MF	8	60	0.00963	tetrapyrrole binding
GO:0008150	BP	535	3016	0.0005353	biological_process	GO:0006629	BP	11	124	0.0124731	lipid metabolic process
GO:0009058	BP	202	524	2.03E-09	biosynthetic process						
GO:1901137	BP	27	66	0.0497099	carbohydrate derivative biosynthetic process						
GO:1901135	BP	46	146	0.0234577	carbohydrate derivative metabolic process						
GO:0005975	BP	40	131	0.0059463	carbohydrate metabolic process						
GO:0098655	BP	28	47	0.0019922	cation transmembrane transport						
GO:0044249	BP	191	463	2.36E-09	cellular biosynthetic process						
GO:0034645	BP	158	322	8.86E-10	cellular macromolecule biosynthetic process						
GO:0044237	BP	268	1171	0.00082	cellular metabolic process						
GO:0009987	BP	309	1494	0.001426	cellular process						
GO:0044267	BP	159	529	0.0027708	cellular protein metabolic process						
GO:0015074	BP	2	3	0.0452803	DNA integration						
GO:0015988	BP	10	19	0.053052	energy coupled proton transmembrane transport, against electrochemical gradient						
GO:0015985	BP	18	24	0.0209443	energy coupled proton transport, down electrochemical gradient						
GO:1901659	BP	25	44	0.0252596	glycosyl compound biosynthetic process						
GO:1901657	BP	37	74	0.0056436	glycosyl compound metabolic process						
GO:1902600	BP	28	43	0.0009853	hydrogen ion transmembrane transport						
GO:0006818	BP	30	45	0.0006111	hydrogen transport						
GO:0098662	BP	28	47	0.0019922	inorganic cation transmembrane transport						
GO:0098660	BP	28	47	0.0019922	inorganic ion transmembrane transport						
GO:0034220	BP	28	60	0.0200742	ion transmembrane transport						
GO:0009059	BP	158	347	3.76E-08	macromolecule biosynthetic process						
GO:0043170	BP	267	1173	0.0031632	macromolecule metabolic process						
GO:0008152	BP	469	1962	4.30E-14	metabolic process						
GO:0032787	BP	18	35	0.0452803	monocarboxylic acid metabolic process						
GO:0015672	BP	30	61	0.0093801	monovalent inorganic cation transport						
GO:0055086	BP	43	113	0.0068775	nucleobase-containing small molecule metabolic process						
GO:0009163	BP	25	44	0.0252596	nucleoside biosynthetic process						
GO:0009116	BP	37	74	0.0056436	nucleoside metabolic process						
GO:0009124	BP	20	33	0.0300997	nucleoside monophosphate biosynthetic process						
GO:0009123	BP	24	40	0.0066678	nucleoside monophosphate metabolic process						
GO:0006753	BP	38	99	0.0134533	nucleoside phosphate metabolic process						
GO:0009142	BP	21	28	0.0079491	nucleoside triphosphate biosynthetic process						
GO:0009141	BP	31	49	0.0014631	nucleoside triphosphate metabolic process						
GO:0009117	BP	38	98	0.0127394	nucleotide metabolic process						
GO:1901576	BP	197	479	4.26E-10	organic substance biosynthetic process						
GO:0071704	BP	374	1550	8.86E-10	organic substance metabolic process						
GO:1901566	BP	30	92	0.0523246	organonitrogen compound biosynthetic process						
GO:0019637	BP	39	127	0.0445914	organophosphate metabolic process						
GO:0055114	BP	74	288	0.0190219	oxidation-reduction process						
GO:0044238	BP	352	1473	1.31E-08	primary metabolic process						
GO:0019538	BP	241	853	1.27E-05	protein metabolic process						
GO:0015992	BP	30	45	0.0006111	proton transport						
GO:0042451	BP	25	40	0.0101366	purine nucleoside biosynthetic process						
GO:0042278	BP	36	62	0.0005921	purine nucleoside metabolic process						
GO:0009127	BP	20	29	0.0093801	purine nucleoside monophosphate biosynthetic process						
GO:0009126	BP	24	36	0.0019922	purine nucleoside monophosphate metabolic process						
GO:0009145	BP	21	28	0.0079491	purine nucleoside triphosphate biosynthetic process						
GO:0009144	BP	31	48	0.0008959	purine nucleoside triphosphate metabolic process						
GO:0006164	BP	24	45	0.0242488	purine nucleotide biosynthetic process						
GO:0006163	BP	35	67	0.0010383	purine nucleotide metabolic process						
GO:0046129	BP	25	40	0.0101366	purine ribonucleoside biosynthetic process						
GO:0046128	BP	36	62	0.0005921	purine ribonucleoside metabolic process						
GO:0009168	BP	20	29	0.0093801	purine ribonucleoside monophosphate biosynthetic process						
GO:0009167	BP	24	36	0.0019922	purine ribonucleoside monophosphate metabolic process						
GO:0009206	BP	21	28	0.0079491	purine ribonucleoside triphosphate biosynthetic process						
GO:0009205	BP	31	48	0.0008959	purine ribonucleoside triphosphate metabolic process						
GO:0009152	BP	23	42	0.0358981	purine ribonucleotide biosynthetic process						
GO:0009150	BP	34	64	0.0015429	purine ribonucleotide metabolic process						
GO:0072522	BP	28	52	0.0053624	purine-containing compound biosynthetic process						
GO:0072521	BP	39	74	0.0002143	purine-containing compound meta Could pick one of these categories related to purine metabolism and mention that several categories related to this process were enriched.						
GO:0042455	BP	25	44	0.0252596	ribonucleoside biosynthetic process						
GO:0009119	BP	36	66	0.0012269	ribonucleoside metabolic process						
GO:0009156	BP	20	33	0.0300997	ribonucleoside monophosphate biosynthetic process						
GO:0009161	BP	24	40	0.0066678	ribonucleoside monophosphate metabolic process						
GO:0009201	BP	21	28	0.0079491	ribonucleoside triphosphate biosynthetic process						
GO:0009199	BP	31	48	0.0008959	ribonucleoside triphosphate metabolic process						
GO:0009260	BP	23	46	0.0741131	ribonucleotide biosynthetic process						
GO:0009259	BP	34	68	0.0031552	ribonucleotide metabolic process						
GO:0046390	BP	23	46	0.0741131	ribose phosphate biosynthetic process						
GO:0019693	BP	37	78	0.0019922	ribose phosphate metabolic process						
GO:0044711	BP	39	150	0.0810334	single-organism biosynthetic process						
GO:0044712	BP	21	57	0.0977539	single-organism catabolic process						
GO:0044710	BP	143	655	0.00082	single-organism metabolic process						
GO:0044699	BP	188	1061	0.0084868	single-organism process						
GO:0044281	BP	71	237	0.0034864	small molecule metabolic process						
GO:0006412	BP	139	216	1.29E-12	translation						
GO:0006414	BP	18	26	0.0148561	translational elongation						
GO:0044444	CC	193	405	1.64E-10	cytoplasmic part						
GO:0005622	CC	102	260	0.013371	intracellular						
GO:0043232	CC	146	253	5.29E-11	intracellular non-membrane-bounded organelle						
GO:0043229	CC	160	479	0.0019922	intracellular organelle						
GO:0044424	CC	222	835	0.0103311	intracellular part						
GO:0030529	CC	146	240	1.43E-11	intracellular ribonucleoprotein complex						
GO:0032991	CC	210	534	1.86E-08	macromolecular complex						
GO:0043228	CC	146	253	5.29E-11	non-membrane-bounded organelle						
GO:0043226	CC	160	479	0.0019922	organelle						
GO:0033178	CC	10	18	0.0445914	proton-transporting two-sector ATPase complex, catalytic domain						
GO:0005840	CC	146	226	3.49E-13	ribosome						
GO:0015078	MF	36	57	0.0005921	hydrogen ion transmembrane transporter activity						
GO:0016787	MF	158	854	0.0510499	hydrolase activity						
GO:0022890	MF	36	103	0.062887	inorganic cation transmembrane transporter activity						
GO:0015077	MF	36	75	0.0074209	monovalent inorganic cation transmembrane transporter activity						
GO:0016491	MF	92	352	0.0179365	oxidoreductase activity						
GO:0016616	MF	19	56	0.0209443	oxidoreductase activity, acting on the CH-OH group of donors, NAD or NADP as acceptor						
GO:0070011	MF	80	304	0.0815075	peptidase activity, acting on L-amino acid peptides						
GO:0042302	MF	27	47	0.0514632	structural constituent of cuticle						

GO:0003735	MF	146	225	3.12E-13	structural constituent of ribosome
GO:0005198	MF	173	287	7.66E-14	structural molecule activity
GO:0003746	MF	11	16	0.0491896	translation elongation factor activity

Table S3: Pfam Enrichment Results

Pfams Enriched in Downregulated DEGs

	PFAM_Name	PFAM_desc	total	Downregulat	pval	fdr
PF00379	Chitin_bind_4	Insect cuticle protein	47	22	6.51E-09	3.93E-06
PF08246	Inhibitor_I29	Cathepsin propeptide inhibit	43	19	2.23E-07	6.73E-05
PF06585	JHBP	Haemolymph juvenile hormo	9	8	4.46E-07	8.99E-05
PF00061	Lipocalin	Lipocalin / cytosolic fatty-aci	12	9	1.06E-06	0.000128
PF00248	Aldo_ket_red	Aldo/keto reductase family	12	9	1.06E-06	0.000128
PF02798	GST_N	Glutathione S-transferase, N	16	10	3.33E-06	0.00022
PF13417	GST_N_3	Glutathione S-transferase, N	16	10	3.33E-06	0.00022
PF00467	KOW	KOW motif	16	10	3.33E-06	0.00022
PF00828	Ribosomal_L18e	Ribosomal protein L18e/L15	6	6	3.65E-06	0.00022
PF08212	Lipocalin_2	Lipocalin-like domain	6	6	3.65E-06	0.00022
PF00112	Peptidase_C1	Papain family cysteine prote	67	22	1.02E-05	0.000559
PF03723	Hemocyanin_C	Hemocyanin, ig-like domain	9	7	1.29E-05	0.00065
PF03722	Hemocyanin_N	Hemocyanin, all-alpha doma	5	5	2.95E-05	0.00137
PF00428	Ribosomal_60s	60s Acidic ribosomal protein	10	7	3.84E-05	0.001658
PF00240	ubiquitin	Ubiquitin family	24	11	5.54E-05	0.002232
PF00043	GST_C	Glutathione S-transferase, C	17	9	6.55E-05	0.002472
PF00736	EF1_GNE	EF-1 guanine nucleotide excl	8	6	8.17E-05	0.002803
PF14560	Ubiquitin_2	Ubiquitin-like domain	14	8	8.35E-05	0.002803
PF03392	OS-D	Insect pheromone-binding fa	6	5	0.000159	0.004589
PF00164	Ribosom_S12_S2	Ribosomal protein S12/S23	6	5	0.000159	0.004589
PF11976	Rad60-SLD	Ubiquitin-2 like Rad60 SUMO	15	8	0.00016	0.004589
PF05193	Peptidase_M16_	Peptidase M16 inactive dom	12	7	0.000202	0.005549
PF00026	Asp	Eukaryotic aspartyl protease	16	8	0.000285	0.007471
PF00372	Hemocyanin_M	Hemocyanin, copper contair	7	5	0.000498	0.011572
PF00177	Ribosomal_S7	Ribosomal protein S7p/S5e	7	5	0.000498	0.011572
PF01849	NAC	NAC domain	7	5	0.000498	0.011572
PF00578	AhpC-TSA	AhpC/TSA family	14	7	0.000698	0.015625
PF03953	Tubulin_C	Tubulin C-terminal domain	11	6	0.000965	0.017497
PF00213	OSCP	ATP synthase delta (OSCP) su	5	4	0.001072	0.017497
PF02772	S-AdoMet_synt_I	S-adenosylmethionine synth	5	4	0.001072	0.017497
PF13409	GST_N_2	Glutathione S-transferase, N	5	4	0.001072	0.017497
PF00573	Ribosomal_L4	Ribosomal protein L4/L1 fam	5	4	0.001072	0.017497
PF01090	Ribosomal_S19e	Ribosomal protein S19e	5	4	0.001072	0.017497
PF01157	Ribosomal_L21e	Ribosomal protein L21e	5	4	0.001072	0.017497
PF01158	Ribosomal_L36e	Ribosomal protein L36e	5	4	0.001072	0.017497
PF01159	Ribosomal_L6e	Ribosomal protein L6e	5	4	0.001072	0.017497
PF00956	NAP	Nucleosome assembly prote	5	4	0.001072	0.017497
PF00128	Alpha-amylase	Alpha amylase, catalytic don	8	5	0.001192	0.018002
PF00210	Ferritin	Ferritin-like domain	8	5	0.001192	0.018002
PF10587	EF-1_beta_acid	Eukaryotic elongation factor	8	5	0.001192	0.018002
PF01248	Ribosomal_L7Ae	Ribosomal protein L7Ae/L30	9	5	0.002409	0.035482
PF00012	HSP70	Hsp70 protein	17	7	0.002824	0.038901
PF13881	Rad60-SLD_2	Ubiquitin-2 like Rad60 SUMO	13	6	0.002875	0.038901
PF00675	Peptidase_M16	Insulinase (Peptidase family	13	6	0.002875	0.038901
PF00464	SHMT	Serine hydroxymethyltransfe	6	4	0.002898	0.038901
PF01576	Myosin_tail_1	Myosin tail	10	5	0.004327	0.056812
PF00431	CUB	CUB domain	14	6	0.004508	0.057933
PF00725	3HCDH	3-hydroxyacyl-CoA dehydrog	7	4	0.006098	0.070835
PF02874	ATP-synt_ab_N	ATP synthase alpha/beta fan	7	4	0.006098	0.070835
PF00056	Ldh_1_N	lactate/malate dehydrogena	7	4	0.006098	0.070835
PF00255	GSHPx	Glutathione peroxidase	7	4	0.006098	0.070835
PF02866	Ldh_1_C	lactate/malate dehydrogena	7	4	0.006098	0.070835
PF00089	Trypsin	Trypsin	88	19	0.010594	0.118692
PF00160	Pro_isomerase	Cyclophilin type peptidyl-prc	12	5	0.010984	0.118692
PF00306	ATP-synt_ab_C	ATP synthase alpha/beta cha	8	4	0.011005	0.118692
PF01479	S4	S4 domain	8	4	0.011005	0.118692
PF00085	Thioredoxin	Thioredoxin	27	8	0.014072	0.134372
PF00137	ATP-synt_C	ATP synthase subunit C	5	3	0.015795	0.134372
PF01294	Ribosomal_L13e	Ribosomal protein L13e	5	3	0.015795	0.134372
PF00252	Ribosomal_L16	Ribosomal protein L16p/L10	5	3	0.015795	0.134372
PF00318	Ribosomal_S2	Ribosomal protein S2	5	3	0.015795	0.134372
PF00327	Ribosomal_L30	Ribosomal protein L30p/L7e	5	3	0.015795	0.134372
PF00380	Ribosomal_S9	Ribosomal protein S9/S16	5	3	0.015795	0.134372
PF00416	Ribosomal_S13	Ribosomal protein S13/S18	5	3	0.015795	0.134372
PF00838	TCTP	Translationally controlled tu	5	3	0.015795	0.134372
PF01246	Ribosomal_L24e	Ribosomal protein L24e	5	3	0.015795	0.134372
PF01283	Ribosomal_S26e	Ribosomal protein S26e	5	3	0.015795	0.134372
PF01929	Ribosomal_L14e	Ribosomal protein L14	5	3	0.015795	0.134372
PF03719	Ribosomal_S5_C	Ribosomal protein S5, C-term	5	3	0.015795	0.134372
PF07650	KH_2	KH domain	5	3	0.015795	0.134372
PF14543	TAXi_N	Xylanase inhibitor N-termina	5	3	0.015795	0.134372
PF01442	Apolipoprotein	Apolipoprotein A1/A4/E dom	9	4	0.017881	0.150005
PF00091	Tubulin	Tubulin/FtsZ family, GTPase	14	5	0.022466	0.185884
PF00456	Transketolase_N	Transketolase, thiamine diph	6	3	0.028693	0.219371
PF02221	E1_DerP2_DerF2	ML domain	6	3	0.028693	0.219371
PF00333	Ribosomal_S5	Ribosomal protein S5, N-term	6	3	0.028693	0.219371
PF00338	Ribosomal_S10	Ribosomal protein S10p/S20	6	3	0.028693	0.219371
PF00687	Ribosomal_L1	Ribosomal protein L1p/L10e	6	3	0.028693	0.219371
PF01201	Ribosomal_S8e	Ribosomal protein S8e	6	3	0.028693	0.219371
PF00153	Mito_carr	Mitochondrial carrier protein	32	8	0.038158	0.288091
PF00006	ATP-synt_ab	ATP synthase alpha/beta fan	7	3	0.045638	0.32816
PF01459	Porin_3	Eukaryotic porin	7	3	0.045638	0.32816
PF13917	zf-CCHC_3	Zinc knuckle	7	3	0.045638	0.32816
PF13019	Telomere_Sde2	Telomere stability and silenc	7	3	0.045638	0.32816
PF03143	GTP_EFTU_D3	Elongation factor Tu C-termi	12	4	0.051847	0.368422
PF00183	HSP90	Hsp90 protein	8	3	0.066418	0.461111
PF08534	Redoxin	Redoxin	8	3	0.066418	0.461111
PF00180	Iso_dh	Isocitrate/isopropylmalate d	9	3	0.090687	0.60192
PF12763	EF-hand_4	Cytoskeletal-regulatory com	9	3	0.090687	0.60192
PF14497	GST_C_3	Glutathione S-transferase, C	9	3	0.090687	0.60192
PF03446	NAD_binding_2	NAD binding domain of 6-ph	9	3	0.090687	0.60192
PF03144	GTP_EFTU_D2	Elongation factor Tu domain	20	5	0.093159	0.611611

Pfams Enriched in Upregulated DEGs

	PFAM_Name	PFAM_desc	total	Upregulate	pval	fdr
PF00379	Chitin_bind_4	Insect cuticle protein	47	10	5.77E-08	3.49E-05
PF00067	p450	Cytochrome P450	35	5	0.000975	0.29456
PF00487	FA_desaturase	Fatty acid desaturase	11	3	0.001571	0.316357
PF00246	Peptidase_M14	Zinc carboxypeptidase	14	3	0.0033	0.408534
PF07993	NAD_binding_4	Male sterility protein	15	3	0.004058	0.408534
PF03098	An_peroxidase	Animal haem peroxidase	15	3	0.004058	0.408534
PF01370	Epimerase	NAD dependent epimerase/(	17	3	0.00587	0.49406
PF01607	CBM_14	Chitin binding Peritrophin-A	34	4	0.006544	0.49406
PF00011	HSP20	Hsp20/alpha crystallin family	7	2	0.009631	0.580119
PF00151	Lipase	Lipase	21	3	0.010758	0.580119
PF00650	CRAL_TRIO	CRAL/TRIO domain	21	3	0.010758	0.580119
PF07716	bZIP_2	Basic region leucine zipper	8	2	0.012655	0.580119
PF00571	CBS	CBS domain	8	2	0.012655	0.580119
PF00089	Trypsin	Trypsin	88	6	0.013446	0.580119
PF02719	Polysacc_synt_2	Polysaccharide biosynthesis	9	2	0.016034	0.605299
PF00170	bZIP_1	bZIP transcription factor	9	2	0.016034	0.605299
PF00640	PID	Phosphotyrosine interaction	10	2	0.019753	0.701798
PF03015	Sterile	Male sterility protein	12	2	0.028139	0.894533
PF04083	Abhydro_lipase	Partial alpha/beta-hydrolase	12	2	0.028139	0.894533
PF00010	HLH	Helix-loop-helix DNA-binding	31	3	0.030939	0.934366
PF01073	3Beta_HSD	3-beta hydroxysteroid dehyc	13	2	0.032776	0.942708
PF00100	Zona_pellucida	Zona pellucida-like domain	17	2	0.053939	1
PF01151	ELO	GNS1/SUR4 family	23	2	0.092087	1

Table S4: Differentially Expressed Unigenes at FDR < 0.05 and log2FC > 0.5

	DEG Results		Best BlastX results							Best BlastP results							Additional Annotations			
Gene.Model	log2FC (	FDR	transcript_id	sprot_Top	%ID	e-val	gene.name	descript	species	prot_id	sprot_Top	%ID	e-val	gene.name	descript	species	Pfam	gene_ontology	KEGG	
TR6071|c9_g1	-14.30	1.90E-83	TR6071|c9_g1_i1	.			.	.	.	TR6071|c9_g1_i1|m.9392	.			.	.	.	.	.	.	.
TR6324|c10_g1	-13.98	7.74E-95	TR6324|c10_g1_i1	APOD_HUI	35.56	1.00E-15	APOD	Apolipoprc	Homo sapi	TR6324|c10_g1_i1|m.17180	APOD_HUI	35.17	8.00E-17	APOD	Apolipoprc	Homo sapi	PF00061.1	.	.	.
TR6289|c0_g1	-13.58	7.52E-68	TR6289|c0_g1_i4	TRY7_ANO	38.11	2.00E-50	TRYP7 AGA	Trypsin-7 (	Anopheles	TR6289|c0_g1_i4|m.15989	TRY7_ANO	38.11	4.00E-51	TRYP7 AGA	Trypsin-7 (	Anopheles	PF00089.2	GO:0004252^mo	Neuroactive ligand-receptor interaction`Neuroactiv	.
TR6235|c10_g1	-13.19	4.40E-59	TR6235|c10_g1_i1	ASPP_AED	60.12	8.00E-144	AAEL0061€	Lysosomal	Aedes aegy	TR6235|c10_g1_i1|m.14316	ASPP_AED	59.48	3.00E-146	AAEL0061€	Lysosomal	Aedes aegy	PF00026.1	GO:0004190^mo	Apoptosis`Autophagy - animal`Lysosome`Sphingoli	.
TR6020|c0_g2	-12.90	1.05E-41	TR6020|c0_g2_i1	RS18_SPOI	91.85	2.00E-71	RpS18	40S riboso	Spodopter	TR6020|c0_g2_i1|m.8358	RS18_SPOI	92.76	8.00E-102	RpS18	40S riboso	Spodopter	PF00416.1	GO:0003723^mo	Ribosome	.
TR6319|c6_g1	-12.78	9.86E-49	TR6319|c6_g1_i1	CATL_SARI	49.07	2.00E-29	0	Cathepsin	Sarcophag	TR6319|c6_g1_i1|m.16998	CATL_SARI	49.07	4.00E-29	0	Cathepsin	Sarcophag	PF00112.1	GO:0008234^mo	Apoptosis`Autophagy - animal`Lysosome`Phagosor	.
TR6241|c6_g1	-12.72	1.21E-38	TR6241|c6_g1_i1	RS8_APIMI	87.37	2.00E-105	RpS8	40S riboso	Apis mellif	TR6241|c6_g1_i1|m.14547	RS8_SPOFI	81.73	1.00E-123	RpS8	40S riboso	Spodopter	PF01201.1	.	Ribosome	.
TR6337|c20_g1	-12.64	1.26E-40	TR6337|c20_g1_i1	RL13_SPOI	73.93	4.00E-98	RpL13	60S riboso	Spodopter	TR6337|c20_g1_i1|m.17667	RL13_SPOI	73.93	5.00E-112	RpL13	60S riboso	Spodopter	PF01294.1	GO:0003735^mo	Ribosome	.
TR1371|c0_g1	-12.60	2.39E-37	TR1371|c0_g1_i1	RL31_RAT	75.21	1.00E-53	Rpl31	60S riboso	Rattus nor	TR1371|c0_g1_i1|m.1158	RL31_RAT	80	1.00E-60	Rpl31	60S riboso	Rattus nor	PF01198.1	GO:0003735^mo	Ribosome	.
TR7863|c0_g1	-12.55	1.73E-37	TR7863|c0_g1_i1	RL27_RAT	67.65	7.00E-60	Rpl27	60S riboso	Rattus nor	TR7863|c0_g1_i1|m.20300	RL27_RAT	67.65	3.00E-59	Rpl27	60S riboso	Rattus nor	PF00467.2	GO:0003735^mo	Ribosome	.
TR6033|c1_g2	-12.55	1.75E-38	TR6033|c1_g2_i1	CATB_BOV	60.06	8.00E-125	CTSB	Cathepsin	Bos taurus	TR6033|c1_g2_i1|m.8478	CATB_PIG	57.4	2.00E-133	CTSB	Cathepsin	Sus scrofa	PF00112.1	GO:0004197^mo	Apoptosis`Autophagy - animal`Lysosome	.
TR6349|c0_g1	-12.52	1.45E-80	TR6349|c0_g1_i2	LIPE_HUM	40	5.00E-39	LIPG UNQ3	Endothelia	Homo sapi	TR6349|c0_g1_i2|m.18094	LIPE_MOU	36.79	2.00E-40	Lipg	Endothelia	Mus muscu	PF00151.1	.	.	.
TR5728|c0_g1	-12.48	4.88E-48	TR5728|c0_g1_i1	PUR6_DRC	71.88	0	ade5 CG39	Multifunct	Drosophila	TR5728|c0_g1_i1|m.6816	PUR6_DRC	71.88	0	ade5 CG39	Multifunct	Drosophila	PF00731.1	GO:0006189^biol	Purine metabolism	.
TR5503|c0_g1	-12.32	2.09E-22	TR5503|c0_g1_i1	CUD2_SCH	49.5	2.00E-26	0	Endocuticl	Schistocer	TR5503|c0_g1_i1|m.6222	CUD2_SCH	49.5	3.00E-25	0	Endocuticl	Schistocer	PF00379.1	GO:0042302^mo	.	.
TR5820|c1_g1	-12.27	3.26E-34	TR5820|c1_g1_i1	RS13_SPOI	90.73	4.00E-93	RpS13	40S riboso	Spodopter	TR5820|c1_g1_i1|m.7129	RS13_SPOI	90.73	2.00E-95	RpS13	40S riboso	Spodopter	PF00312.1	GO:0003735^mo	Ribosome`Ribosome	.
TR5637|c0_g1	-12.27	4.70E-48	TR5637|c0_g1_i1	APL3_GALI	32.07	7.00E-12	0	Apolipoph	Galleria me	TR5637|c0_g1_i1|m.6550	APL3_GALI	32.07	6.00E-09	0	Apolipoph	Galleria me	PF01442.1	GO:0008289^mo	.	.
TR8141|c0_g1	-12.25	1.35E-35	TR8141|c0_g1_i1	RL12_MOU	78.53	3.00E-90	Rpl12	60S riboso	Mus muscu	TR8141|c0_g1_i1|m.20469	RL12_MOU	78.53	7.00E-93	Rpl12	60S riboso	Mus muscu	PF00298.1	GO:0003735^mo	Ribosome	.
TR3333|c0_g1	-12.18	4.52E-34	TR3333|c0_g1_i1	RL35A_POI	60.91	2.00E-42	RPL35A	60S riboso	Pongo abe	TR3333|c0_g1_i1|m.3145	RL35A_POI	60.91	8.00E-44	RPL35A	60S riboso	Pongo abe	PF01247.1	GO:0003735^mo	Ribosome	.
TR6066|c0_g2	-12.15	7.63E-35	TR6066|c0_g2_i1	RL4_DRON	61.26	7.00E-72	RpL4 RpL1	60S riboso	Drosophila	TR6066|c0_g2_i1|m.9297	RL4_UREC	62.43	7.00E-70	RPL4 RPL1	60S riboso	Urechis ca	PF00573.1	GO:0003735^mo	Ribosome	.
TR6146|c9_g1	-12.12	6.34E-32	TR6146|c9_g1_i1	LIPP_MOU	34.12	2.00E-35	Pnlip	Pancreatic	Mus muscu	TR6146|c9_g1_i1|m.11719	LIPP_MOU	33.59	8.00E-38	Pnlip	Pancreatic	Mus muscu	PF00151.1	.	.	.
TR6325|c5_g2	-12.08	1.93E-44	TR6325|c5_g2_i1	SERB_BOV	58.06	5.00E-91	PSPH	Phosphose	Bos taurus	TR6325|c5_g2_i1|m.17230	SERB_BOV	58.06	9.00E-95	PSPH	Phosphose	Bos taurus	PF00702.2	GO:0016791^mo	Biosynthesis of amino acids`Carbon metabolism`Gl	.
TR5862|c0_g1	-12.08	1.06E-32	TR5862|c0_g1_i1	CTRL_HUN	37.45	3.00E-36	CTRL CTRL	Chymotryp	Homo sapi	TR5862|c0_g1_i1|m.7307	TRYP_AST	34.01	1.00E-39	0	Trypsin-1 (	Astacus as	PF00089.2	GO:0004252^mo	.	.
TR5764|c0_g2	-12.07	2.43E-30	TR5764|c0_g2_i1	RL15_CHIT	81.15	8.00E-107	RpL15	60S riboso	Chironomu	TR5764|c0_g2_i1|m.6947	RL15_CHIT	81.15	4.00E-114	RpL15	60S riboso	Chironomu	PF00827.1	GO:0003735^mo	Ribosome	.
TR6054|c5_g1	-12.07	2.47E-31	TR6054|c5_g1_i1	CU12_HYA	50.6	4.00E-20	CP12	Flexible cu	Hyalophor	TR6054|c5_g1_i1|m.9039	CU12_HYA	49.41	3.00E-19	CP12	Flexible cu	Hyalophor	PF00379.1	GO:0042302^mo	.	.
TR6430|c28_g1	-12.01	1.10E-32	TR6430|c28_g1_i1	RL35_RAT	75.61	2.00E-56	Rpl35	60S riboso	Rattus nor	TR6430|c28_g1_i1|m.19225	RL35_RAT	75.61	1.00E-55	Rpl35	60S riboso	Rattus nor	PF00831.1	GO:0003735^mo	Ribosome	.
TR5893|c1_g1	-11.97	1.09E-38	TR5893|c1_g1_i1	Y3800_DR	50.3	1.00E-48	CG3800	CCHC-type	Drosophila	TR5893|c1_g1_i1|m.7381	Y3800_DR	50.89	4.00E-44	CG3800	CCHC-type	Drosophila	PF00098.1	GO:0003676^mo	.	.
TR6354|c5_g1	-11.96	1.18E-31	TR6354|c5_g1_i1	.			.	.	.	TR6354|c5_g1_i1|m.18173	.			.	.	.	PF06585.6	.	.	.
TR1279|c0_g1	-11.96	1.86E-33	TR1279|c0_g1_i1	RL23A_RAT	67.95	6.00E-65	Rpl23a	60S riboso	Rattus nor	TR1279|c0_g1_i1|m.1082	RL23A_RAT	73.81	3.00E-58	Rpl23a	60S riboso	Rattus nor	PF00276.1	GO:0003735^mo	Ribosome	.
TR6319|c0_g1	-11.94	4.45E-36	TR6319|c0_g1_i1	CATL_SARI	40.74	2.00E-19	0	Cathepsin	Sarcophag	TR6319|c0_g1_i1|m.16994	CATL_SARI	40.74	1.00E-18	0	Cathepsin	Sarcophag	PF08246.7	.	Apoptosis`Autophagy - animal`Lysosome`Phagosor	.
TR6086|c8_g1	-11.94	5.01E-33	TR6086|c8_g1_i1	COX3_SPO	58.39	1.00E-46	COIII	Cytochrom	Spodopter	TR6086|c8_g1_i1|m.9848	COX3_COT	60.34	3.00E-41	MT-CO3 C(	Cytochrom	Coturnix cc	PF00510.1	GO:0015002^mo	Oxidative phosphorylation	.
TR6303|c5_g1	-11.93	4.82E-107	TR6303|c5_g1_i3	CRPI_PERA	40.17	9.00E-131	0	Allergen Cr	Periplaneta	TR6303|c5_g1_i3|m.16477	CRPI_PERA	40	9.00E-131	0	Allergen Cr	Periplaneta	PF00372.1	.	.	.
TR6181|c3_g1	-11.86	4.90E-30	TR6181|c3_g1_i1	RL13A_CH	78.52	3.00E-84	RpL13A	60S riboso	Choristone	TR6181|c3_g1_i1|m.12669	RL13A_CH	77.48	4.00E-83	RpL13A	60S riboso	Choristone	PF00572.1	GO:0003735^mo	Ribosome	.
TR5545|c0_g2	-11.86	5.29E-31	TR5545|c0_g2_i1	RS6_MANS	84.12	2.00E-128	RpS6	40S riboso	Manduca s	TR5545|c0_g2_i1|m.6308	RS6_MANS	84.86	4.00E-145	RpS6	40S riboso	Manduca s	PF01092.1	GO:0003735^mo	mTOR signaling pathway`Ribosome	.
TR6199|c10_g2	-11.85	8.58E-30	TR6199|c10_g2_i1	RL9_SPOFI	80.42	1.00E-104	RpL9	60S riboso	Spodopter	TR6199|c10_g2_i1|m.13197	RL9_SPOFI	80.42	6.00E-110	RpL9	60S riboso	Spodopter	PF00347.1	GO:0003735^mo	Ribosome	.
TR2590|c0_g1	-11.83	1.17E-26	TR2590|c0_g1_i1	RL36_DROI	73.04	9.00E-50	RpL36 M(1	60S riboso	Drosophila	TR2590|c0_g1_i1|m.2290	RL36_DROI	73.04	2.00E-49	RpL36 M(1	60S riboso	Drosophila	PF01158.1	GO:0003735^mo	Ribosome	.
TR396|c0_g1	-11.83	1.18E-31	TR396|c0_g1_i1	RL6_PIG^^	48.12	2.00E-69	RPL6	60S riboso	Sus scrofa	TR396|c0_g1_i1|m.372	RL6_PIG^^	48.95	4.00E-66	RPL6	60S riboso	Sus scrofa	PF01159.1	GO:0003735^mo	Ribosome	.
TR2173|c0_g1	-11.77	5.26E-25	TR2173|c0_g1_i1	RL371_DR	90.22	6.00E-47	RpL37a CG	Probable 6	Drosophila	TR2173|c0_g1_i1|m.1915	RL371_DR	90.22	3.00E-54	RpL37a CG	Probable 6	Drosophila	PF01907.1	GO:0003735^mo	Ribosome	.
TR8337|c0_g1	-11.75	5.40E-30	TR8337|c0_g1_i1	RL21_HUN	66.25	9.00E-72	RPL21	60S riboso	Homo sapi	TR8337|c0_g1_i1|m.20590	RL21_HUN	66.25	2.00E-71	RPL21	60S riboso	Homo sapi	PF01157.1	GO:0003735^mo	Ribosome	.
TR3235|c0_g1	-11.75	2.05E-28	TR3235|c0_g1_i1	PUR6_DRC	71.23	0	ade5 CG39	Multifunct	Drosophila	TR3235|c0_g1_i1|m.3070	PUR6_DRC	71.23	0	ade5 CG39	Multifunct	Drosophila	PF00731.1	GO:0006189^biol	Purine metabolism	.
TR2045|c0_g1	-11.72	7.11E-32	TR2045|c0_g1_i1	GST1_BLA(	55.5	4.00E-68	0	Glutathion	Blattella ge	TR2045|c0_g1_i1|m.1772	GST1_BLA(	55.5	3.00E-68	0	Glutathion	Blattella ge	PF00043.2	GO:0005515^mo	Arachidonic acid metabolism`Drug metabolism - cy	.
TR5976|c1_g2	-11.68	1.41E-27	TR5976|c1_g2_i1	IF4A2_RAT	76.41	5.00E-156	Eif4a2	Eukaryotic	Rattus nor	TR5976|c1_g2_i1|m.8068	IF4A1_MA(	76.14	4.00E-164	EIF4A1 Qts	Eukaryotic	Macaca fas	PF00270.2	GO:0003676^mo	RNA transport	.
TR4753|c0_g1	-11.64	2.65E-25	TR4753|c0_g1_i1	RL40_DROI	96.88	5.00E-87	RpL40 Ubi-	Ubiquitin-€	Drosophila	TR4753|c0_g1_i1|m.4818	RL40_DROI	96.88	1.00E-87	RpL40 Ubi-	Ubiquitin-€	Drosophila	PF00240.1	GO:0005515^mo	Ribosome	.
TR2041|c0_g1	-11.63	1.76E-26	TR2041|c0_g1_i1	RL34_AED	73.95	2.00E-55	RpL34 RpL	60S riboso	Aedes albo	TR2041|c0_g1_i1|m.1769	RL34_AED	73.95	3.00E-54	RpL34 RpL	60S riboso	Aedes albo	PF01199.1	GO:0003735^mo	Ribosome	.
TR5916|c0_g1	-11.58	2.54E-33	TR5916|c0_g1_i1	AK1A1_XEI	42.86	5.00E-76	akr1a1 TEg	Alcohol de	Xenopus tr	TR5916|c0_g1_i1|m.7470	AK1A1_MC	44.07	8.00E-81	Akr1a1 Akr	Alcohol de	Mus muscu	PF00248.1	.	.	.
TR616|c0_g1	-11.58	1.81E-24	TR616|c0_g1_i1	RS16_DRO	86.99	1.00E-90	RpS16 CG4	40S riboso	Drosophila	TR616|c0_g1_i1|m.543	RS16_DRO	86.99	5.00E-91	RpS16 CG4	40S riboso	Drosophila	PF00380.1	GO:0003735^mo	Ribosome	.
TR5332|c0_g2	-11.58	2.12E-29	TR5332|c0_g2_i1	RL32_APIN	85.82	2.00E-80	RpL32 rp49	60S riboso	Apis mellif	TR5332|c0_g2_i1|m.5858	RL32_APIN	85.82	6.00E-82	RpL32 rp49	60S riboso	Apis mellif	PF01655.1	GO:0003735^mo	Ribosome	.
TR6131|c6_g1	-11.57	8.11E-29	TR6131|c6_g1_i1	RS19A_DR	66.41	1.00E-51	RpS19a Rp	40S riboso	Drosophila	TR6131|c6_g1_i1|m.11042	RS19A_DR	61.04	3.00E-62	RpS19a Rp	40S riboso	Drosophila	PF01090.1	GO:0003735^mo	Ribosome	.
TR6259|c12_g1	-11.55	7.57E-28	TR6259|c12_g1_i1	ATPG_DRC	73.17	3.00E-138	ATPsyngan	ATP syntha	Drosophila	TR6259|c12_g1_i1|m.15207	ATPG_DRC	73.17	1.00E-149	ATPsyngan	ATP syntha	Drosophila	PF00231.1	GO:0046933^mo	Oxidative phosphorylation	.
TR6066|c0_g1	-11.54	9.07E-29	TR6066|c0_g1_i1	RL4_DRON	74.11	1.00E-98	RpL4 RpL1	60S riboso	Drosophila	TR6066|c0_g1_i1|m.9296	RL4_DRON	74.11	7.00E-101	RpL4 RpL1	60S riboso	Drosophila	PF00573.1	GO:0003735^mo	Ribosome	.
TR6224|c4_g2	-11.53	4.14E-28	TR6224|c4_g2_i1	RL23_AED	94.92	4.00E-77	RpL23-A Rp	60S riboso	Aedes aegy	TR6224|c4_g2_i1|m.14021	RL23_DROI	95.28	6.00E-84	RpL23 RpL	60S riboso	Drosophila	PF00238.1	GO:0003735^mo	Ribosome	.
TR6208|c4_g1	-11.47	1.38E-50	TR6208|c4_g1_i1	RS4_CARG	88.42	1.00E-169	RpS4	40S riboso	Carabus gr	TR6208|c4_g1_i1|m.13468	RS4_CARG	88.08	3.00E-172	RpS4	40S riboso	Carabus gr	PF00467.2	GO:0003723^mo	Ribosome	.
TR6164|c8_g1	-11.43	3.74E-29	TR6164|c8_g1_i1	HSP70_ON	90.49	2.00E-145	0	Heat shock	Onchocerc	TR6164|c8_g1_i1|m.12220	HSP70_ON	90.49	3.00E-176	0	Heat shock	Onchocerc	PF00012.1	.	Endocytosis`Longevity regulating pathway - multipl	.
TR1535|c0_g1	-11.43	5.69E-25	TR1535|c0_g1_i1	RL26_LITLI	75.51	1.00E-72	RPL26	60S riboso	Littorina lit	TR1535|c0_g1_i1|m.1295	RL26_LITLI	75.51	1.00E-75	RPL26	60S riboso	Littorina lit	PF00467.2	.	Ribosome	.
TR5984|c0_g1	-11.43	2.21E-28	TR5984|c0_g1_i1	CYC_SAMC	86.92	1.00E-62	0	Cytochrom	Samia cynt	TR5984|c0_g1_i1|m.8117	CYC_SAMC	87.04	2.00E-64	0	Cytochrom	Samia cynt	PF00034.1	GO:0009055^mo	Apoptosis`Apoptosis - fly`Apoptosis - multiple spec	.
TR5863|c1_g1	-11.42	7.42E-30	TR5863|c1_g1_i1	DDX17_DR	64.21	0	Rm62 Dmp	ATP-deper	Drosophila	TR5863|c1_g1_i1|m.7308	DDX17_DR	67.13	0	Rm62 Dmp	ATP-deper	Drosophila	PF00270.2	GO:0003676^mo	Spliceosome	.
TR6020|c0_g3	-11.40	2.72E-28	TR6020|c0_g3_i1	RS18_SPOI	93.33	4.00E-88	RpS18	40S riboso	Spodopter	TR6020|c0_g3_i1|m.8359	RS18_SPOI	94.08	5.00E-103	RpS18	40S riboso	Spodopter	PF00416.1	GO:0003723^mo	Ribosome	.
TR6435|c5_g2	-11.34	2.12E-96	TR6435|c5_g2_i2	CRPI_PERA	36.35	8.00E-135	0	Allergen Cr	Periplaneta	TR6435|c5_g2_i4|m.19238	HEXA_BLA	34.8	7.00E-134	0	Hexamerin	Blaberus d	PF00372.1	.	.	.
TR6355|c4_g1	-11.31	2.58E-27	TR6355|c4_g1_i1	ATPA_DRC	80.95	5.00E-72	blw ATPSY	ATP syntha	Drosophila	TR6355|c4_g1_i1|m.18205	ATPA_DRC	80.95	2.00E-79	blw ATPSY	ATP syntha	Drosophila	PF00306.2	GO:0016820^mo	Oxidative phosphorylation	.
TR5786|c0_g1	-11.29	5.26E-29	TR5786|c0_g1_i1	EF1G_ART	82.1	1.00E-98	0	Elongation	Artemia sa	TR5786|c0_g1_i1|m.7008	EF1G_ART	71.3	5.00E-103	0	Elongation	Artemia sa	PF00647.1	GO:0003746^mo	.	.
TR4704|c0_g1	-11.27	1.38E-50	TR4704|c0_g1_i1	RL10_BOM	88.13	2.00E-134	RpL10	60S riboso	Bombyx m	TR4704|c0_g1_i1|m.4730	RL10_BOM	88.13	1.00E-142	RpL10	60S riboso	Bombyx m	PF00252.1	GO:0003735^mo	Ribosome	.
TR4745|c0_g1	-11.25	5.57E-15	TR4745|c0_g1_i1	CUO6_BLA	45.21	3.00E-12	0	Cuticle pro	Blaberus cr	TR4745|c0_g1_i1|m.4805	CUO7_BLA	35.8	4.00E-14	0	Cuticle pro	Blaberus cr	PF00379.1	GO:0042302^mo	.	.
TR6105|c0_g1	-11.22	1.78E-25	TR6105|c0_g1_i1	RL27A_MA	75	6.00E-53	RPL27A Qt	60S riboso	Macaca fas	TR6105|c0_g1_i1|m.10256	RL27A_BO	75	1.00E-53	RPL27A	60S riboso	Bos taurus	PF00828.1	.	Ribosome	.
TR6497|c0_g1	-11.22	1.13E-26	TR6497|c0_g1_i1	RL17_PHLF	84.24	2.00E-100	RpL17	60S riboso	Phlebotom	TR6497|c0_g1_i1|m.19550	RL17_PHLF	83.7	3.00E-108	RpL17	60S riboso	Phlebotom	PF00237.1	GO:0003735^mo	Ribosome	.
TR6097|c7_g1	-11.15	2.39E-22	TR6097|c7_g1_i1	.			.	.	.	TR6097|c7_g1_i1|m.10163	.			.	.	.	PF00050.1	GO:0005515^mo	.	.
TR5786|c0_g2	-11.13	1.62E-28	TR5786|c0_g2_i1	EF1G_ART	74.54	1.00E-112	0	Elongation	Artemia sa	TR5786|c0_g2_i1|m.7010	EF1G_ART	74.54	2.00E-117	0	Elongation	Artemia sa	PF00043.2	GO:0005515^mo	.	.
TR396|c0_g2	-11.10	3.88E-26	TR396|c0_g2_i1	RL6_PIG^^	51.18	6.00E-66	RPL6	60S riboso	Sus scrofa	TR396|c0_g2_i1|m.373	RL6_PIG^^	52.74	2.00E-64	RPL6	60S riboso	Sus scrofa	PF01159.1	GO:0003735^mo	Ribosome	.
TR4646|c0_g1	-11.10	5.65E-24	TR4646|c0_g1_i1	RS23_SPOI	94.95	1.00E-66	RpS23	40S riboso	Spodopter	TR4646|c0_g1_i1|m.4644	RS23_DRO	96.97	4.00E-66	RpS23 CG8	40S riboso	Drosophila	PF00164.2	GO:0003735^mo	Ribosome	.
TR5430|c0_g2	-11.09	4.53E-25	TR5430|c0_g2_i1	EF1B2_BOI	69.83	3.00E-96	0	Elongation	Bombyx m	TR5430|c0_g2_i1|m.6033	EF1B2_BOI	70.26	6.00E-94	0	Elongation	Bombyx m	PF00736.1	GO:0003746^mo	.	.
TR5545|c0_g1	-11.09	1.98E-25	TR5545|c0_g1_i1	RS6_MANS	83.69	8.00E-129	RpS6	40S riboso	Manduca s	TR5545|c0_g1_i1|m.6307	RS6_MANS	84.46	1.00E-145	RpS6	40S riboso	Manduca s	PF01092.1	GO:0003735^mo	mTOR signaling pathway`Ribosome	.
TR3233|c0_g1	-11.08	4.72E-23	TR3233|c0_g1_i1	DERP3_DE	35.27	2.00E-39	DERP3	Mite allerg	Dermatopl	TR3233|c0_g1_i1|m.3066	DERP3_DE	35.27	2.00E-39	DERP3	Mite allerg	Dermatopl	PF00089.2	GO:0004252^mo	.	.
TR4702|c0_g1	-11.02	2.77E-26	TR4702|c0_g1_i1	BT3L4_XEN	72.5	2.00E-55	btf3l4 TNe	Transcripti	Xenopus tr	TR4702|c0_g1_i1|m.4726	BT3L4_XEN	73.12	9.00E-70	btf3l4 TNe	Transcripti	Xenopus tr	PF01849.1	.	Apoptosis - fly	.
TR5894|c1_g1	-10.95	1.56E-26	TR5894|c1_g1_i1	TKTL2_MO	66.67	1.00E-132	Tktl2	Transketol	Mus muscu	TR5894|c1_g1_i1|m.7387	TKTL2_MO	66.67	3.00E-138	Tktl2	Transketol	Mus muscu	PF02779.1	GO:0003824^mo	Biosynthesis of amino acids`Carbon metabolism`Pe	.
TR6286|c7_g1	-10.94	3.42E-21	TR6286|c7_g1_i1	RS12_PIG^	81.4	2.00E-43	RPS12	40S riboso	Sus scrofa	TR6286|c7_g1_i1|m.15902	RS12_PIG^	81.4	6.00E-43	RPS12	40S riboso	Sus scrofa	PF01248.2	.	Ribosome	.
TR5958|c0_g2	-10.91	1.07E-73	TR5958|c0_g2_i1	TCTP_BOM	79.07	8.00E-96	Tctp	Translatior	Bombyx m	TR5958|c0_g2_i1|m.7795	TCTP_BOM	79.07	7.00E-97	Tctp	Translatior	Bombyx m	PF00838.1	.	.	.
TR1535|c0_g2	-10.85	8.64E-22	TR1535|c0_g2_i1	RL26_LITLI	75.51	9.00E-73	RPL26	60S riboso	Littorina lit	TR1535|c0_g2_i1|m.1296	RL26_LITLI	75.51	3.00E-75	RPL26	60S riboso	Littorina lit	PF00467.2	.	Ribosome	.
TR6008|c0_g2	-10.84	3.58E-26	TR6008|c0_g2_i1	ALF_DRON	84.95	5.00E-166	Ald CG605	Fructose-b	Drosophila	TR6008|c0_g2_i1|m.8297	ALF_DRON	84.95	1.00E-173	Ald CG605	Fructose-b	Drosophila	PF00274.1	GO:0004332^mo	Biosynthesis of amino acids`Carbon metabolism`Fr	.
TR5921|c0_g1	-10.81	4.51E-23	TR5921|c0_g1_i1	YPF05_PLA	21.6	1.00E-08	PF11_0207	Uncharact	Plasmodiu	TR5921|c0_g1_i1|m.7485	.			.	.	.	PF01442.1	GO:0008289^mo	.	.
TR629|c0_g1	-10.80	5.35E-25	TR629|c0_g1_i1	CATL_SARI	55.21	2.00E-118	0	Cathepsin	Sarcophag	TR629|c0_g1_i1|m.554	CATL_SARI	55.21	2.00E-118	0	Cathepsin	Sarcophag	PF00112.1	GO:0008234^mo	Apoptosis`Autophagy - animal`Lysosome`Phagosor	.
TR6001|c0_g1	-10.79	8.97E-24	TR6001|c0_g1_i1	.			.	.	.	TR6001|c0_g1_i1|m.8273	.			.	.	.	PF06585.6	.	.	.
TR5891|c0_g1	-10.79	8.41E-43	TR5891|c0_g1_i1	ASPP_AED	59.67	2.00E-152	AAEL0061€	Lysosomal	Aedes aegy	TR5891|c0_g1_i1|m.7377	ASPP_AED	58.9	3.00E-169	AAEL0061€	Lysosomal	Aedes aegy	PF00026.1	GO:0004190^mo	Apoptosis`Autophagy - animal`Lysosome`Sphingoli	.
TR7509|c0_g1	-10.78	3.66E-24	TR7509|c0_g1_i1	DHSO_BOV	56.57	2.00E-137	SORD	Sorbitol de	Bos taurus	TR7509|c0_g1_i1|m.20079	DHSO_BOV	56.94	9.00E-140	SORD	Sorbitol de	Bos taurus	PF00107.2	GO:0016491^mo	Fructose and mannose metabolism`Pentose and gl	.
TR4779|c0_g2	-10.77	6.13E-22	TR4779|c0_g2_i1	TRY1_ANO	40.43	6.00E-51	TRYP1 AGA	Trypsin-1 (	Anopheles	TR4779|c0_g2_i1|m.4874	TRY4_ANO	38.55	6.00E-52	TRYP4 AGA	Trypsin-4 (	Anopheles	PF00089.2	GO:0004252^mo	Neuroactive ligand-receptor interaction	.
TR7829|c0_g1	-10.76	1.14E-20	TR7829|c0_g1_i1	ATP5L_POI	47.83	1.00E-21	ATP5L	ATP syntha	Pongo abe	TR7829|c0_g1_i1|m.20281	ATP5L_POI	47.83	3.00E-22	ATP5L	ATP syntha	Pongo abe	PF04718.1	GO:0015078^mo	Oxidative phosphorylation	.
TR1462|c0_g1	-10.71	1.30E-21	TR1462|c0_g1_i1	.			.	.	.	TR1462|c0_g1_i1|m.1229	.			.	.	.	PF02937.1	GO:0004129^mo	.	.
TR6346|c4_g1	-10.70	6.28E-23	TR6346|c4_g1_i1	NACA_DRC	65.47	4.00E-64	Nacalpha a	Nascent pc	Drosophila	TR6346|c4_g1_i1|m.18024	NACA_DRC	65.92	7.00E-75	Nacalpha a	Nascent pc	Drosophila	PF01849.1	.	.	.
TR6329|c5_g2	-10.69	9.79E-28	TR6329|c5_g2_i1	SAHHA_XE	83.73	0	ahcy-a ahc	Adenosylh	Xenopus la	TR6329|c5_g2_i1|m.17361	SAHHA_XE	83.73	0	ahcy-a ahc	Adenosylh	Xenopus la	PF00670.1	GO:0004013^mo	Cysteine and methionine metabolism	.
TR5670|c0_g1	-10.67	1.17E-25	TR5670|c0_g1_i1	NP1L1_HU	64.18	1.00E-66	NAP1L1 NF	Nucleosom	Homo sapi	TR5670|c0_g1_i1|m.6683	NP1L4_HU	66	6.00E-81	NAP1L4 NA	Nucleosom	Homo sapi	PF00956.1	GO:0006334^biol	.	.
TR2247|c0_g1	-10.66	9.43E-21	TR2247|c0_g1_i1	.			.	.	.	TR2247|c0_g1_i1|m.1984	.			.	.	.	PF05680.7	GO:0015078^mo	Oxidative phosphorylation	.
TR6142|c0_g1	-10.64	7.91E-36	TR6142|c0_g1_i1	RS11_XENI	80.69	2.00E-77	rps11	40S riboso	Xenopus la	TR6142|c0_g1_i1|m.11531	RS11_RAT	78.48	1.00E-85	Rps11	40S riboso	Rattus nor	PF00366.1	GO:0003735^mo	Ribosome	.
TR7805|c0_g1	-10.61	2.97E-38	TR7805|c0_g1_i1	RL17_PHLF	82.53	1.00E-99	RpL17	60S riboso	Phlebotom	TR7805|c0_g1_i1|m.20272	RL17_PHLF	81.52	7.00E-104	RpL17	60S riboso	Phlebotom	PF00237.1	GO:0003735^mo	Ribosome	.
TR5742|c0_g2	-10.60	2.13E-38	TR5742|c0_g2_i1	SERB_BOV	56.95	6.00E-88	PSPH	Phosphose	Bos taurus	TR5742|c0_g2_i1|m.6841	SERB_BOV	56.95	2.00E-95	PSPH	Phosphose	Bos taurus	PF00702.2	GO:0016791^mo	Biosynthesis of amino acids`Carbon metabolism`Gl	.
TR1542|c0_g1	-10.60	4.66E-42	TR1542|c0_g1_i1	NDKA_DRC	79.73	5.00E-84	awd	Nucleoside	Drosophila	TR1542|c0_g1_i1|m.1303	NDKA_DRC	77.78	2.00E-86	awd K-pn (	Nucleoside	Drosophila	PF00334.1	GO:0004550^mo	Purine metabolism`Pyrimidine metabolism	.
TR8561|c0_g1	-10.55	2.59E-20	TR8561|c0_g1_i1	DFP11_HYI	37.06	1.00E-24	0	Putative de	Hyphantria	TR8561|c0_g1_i1|m.20699	DFP_MANS	38.89	2.00E-23	0	Putative de	Manduca s	PF02014.1	.	.	.
TR5949|c25_g1	-10.54	5.07E-20	TR5949|c25_g1_i1	MPCP_BOV	69.38	1.00E-147	SLC25A3 P	Phosphate	Bos taurus	TR5949|c25_g1_i1|m.7636	MPCP_MO	68.44	5.00E-159	Slc25a3	Phosphate	Mus muscu	PF00153.2	.	.	.
TR5923|c0_g1	-10.54	1.54E-35	TR5923|c0_g1_i1	.			.	.	.	TR5923|c0_g1_i1|m.7487	.			.	.	.	.	.	.	.
TR4354|c0_g1	-10.53	2.86E-20	TR4354|c0_g1_i1	TRY7_ANO	41.88	3.00E-42	TRYP7 AGA	Trypsin-7 (	Anopheles	TR4354|c0_g1_i1|m.4241	TRY7_ANO	41.88	1.00E-58	TRYP7 AGA	Trypsin-7 (	Anopheles	PF00089.2	GO:0004252^mo	Neuroactive ligand-receptor interaction	.
TR6139|c12_g1	-10.52	4.76E-35	TR6139|c12_g1_i1	RL18A_SP(	72.88	7.00E-84	RpL18A	60S riboso	Spodopter	TR6139|c12_g1_i1|m.11379	RL18A_SP(	72.88	2.00E-93	RpL18A	60S riboso	Spodopter	PF01775.1	GO:0003735^mo	Ribosome	.
TR8923|c0_g1	-10.52	1.80E-22	TR8923|c0_g1_i1	ALDR_RAB	60.13	4.00E-130	AKR1B1	Aldose red	Oryctolagu	TR8923|c0_g1_i1|m.20921	ALDR_RAB	60.13	2.00E-122	AKR1B1	Aldose red	Oryctolagu	PF00248.1	.	Fructose and mannose metabolism`Galactose met	.
TR7229|c0_g1	-10.51	1.72E-23	TR7229|c0_g1_i1	CD53_MOU	39.37	1.00E-21	Cd53	Leukocyte	Mus muscu	TR7229|c0_g1_i1|m.19967	CD53_RAT	37.04	1.00E-26	Cd53 Ox-4	Leukocyte	Rattus nor	PF00335.1	GO:0016021^cell	Lysosome	.
TR955|c0_g1	-10.46	8.87E-24	TR955|c0_g1_i1	COX5B_BO	44.19	8.00E-19	COX5B	Cytochrom	Bos taurus	TR955|c0_g1_i1|m.800	COX5B_BO	41.18	2.00E-20	COX5B	Cytochrom	Bos taurus	PF01215.1	GO:0004129^mo	Oxidative phosphorylation	.
TR1313|c0_g1	-10.44	8.86E-24	TR1313|c0_g1_i1	RL21_HUN	61.88	6.00E-69	RPL21	60S riboso	Homo sapi	TR1313|c0_g1_i1|m.1110	RL21_HUN	61.88	2.00E-67	RPL21	60S riboso	Homo sapi	PF01157.1	GO:0003735^mo	Ribosome	.
TR407|c0_g1	-10.43	1.53E-34	TR407|c0_g1_i1	RL14_DRO	45.65	2.00E-41	RpL14 GJ1	60S riboso	Drosophila	TR407|c0_g1_i1|m.381	RL14_DRO	44.65	6.00E-45	RpL14 GJ1	60S riboso	Drosophila	PF01929.1	GO:0003735^mo	Ribosome	.
TR6044|c31_g1	-10.40	2.57E-20	TR6044|c31_g1_i1	RS5_HUMA	85.11	1.00E-50	RPS5	40S riboso	Homo sapi	TR6044|c31_g1_i1|m.8785	RS5_HUMA	85.11	8.00E-54	RPS5	40S riboso	Homo sapi	PF00177.1	.	Ribosome	.
TR807|c0_g1	-10.38	1.33E-19	TR807|c0_g1_i1	THIO2_DR	62.75	2.00E-38	Trx-2	Thioredoxi	Drosophila	TR807|c0_g1_i1|m.703	THIO2_DR	62.75	9.00E-41	Trx-2	Thioredoxi	Drosophila	PF00085.1	GO:0045454^biol	.	.
TR6123|c30_g1	-10.37	1.89E-22	TR6123|c30_g1_i1	MDHM_HU	69.49	6.00E-111	MDH2	Malate del	Homo sapi	TR6123|c30_g1_i1|m.10766	MDHM_HU	69.49	3.00E-116	MDH2	Malate del	Homo sapi	PF00056.1	GO:0016491^mo	Carbon metabolism`Citrate cycle (TCA cycle)`Cystei	.
TR5752|c0_g3	-10.36	6.47E-23	TR5752|c0_g3_i1	EF1D_XEN	49.81	9.00E-69	eef1d	Elongation	Xenopus la	TR5752|c0_g3_i1|m.6900	EF1D_XEN	50	2.00E-79	eef1d	Elongation	Xenopus la	PF00736.1	GO:0003746^mo	.	.
TR6003|c1_g1	-10.36	5.90E-33	TR6003|c1_g1_i1	APOD_HUI	33.51	7.00E-26	APOD	Apolipoprc	Homo sapi	TR6003|c1_g1_i1|m.8283	APOD_MO	34.03	7.00E-27	Apod	Apolipoprc	Mus muscu	PF00061.1	.	.	.
TR4967|c0_g1	-10.33	3.10E-21	TR4967|c0_g1_i1	OB10_DRC	40.58	6.00E-12	a10 OS-D (	Putative oc	Drosophila	TR4967|c0_g1_i1|m.5245	OB10_DRC	40.58	4.00E-12	a10 OS-D (	Putative oc	Drosophila	PF03392.8	.	.	.
TR3464|c0_g2	-10.32	1.06E-13	TR3464|c0_g2_i1	PTGR1_BO	56.74	1.00E-59	PTGR1 LTB	Prostaglan	Bos taurus	TR3464|c0_g2_i1|m.3265	PTGR1_BO	56.74	3.00E-62	PTGR1 LTB	Prostaglan	Bos taurus	PF00107.2	GO:0008270^mo	.	.
TR661|c0_g2	-10.30	3.07E-20	TR661|c0_g2_i1	ATPK_DRC	64.42	2.00E-48	CG4692	Putative A	Drosophila	TR661|c0_g2_i1|m.588	ATPK_DRO	63.81	6.00E-45	CG4692	Putative A	Drosophila	PF10206.4	.	Oxidative phosphorylation	.
TR5864|c0_g1	-10.29	4.88E-48	TR5864|c0_g1_i1	RL7_DRON	69.42	3.00E-112	RpL7 CG48	60S riboso	Drosophila	TR5864|c0_g1_i1|m.7310	RL7_DRON	69.42	1.00E-119	RpL7 CG48	60S riboso	Drosophila	PF00327.1	.	Ribosome	.
TR853|c0_g1	-10.28	5.57E-21	TR853|c0_g1_i1	GSTT1_LU(	39.47	7.00E-29	GST1	Glutathion	Lucilia cup	TR853|c0_g1_i1|m.738	GST1D_AN	39.8	3.00E-45	GstD1 GST	Glutathion	Anopheles	PF00043.2	GO:0005515^mo	Drug metabolism - cytochrome P450`Glutathione n	.
TR2455|c0_g1	-10.26	1.09E-21	TR2455|c0_g1_i1	FRIL_XENL	29.09	6.00E-13	0	Ferritin ligl	Xenopus la	TR2455|c0_g1_i1|m.2190	FRIL_XENL	29.38	2.00E-13	0	Ferritin ligl	Xenopus la	PF00210.1	GO:0008199^mo	.	.
TR4390|c0_g1	-10.20	4.56E-23	TR4390|c0_g1_i1	ATP5H_DR	34.76	2.00E-23	ATPsynD A	ATP syntha	Drosophila	TR4390|c0_g1_i1|m.4282	ATP5H_DR	34.76	2.00E-21	ATPsynD A	ATP syntha	Drosophila	PF05873.7	GO:0015078^mo	Oxidative phosphorylation	.
TR6261|c2_g1	-10.19	3.00E-17	TR6261|c2_g1_i1	LIPH_RABI	34.7	4.00E-34	LIPH	Lipase mer	Oryctolagu	TR6261|c2_g1_i1|m.15239	LIPH_RABI	34.78	6.00E-37	LIPH	Lipase mer	Oryctolagu	PF00151.1	.	.	.
TR5863|c1_g2	-10.17	2.11E-20	TR5863|c1_g2_i1	DDX17_DR	69.67	0	Rm62 Dmp	ATP-deper	Drosophila	TR5863|c1_g2_i1|m.7309	DDX17_DR	69.67	0	Rm62 Dmp	ATP-deper	Drosophila	PF00270.2	GO:0003676^mo	Spliceosome	.
TR4261|c1_g1	-10.16	1.19E-20	TR4261|c1_g1_i1	METK_DRC	76.27	3.00E-116	Sam-S M(2	S-adenosyl	Drosophila	TR4261|c1_g1_i1|m.4147	METK_DRC	76.27	1.00E-117	Sam-S M(2	S-adenosyl	Drosophila	PF02772.1	GO:0004478^mo	Biosynthesis of amino acids`Cysteine and methioni	.
TR6171|c1_g2	-10.13	4.35E-23	TR6171|c1_g2_i1	IF5A_SPOF	92.5	5.00E-105	eIF-5A eIF5	Eukaryotic	Spodopter	TR6171|c1_g2_i1|m.12452	IF5A_SPOF	92.5	5.00E-108	eIF-5A eIF5	Eukaryotic	Spodopter	PF01287.1	GO:0003723^mo	.	.
TR6001|c1_g1	-10.13	1.93E-19	TR6001|c1_g1_i1	.			.	.	.	TR6001|c1_g1_i1|m.8275	.			.	.	.	PF06585.6	.	.	.
TR6317|c4_g1	-10.12	4.64E-22	TR6317|c4_g1_i1	METK_DRC	78.71	2.00E-130	Sam-S M(2	S-adenosyl	Drosophila	TR6317|c4_g1_i1|m.16945	METK_DRC	78.71	4.00E-131	Sam-S M(2	S-adenosyl	Drosophila	PF02772.1	GO:0004478^mo	Biosynthesis of amino acids`Cysteine and methioni	.
TR6442|c16_g2	-10.12	4.97E-31	TR6442|c16_g2_i1	AMYA_DR(	61.49	0	Amy-d; Am	Alpha-amy	Drosophila	TR6442|c16_g2_i1|m.19442	AMYA_DR(	60.29	0	Amy-d; Am	Alpha-amy	Drosophila	PF00128.1	GO:0003824^mo	Starch and sucrose metabolism	.
TR8093|c0_g1	-10.12	2.97E-19	TR8093|c0_g1_i1	REEP5_BO	57.14	2.00E-53	REEP5	Receptor e	Bos taurus	TR8093|c0_g1_i1|m.20429	REEP5_RA	49.4	7.00E-54	Reep5 Dp1	Receptor e	Rattus nor	PF03134.1	.	.	.
TR7692|c0_g1	-10.12	7.82E-15	TR7692|c0_g1_i1	PEB3_DRO	42.35	1.00E-21	EbpIII PebI	Ejaculatory	Drosophila	TR7692|c0_g1_i1|m.20214	PEB3_DRO	43.37	3.00E-20	EbpIII PebI	Ejaculatory	Drosophila	PF03392.8	.	.	.
TR6315|c7_g1	-10.12	1.96E-29	TR6315|c7_g1_i1	AMYB_DR(	61.3	0	Amy-d Am	Alpha-amy	Drosophila	TR6315|c7_g1_i1|m.16862	AMYB_DR(	62.19	0	Amy-d Am	Alpha-amy	Drosophila	PF00128.1	GO:0003824^mo	Starch and sucrose metabolism	.
TR8715|c0_g1	-10.11	5.00E-19	TR8715|c0_g1_i1	GST_MUSD	40.1	4.00E-45	0	Glutathion	Musca don	TR8715|c0_g1_i1|m.20819	HPGDS_CH	40.69	3.00E-48	HPGDS GS	Hematopo	Gallus gallu	PF00043.2	GO:0005515^mo	Arachidonic acid metabolism`Drug metabolism - cy	.
TR5225|c0_g1	-10.11	1.90E-16	TR5225|c0_g1_i1	AT5F1_DR(	48.21	2.00E-26	ATPsynB A	ATP syntha	Drosophila	TR5225|c0_g1_i1|m.5668	AT5F1_DR(	48.21	1.00E-25	ATPsynB A	ATP syntha	Drosophila	PF05405.9	GO:0015078^mo	Oxidative phosphorylation	.
TR8775|c0_g1	-10.11	4.84E-18	TR8775|c0_g1_i1	COX6A_ON	39.25	1.00E-17	0	Cytochrom	Oncorhync	TR8775|c0_g1_i1|m.20863	COX6A_ON	40	2.00E-17	0	Cytochrom	Oncorhync	PF02046.1	GO:0004129^mo	Oxidative phosphorylation	.
TR5225|c0_g2	-10.11	2.92E-18	TR5225|c0_g2_i1	AT5F1_DR(	52.13	3.00E-29	ATPsynB A	ATP syntha	Drosophila	TR5225|c0_g2_i1|m.5669	AT5F1_DR(	53	4.00E-31	ATPsynB A	ATP syntha	Drosophila	PF05405.9	GO:0015078^mo	Oxidative phosphorylation	.
TR5739|c0_g1	-10.09	2.63E-18	TR5739|c0_g1_i1	GNMT_RA	51.9	6.00E-78	Gnmt	Glycine N-r	Rattus nor	TR5739|c0_g1_i1|m.6831	GNMT_RA	51.9	2.00E-81	Gnmt	Glycine N-r	Rattus nor	PF08241.7	GO:0008168^mo	Glycine, serine and threonine metabolism	.
TR5994|c0_g3	-10.08	2.25E-20	TR5994|c0_g3_i1	CRYL1_RAE	50.69	3.00E-44	CRYL1 GUL	Lambda-cr	Oryctolagu	TR5994|c0_g3_i1|m.8237	CRYL1_POI	50.96	3.00E-49	CRYL1	Lambda-cr	Pongo abe	PF02737.1	GO:0004616^mo	Pentose and glucuronate interconversions	.
TR5752|c0_g1	-10.07	7.68E-20	TR5752|c0_g1_i1	EF1D_XEN	54.21	2.00E-62	eef1d	Elongation	Xenopus la	TR5752|c0_g1_i1|m.6898	EF1D_XEN	54.67	3.00E-74	eef1d	Elongation	Xenopus la	PF00736.1	GO:0003746^mo	.	.

TR6096|c5_g1	-10.05	3.46E-19	TR6096|c5_g1_i1	MDHC_CH	74.24	1.00E-98	MDH1 RCJI	Malate del	Gallus gallu	TR6096|c5_g1_i1|m.10136	MDHC_HU	73.74	1.00E-102	MDH1 MD	Malate del	Homo sapi	PF00056.1	GO:0016491^mo	Carbon metabolism`Citrate cycle (TCA cycle)`Cystei	.
TR8989|c0_g1	-10.04	5.35E-18	TR8989|c0_g1_i1	.			.	.	.	TR8989|c0_g1_i1|m.20942	.			.	.	.	PF02178.1	GO:0003677^mo	.	.
TR6226|c7_g1	-10.03	6.85E-19	TR6226|c7_g1_i1	.			.	.	.	TR6226|c7_g1_i1|m.14038	.			.	.	.	PF03103.1	.	.	.
TR6442|c16_g1	-10.02	4.29E-17	TR6442|c16_g1_i1	AM4N_DR	63.69	7.00E-64	Amy4N GF	Alpha-amy	Drosophila	TR6442|c16_g1_i1|m.19441	AM4N_DR	63.69	1.00E-64	Amy4N GF	Alpha-amy	Drosophila	PF02806.1	GO:0003824^mo	Starch and sucrose metabolism	.
TR2372|c0_g1	-10.01	3.86E-17	TR2372|c0_g1_i1	ATPO_DRC	66.36	3.00E-40	ATPsynO C	ATP syntha	Drosophila	TR2372|c0_g1_i1|m.2099	ATPO_DRC	66.36	6.00E-43	ATPsynO C	ATP syntha	Drosophila	PF00213.1	GO:0046933^mo	Oxidative phosphorylation	.
TR6165|c10_g1	-9.97	6.24E-20	TR6165|c10_g1_i1	IDHC_MICI	75.93	2.00E-147	IDH1 IDP2	Isocitrate c	Microtus n	TR6165|c10_g1_i1|m.12280	IDHC_MICI	75.93	2.00E-154	IDH1 IDP2	Isocitrate c	Microtus n	PF00180.1	GO:0016616^mo	2-Oxocarboxylic acid metabolism`Biosynthesis of ai	.
TR8897|c0_g1	-9.97	8.81E-18	TR8897|c0_g1_i1	ATP5J_DR	45.45	5.00E-24	ATPsynCf6	ATP syntha	Drosophila	TR8897|c0_g1_i1|m.20917	ATP5J_DR	45.45	2.00E-25	ATPsynCf6	ATP syntha	Drosophila	PF05511.6	GO:0015078^mo	Oxidative phosphorylation	.
TR5488|c1_g1	-9.94	2.13E-09	TR5488|c1_g1_i1	.			.	.	.	TR5488|c1_g1_i1|m.6182	.			.	.	.	.	.	.	.
TR427|c0_g1	-9.91	2.35E-16	TR427|c0_g1_i1	TPIS_CULT	73.28	2.00E-129	Tpi	Triosephos	Culex tarsa	TR427|c0_g1_i1|m.405	TPIS_CULT	73.28	7.00E-135	Tpi	Triosephos	Culex tarsa	PF00121.1	GO:0004807^mo	Biosynthesis of amino acids`Carbon metabolism`Fr	.
TR6261|c2_g2	-9.91	5.43E-17	TR6261|c2_g2_i1	LIPH_RABI	34.7	3.00E-34	LIPH	Lipase mer	Oryctolagu	TR6261|c2_g2_i1|m.15241	LIPH_RABI	34.78	5.00E-37	LIPH	Lipase mer	Oryctolagu	PF00151.1	.	.	.
TR3937|c0_g1	-9.91	1.74E-27	TR3937|c0_g1_i1	RS15A_DR	91.67	3.00E-74	RpS15Aa G	40S riboso	Drosophila	TR3937|c0_g1_i1|m.3755	RS15A_DR	92.31	2.00E-84	RpS15Aa G	40S riboso	Drosophila	PF00410.1	GO:0003735^mo	Ribosome	.
TR3231|c1_g1	-9.90	4.09E-18	TR3231|c1_g1_i1	NP1L1_XEI	52.04	3.00E-104	nap1l1 TNe	Nucleosom	Xenopus tr	TR3231|c1_g1_i1|m.3064	NP1L4_MC	52.57	9.00E-102	Nap1l4	Nucleosom	Mus muscu	PF00956.1	GO:0006334^biol	.	.
TR5888|c0_g1	-9.90	1.75E-23	TR5888|c0_g1_i1	CUD2_SCH	45.28	1.00E-23	0	Endocuticl	Schistocer	TR5888|c0_g1_i1|m.7369	CUD2_SCH	47.37	4.00E-22	0	Endocuticl	Schistocer	PF00379.1	GO:0042302^mo	.	.
TR6087|c1_g1	-9.89	4.30E-30	TR6087|c1_g1_i1	YELL_DROI	41.33	2.00E-100	y	Protein yel	Drosophila	TR6087|c1_g1_i1|m.9853	YELL_DROI	40.94	5.00E-103	y	Protein yel	Drosophila	PF03022.1	.	.	.
TR8769|c0_g1	-9.89	9.38E-21	TR8769|c0_g1_i1	NSA2_MOI	73.31	7.00E-118	Nsa2 Tinp1	Ribosome	Mus muscu	TR8769|c0_g1_i1|m.20859	NSA2_HUI	73.71	1.00E-135	NSA2 TINP	Ribosome I	Homo sapi	PF01201.1	.	.	.
TR6365|c4_g1	-9.88	5.40E-30	TR6365|c4_g1_i1	CUD2_SCH	44.54	1.00E-21	0	Endocuticl	Schistocer	TR6365|c4_g1_i1|m.18289	CUD2_SCH	45.95	2.00E-19	0	Endocuticl	Schistocer	PF00379.1	GO:0042302^mo	.	.
TR1828|c0_g1	-9.87	5.65E-19	TR1828|c0_g1_i1	GLYC_RABI	55.93	3.00E-61	SHMT1	Serine hyd	Oryctolagu	TR1828|c0_g1_i1|m.1567	GLYC_RABI	55.93	3.00E-64	SHMT1	Serine hyd	Oryctolagu	PF00464.1	GO:0004372^mo	Biosynthesis of amino acids`Carbon metabolism`Gl	.
TR5754|c1_g1	-9.85	7.79E-31	TR5754|c1_g1_i1	VDAC_DRC	57.8	7.00E-118	porin POR-	Voltage-de	Drosophila	TR5754|c1_g1_i1|m.6904	VDAC_DRC	57.8	2.00E-120	porin POR-	Voltage-de	Drosophila	PF01459.1	GO:0055085^biol	Calcium signaling pathway	.
TR5346|c0_g2	-9.85	2.38E-15	TR5346|c0_g2_i1	HEXA_BLA	36.96	5.00E-156	0	Hexamerin	Blaberus di	TR5346|c0_g2_i1|m.5877	HEXA_BLA	37.18	2.00E-145	0	Hexamerin	Blaberus d	PF00372.1	.	.	.
TR2322|c1_g1	-9.84	3.58E-21	TR2322|c1_g1_i1	DNJA1_PO	59.74	3.00E-119	DNAJA1	DnaJ homc	Pongo abe	TR2322|c1_g1_i1|m.2039	DNJA1_PO	60.06	9.00E-125	DNAJA1	DnaJ homc	Pongo abe	PF00684.1	GO:0031072^mo	Protein processing in endoplasmic reticulum	.
TR8306|c0_g1	-9.83	1.22E-10	TR8306|c0_g1_i1	.			.	.	.	TR8306|c0_g1_i1|m.20572	.			.	.	.	.	.	.	.
TR5128|c1_g1	-9.83	3.75E-17	TR5128|c1_g1_i1	CY1_BOVII	65.06	2.00E-96	CYC1	Cytochrom	Bos taurus	TR5128|c1_g1_i1|m.5497	CY1_BOVII	65.31	4.00E-111	CYC1	Cytochrom	Bos taurus	PF02167.1	GO:0005506^mo	Oxidative phosphorylation	.
TR6169|c24_g1	-9.81	2.35E-14	TR6169|c24_g1_i1	COGS_UCA	40.18	3.00E-41	0	Brachyurin	Uca pugilat	TR6169|c24_g1_i1|m.12421	CTRB1_LIT	36.6	2.00E-40	0	Chymotryp	Litopenaeu	PF00089.2	GO:0004252^mo	.	.
TR2030|c0_g1	-9.80	6.50E-17	TR2030|c0_g1_i1	UCRI_MOU	69.23	2.00E-96	Uqcrfs1	Cytochrom	Mus muscu	TR2030|c0_g1_i1|m.1761	UCRI_AOT	69.74	5.00E-101	UQCRFS1	Cytochrom	Aotus azar	PF00355.2	GO:0008121^mo	Oxidative phosphorylation	.
TR5837|c0_g1	-9.80	3.42E-28	TR5837|c0_g1_i1	RL28_SPOI	66.67	4.00E-55	RpL28	60S riboso	Spodopter	TR5837|c0_g1_i1|m.7186	RL28_SPOI	66.13	1.00E-55	RpL28	60S riboso	Spodopter	PF01778.1	.	Ribosome	.
TR3339|c2_g1	-9.77	2.39E-18	TR3339|c2_g1_i1	FRIL_XENL	27.11	3.00E-14	0	Ferritin ligl	Xenopus la	TR3339|c2_g1_i1|m.3148	FRIL_XENL	28.57	5.00E-13	0	Ferritin ligl	Xenopus la	PF00210.1	GO:0008199^mo	.	.
TR1255|c0_g1	-9.75	1.66E-14	TR1255|c0_g1_i1	.			.	.	.	TR1255|c0_g1_i1|m.1061	.			.	.	.	.	.	.	.
TR757|c0_g1	-9.74	9.80E-19	TR757|c0_g1_i1	SER3_DRO	37.39	6.00E-14	Jon99Ci SE	Serine prot	Drosophila	TR757|c0_g1_i1|m.674	TMPS3_HU	38.46	2.00E-14	TMPRSS3 E	Transmem	Homo sapi	PF00089.2	GO:0004252^mo	.	.
TR5386|c0_g1	-9.73	2.81E-14	TR5386|c0_g1_i1	CBPB_AST	44.2	4.00E-60	0	Carboxype	Astacus as	TR5386|c0_g1_i1|m.5946	CBPB_AST	44.2	3.00E-59	0	Carboxype	Astacus as	PF00246.1	GO:0004181^mo	.	.
TR5126|c0_g1	-9.72	5.87E-17	TR5126|c0_g1_i1	SODC_CER	73.86	8.00E-79	Sod	Superoxide	Ceratitis ca	TR5126|c0_g1_i1|m.5496	SODC_CER	73.86	2.00E-75	Sod	Superoxide	Ceratitis ca	PF00080.1	GO:0046872^mo	Longevity regulating pathway - multiple species`Pe	.
TR4550|c0_g1	-9.72	2.73E-16	TR4550|c0_g1_i1	FIBC_LUMI	37.85	4.00E-21	0	Fibrinolytic	Lumbricus	TR4550|c0_g1_i1|m.4495	FIBC_LUMI	37.99	5.00E-22	0	Fibrinolytic	Lumbricus	PF00089.2	GO:0004252^mo	.	.
TR5874|c0_g1	-9.72	1.03E-23	TR5874|c0_g1_i1	PPIA_BLAG	84.15	2.00E-98	CYPA	Peptidyl-pr	Blattella ge	TR5874|c0_g1_i1|m.7328	PPIA_DROI	84.57	3.00E-100	Cyp1 Cyp-1	Peptidyl-pr	Drosophila	PF00160.1	GO:0003755^mo	Calcium signaling pathway	.
TR5346|c0_g1	-9.71	1.14E-16	TR5346|c0_g1_i1	CRPI_PERA	37.08	1.00E-143	0	Allergen Cr	Periplaneta	TR5346|c0_g1_i1|m.5876	CRPI_PERA	37.19	4.00E-133	0	Allergen Cr	Periplaneta	PF00372.1	.	.	.
TR436|c0_g1	-9.69	9.00E-18	TR436|c0_g1_i1	COX42_TH	41.35	7.00E-23	0	Cytochrom	Thunnus o	TR436|c0_g1_i1|m.407	COX42_TH	41.35	9.00E-22	0	Cytochrom	Thunnus o	PF02936.9	GO:0004129^mo	Oxidative phosphorylation	.
TR5830|c0_g1	-9.67	1.92E-13	TR5830|c0_g1_i1	LIPP_RABI	33.12	8.00E-29	PNLIP	Pancreatic	Oryctolagu	TR5830|c0_g1_i1|m.7155	LIPP_RABI	32.79	5.00E-34	PNLIP	Pancreatic	Oryctolagu	PF00151.1	.	.	.
TR1910|c0_g1	-9.67	6.55E-16	TR1910|c0_g1_i1	YOCA_CAE	41.67	4.00E-31	.	.	.	TR1910|c0_g1_i1|m.1625	YC17_DRO	38.22	2.00E-24	CG16817	Uncharact	Drosophila	PF04969.1	.	Arachidonic acid metabolism	.
TR6275|c10_g2	-9.66	4.43E-45	TR6275|c10_g2_i1	RL3_DROM	83.92	0	RpL3 CG48	60S riboso	Drosophila	TR6275|c10_g2_i1|m.15649	RL3_DROM	84	0	RpL3 CG48	60S riboso	Drosophila	PF00297.1	GO:0003735^mo	Ribosome	.
TR4653|c0_g1	-9.66	6.51E-18	TR4653|c0_g1_i1	ACDSB_MO	64.47	0	Acadsb	Short/bran	Mus muscu	TR4653|c0_g1_i1|m.4653	ACDSB_MO	64.47	0	Acadsb	Short/bran	Mus muscu	PF00441.1	GO:0016627^mo	Fatty acid degradation`Fatty acid metabolism`Valin	.
TR7502|c0_g1	-9.65	7.99E-15	TR7502|c0_g1_i1	ATP5L_POI	50	2.00E-20	ATP5L	ATP syntha	Pongo abe	TR7502|c0_g1_i1|m.20071	ATP5L_POI	50	3.00E-21	ATP5L	ATP syntha	Pongo abe	PF04718.1	GO:0015078^mo	Oxidative phosphorylation	.
TR5894|c0_g3	-9.65	1.92E-18	TR5894|c0_g3_i1	TKT_PONA	69.31	5.00E-88	TKT	Transketol	Pongo abe	TR5894|c0_g3_i1|m.7385	TKT_PONA	69.31	2.00E-93	TKT	Transketol	Pongo abe	PF00456.1	GO:0008661^mo	Biosynthesis of amino acids`Carbon metabolism`Pe	.
TR436|c0_g2	-9.65	3.57E-16	TR436|c0_g2_i1	COX42_TH	41.35	7.00E-23	0	Cytochrom	Thunnus o	TR436|c0_g2_i1|m.408	COX42_TH	41.35	8.00E-22	0	Cytochrom	Thunnus o	PF02936.9	GO:0004129^mo	Oxidative phosphorylation	.
TR6096|c6_g1	-9.64	1.05E-14	TR6096|c6_g1_i1	MDHC_CH	69.23	7.00E-113	MDH1 RCJI	Malate del	Gallus gallu	TR6096|c6_g1_i1|m.10137	MDHC_HU	67.69	2.00E-125	MDH1 MD	Malate del	Homo sapi	PF00056.1	GO:0016491^mo	Carbon metabolism`Citrate cycle (TCA cycle)`Cystei	.
TR9350|c0_g1	-9.63	4.51E-23	TR9350|c0_g1_i1	RS26_ANO	77.39	2.00E-57	RpS26 AGA	40S riboso	Anopheles	TR9350|c0_g1_i1|m.21173	RS26_ANO	77.39	1.00E-55	RpS26 AGA	40S riboso	Anopheles	PF01283.1	GO:0003735^mo	Ribosome	.
TR6355|c9_g1	-9.63	2.31E-16	TR6355|c9_g1_i1	ATPA_DRC	68	2.00E-34	blw ATPSY	ATP syntha	Drosophila	TR6355|c9_g1_i1|m.18213	ATPA_DRC	68	1.00E-33	blw ATPSY	ATP syntha	Drosophila	PF02874.1	GO:0015992^biol	Oxidative phosphorylation	.
TR5890|c0_g2	-9.63	1.66E-18	TR5890|c0_g2_i1	SUI1_ANO	97.27	6.00E-73	AGAP0064	Protein tra	Anopheles	TR5890|c0_g2_i1|m.7376	SUI1_ANO	97.27	5.00E-75	AGAP0064	Protein tra	Anopheles	PF01253.1	GO:0003743^mo	RNA transport	.
TR1045|c0_g1	-9.63	7.33E-17	TR1045|c0_g1_i1	GST1_BLA	35.78	3.00E-43	0	Glutathion	Blattella ge	TR1045|c0_g1_i1|m.864	GST1_BLA	35.78	9.00E-44	0	Glutathion	Blattella ge	PF00043.2	GO:0005515^mo	Arachidonic acid metabolism`Drug metabolism - cy	.
TR4647|c0_g2	-9.62	8.25E-14	TR4647|c0_g2_i1	ACO11_TR	55.92	1.00E-136	D11DS PGI	Acyl-CoA D	Trichoplusi	TR4647|c0_g2_i1|m.4646	ACO11_TR	54.44	4.00E-135	D11DS PGI	Acyl-CoA D	Trichoplusi	PF00487.1	GO:0006629^biol	Biosynthesis of unsaturated fatty acids`Fatty acid n	.
TR2896|c0_g1	-9.61	8.29E-24	TR2896|c0_g1_i1	RL24_SPOI	78.71	5.00E-56	RpL24	60S riboso	Spodopter	TR2896|c0_g1_i1|m.2638	RL24_PLU	78.71	2.00E-74	RpL24	60S riboso	Plutella xyl	PF01246.1	.	Ribosome	.
TR5800|c1_g1	-9.59	9.91E-17	TR5800|c1_g1_i1	URIC_DRO	50.16	4.00E-97	Uro UO GA	Uricase (EC	Drosophila	TR5800|c1_g1_i1|m.7069	URIC_DRO	51.27	8.00E-101	Uro UO GA	Uricase (EC	Drosophila	PF01014.1	.	Purine metabolism	.
TR1733|c0_g2	-9.59	5.33E-17	TR1733|c0_g2_i1	RAN_DROI	95.53	3.00E-129	Ran Ran10	GTP-bindir	Drosophila	TR1733|c0_g2_i1|m.1490	RAN_DROI	94.05	1.00E-129	Ran Ran10	GTP-bindir	Drosophila	PF00025.1	GO:0005525^mo	Ribosome biogenesis in eukaryotes`RNA transport	.
TR6442|c15_g1	-9.58	1.95E-22	TR6442|c15_g1_i2	CUD2_SCH	56.19	6.00E-34	0	Endocuticl	Schistocer	TR6442|c15_g1_i2|m.19440	CUD2_SCH	57.14	9.00E-31	0	Endocuticl	Schistocer	PF00379.1	GO:0042302^mo	.	.
TR7379|c0_g1	-9.58	1.50E-14	TR7379|c0_g1_i1	.			.	.	.	TR7379|c0_g1_i1|m.20025	.			.	.	.	.	.	.	.
TR6186|c0_g2	-9.58	1.21E-64	TR6186|c0_g2_i1	ADT1_ANC	77.7	1.00E-78	AGAP0067	ADP,ATP ca	Anopheles	TR6186|c0_g2_i1|m.12768	ADT1_ANC	77.7	3.00E-82	AGAP0067	ADP,ATP ca	Anopheles	PF00153.2	.	Calcium signaling pathway	.
TR6317|c4_g2	-9.54	5.21E-20	TR6317|c4_g2_i1	METK_DRC	82.98	2.00E-79	Sam-S M(2	S-adenosyl	Drosophila	TR6317|c4_g2_i1|m.16946	METK_DRC	82.98	3.00E-82	Sam-S M(2	S-adenosyl	Drosophila	PF00438.1	GO:0004478^mo	Biosynthesis of amino acids`Cysteine and methioni	.
TR5917|c0_g1	-9.54	4.52E-35	TR5917|c0_g1_i1	RL22_PIG^	74.49	3.00E-28	RPL22	60S riboso	Sus scrofa	TR5917|c0_g1_i1|m.7471	RL22_DROI	66.67	7.00E-43	RpL22 CG7	60S riboso	Drosophila	PF01776.1	GO:0003735^mo	Ribosome	.
TR5902|c0_g2	-9.53	1.10E-17	TR5902|c0_g2_i1	AQP_AEDA	35.98	3.00E-29	AAEL00351	Aquaporin	Aedes aegy	TR5902|c0_g2_i1|m.7417	AQP_AEDA	35.98	1.00E-27	AAEL00351	Aquaporin	Aedes aegy	PF00230.1	GO:0005215^mo	.	.
TR2372|c0_g2	-9.52	3.59E-15	TR2372|c0_g2_i1	ATPO_DRC	50.5	4.00E-24	ATPsynO C	ATP syntha	Drosophila	TR2372|c0_g2_i1|m.2100	ATPO_DRC	50.5	7.00E-25	ATPsynO C	ATP syntha	Drosophila	PF00213.1	GO:0046933^mo	Oxidative phosphorylation	.
TR9530|c0_g1	-9.52	4.02E-14	TR9530|c0_g1_i1	DPGN_DIP	58.33	1.00E-05	0	Serine prot	Dipetaloga	TR9530|c0_g1_i1|m.21243	.			.	.	.	PF00050.1	GO:0005515^mo	.	.
TR1316|c0_g1	-9.52	5.62E-17	TR1316|c0_g1_i1	ATP5J_DR	47.52	2.00E-23	ATPsynCf6	ATP syntha	Drosophila	TR1316|c0_g1_i1|m.1115	ATP5J_DR	50.51	6.00E-25	ATPsynCf6	ATP syntha	Drosophila	PF05511.6	GO:0015078^mo	Oxidative phosphorylation	.
TR6754|c0_g1	-9.52	5.29E-31	TR6754|c0_g1_i1	RS25_SPOI	84	3.00E-37	RpS25	40S riboso	Spodopter	TR6754|c0_g1_i1|m.19725	RS25_SPOI	79.83	4.00E-44	RpS25	40S riboso	Spodopter	PF03297.1	.	Ribosome	.
TR8107|c0_g1	-9.52	2.05E-13	TR8107|c0_g1_i1	CX6A1_RA	38.89	6.00E-12	COX6A1 CC	Cytochrom	Oryctolagu	TR8107|c0_g1_i1|m.20443	CX6A1_BO	39.45	8.00E-18	COX6A1	Cytochrom	Bos taurus	PF02046.1	GO:0004129^mo	Oxidative phosphorylation	.
TR7859|c0_g1	-9.51	9.68E-20	TR7859|c0_g1_i1	.			.	.	.	TR7859|c0_g1_i1|m.20298	.			.	.	.	PF03103.1	.	.	.
TR2200|c0_g1	-9.51	2.02E-15	TR2200|c0_g1_i1	MPPB_BOV	67.63	1.00E-95	PMPCB	Mitochond	Bos taurus	TR2200|c0_g1_i1|m.1940	MPPB_BOV	67.31	1.00E-98	PMPCB	Mitochond	Bos taurus	PF05193.1	.	.	.
TR4550|c0_g2	-9.51	4.71E-15	TR4550|c0_g2_i1	FIBC_LUMI	37.85	4.00E-21	0	Fibrinolytic	Lumbricus	TR4550|c0_g2_i1|m.4496	FIBC_LUMI	37.99	5.00E-22	0	Fibrinolytic	Lumbricus	PF00089.2	GO:0004252^mo	.	.
TR5956|c3_g1	-9.50	5.36E-26	TR5956|c3_g1_i1	.			.	.	.	TR5956|c3_g1_i1|m.7743	TROP_HUI	35.07	3.00E-06	TRO KIAA1	Trophinin (	Homo sapi	.	.	.	.
TR5987|c2_g1	-9.49	4.99E-53	TR5987|c2_g1_i2	RLA2_DRO	74.24	1.00E-24	RpLP2 rpA	60S acidic	Drosophila	TR5987|c2_g1_i2|m.8132	RLA2_DRO	73.85	2.00E-25	RpLP2 rpA	60S acidic	Drosophila	PF00428.1	GO:0003735^mo	Ribosome`Ribosome	.
TR3750|c0_g1	-9.48	9.44E-14	TR3750|c0_g1_i1	GST1D_AN	69.87	4.00E-77	GstD1 GST	Glutathion	Anopheles	TR3750|c0_g1_i1|m.3575	GST1D_AN	69.87	2.00E-78	GstD1 GST	Glutathion	Anopheles	PF02798.1	GO:0005515^mo	Drug metabolism - cytochrome P450`Glutathione n	.
TR4854|c0_g1	-9.48	3.57E-16	TR4854|c0_g1_i1	APOD_HUI	27.49	2.00E-11	APOD	Apolipopro	Homo sapi	TR4854|c0_g1_i1|m.5013	APOD_BOV	29.24	2.00E-12	APOD	Apolipopro	Bos taurus	PF00061.1	.	.	.
TR4479|c0_g1	-9.47	5.85E-14	TR4479|c0_g1_i1	CTRB2_LIT	37.43	3.00E-24	0	Chymotryp	Litopenaeu	TR4479|c0_g1_i1|m.4385	CTRB2_LIT	37.43	9.00E-23	0	Chymotryp	Litopenaeu	PF00089.2	GO:0004252^mo	.	.
TR4261|c0_g1	-9.47	1.24E-16	TR4261|c0_g1_i1	METK_DRC	81.01	2.00E-87	Sam-S M(2	S-adenosyl	Drosophila	TR4261|c0_g1_i1|m.4146	METK_DRC	81.01	1.00E-88	Sam-S M(2	S-adenosyl	Drosophila	PF00438.1	GO:0004478^mo	Biosynthesis of amino acids`Cysteine and methioni	.
TR884|c0_g1	-9.47	1.23E-16	TR884|c0_g1_i1	ACH2_BOM	38.61	4.00E-61	0	Antichymo	Bombyx m	TR884|c0_g1_i1|m.754	SERA_MAN	40.27	1.00E-58	0	Alaserpin (	Manduca s	PF00079.1	.	.	.
TR5262|c1_g1	-9.46	9.21E-15	TR5262|c1_g1_i1	PUR9_CHI	69.88	4.00E-169	ATIC PURH	Bifunctiona	Gallus gallu	TR5262|c1_g1_i1|m.5757	PUR9_CHI	69.88	5.00E-178	ATIC PURH	Bifunctiona	Gallus gallu	PF01808.1	GO:0003937^mo	One carbon pool by folate`Purine metabolism	.
TR5980|c1_g2	-9.46	6.63E-39	TR5980|c1_g2_i1	RS3A_PER	96.31	1.00E-166	Parcxpwex	40S riboso	Periplaneta	TR5980|c1_g2_i1|m.8083	RS3A_PER	96.31	2.00E-173	Parcxpwex	40S riboso	Periplaneta	PF01015.1	GO:0003735^mo	Ribosome	.
TR4894|c1_g1	-9.45	6.44E-16	TR4894|c1_g1_i1	YM67_CAE	37.93	4.00E-33	K12H4.7	Putative se	Caenorhab	TR4894|c1_g1_i1|m.5089	YM67_CAE	36.02	4.00E-42	K12H4.7	Putative se	Caenorhab	PF00326.1	GO:0008236^mo	.	.
TR7351|c0_g1	-9.43	9.54E-17	TR7351|c0_g1_i1	DFP_MAN	39.02	4.00E-14	0	Putative de	Manduca s	TR7351|c0_g1_i1|m.20017	DFP_MAN	39.02	1.00E-14	0	Putative de	Manduca s	PF02014.1	.	.	.
TR8351|c0_g1	-9.43	5.25E-16	TR8351|c0_g1_i1	CRUST_PA	50	2.00E-11	Cys	Crustapain	Pandalus b	TR8351|c0_g1_i1|m.20597	CATLL_PHA	38.3	1.00E-16	0	Cathepsin	Phaedon c	PF08246.7	.	.	.
TR6346|c3_g1	-9.41	5.45E-13	TR6346|c3_g1_i1	COGS_UCA	28.26	1.00E-07	0	Brachyurin	Uca pugilat	TR6346|c3_g1_i1|m.18023	COGS_UCA	29.71	8.00E-08	0	Brachyurin	Uca pugilat	PF00089.2	GO:0004252^mo	.	.
TR4650|c1_g1	-9.41	7.48E-25	TR4650|c1_g1_i1	FABPM_SC	48.85	9.00E-32	0	Fatty acid-l	Schistocer	TR4650|c1_g1_i1|m.4649	FABP7_CH	50.41	8.00E-34	FABP7	Fatty acid-l	Gallus gallu	PF00061.1	.	PPAR signaling pathway	.
TR1956|c0_g1	-9.39	1.42E-15	TR1956|c0_g1_i1	SERC_DRO	65.65	2.00E-44	CG11899	Probable p	Drosophila	TR1956|c0_g1_i1|m.1672	SERC_DRO	65.65	6.00E-48	CG11899	Probable p	Drosophila	PF00266.1	GO:0008152^biol	Biosynthesis of amino acids`Carbon metabolism`Gl	.
TR5564|c0_g1	-9.38	1.58E-26	TR5564|c0_g1_i1	RSSA_MAC	93.28	5.00E-84	0	40S riboso	Maconellic	TR5564|c0_g1_i1|m.6357	RSSA_BOM	75.26	7.00E-93	0	40S riboso	Bombyx m	PF00318.1	GO:0003735^mo	Ribosome	.
TR1956|c0_g2	-9.35	2.14E-16	TR1956|c0_g2_i1	SERC_DRO	65.37	5.00E-90	CG11899	Probable p	Drosophila	TR1956|c0_g2_i1|m.1673	SERC_DRO	65.67	3.00E-109	CG11899	Probable p	Drosophila	PF00266.1	GO:0008152^biol	Biosynthesis of amino acids`Carbon metabolism`Gl	.
TR2022|c0_g1	-9.34	4.82E-23	TR2022|c0_g1_i1	APL3_GALI	27.67	2.00E-07	0	Apolipoph	Galleria me	TR2022|c0_g1_i1|m.1752	APL3_GALI	29.89	1.00E-07	0	Apolipoph	Galleria me	PF01442.1	GO:0008289^mo	.	.
TR2145|c2_g1	-9.34	8.87E-18	TR2145|c2_g1_i1	TRAM1_BC	50.9	2.00E-48	TRAM1 TRA	Translocati	Bos taurus	TR2145|c2_g1_i1|m.1887	TRAM1_BC	50.9	1.00E-56	TRAM1 TRA	Translocati	Bos taurus	PF08390.6	.	Protein processing in endoplasmic reticulum	.
TR1405|c0_g1	-9.33	8.72E-17	TR1405|c0_g1_i1	UAF30_SCI	40.58	1.00E-09	spp27 uaf3	Upstream	Schizosacc	TR1405|c0_g1_i1|m.1179	UAF30_SCI	27.13	2.00E-19	spp27 uaf3	Upstream	Schizosacc	PF02201.1	GO:0005515^mo	.	.
TR4699|c0_g2	-9.32	1.82E-12	TR4699|c0_g2_i1	K1161_HU	35.63	6.00E-72	KIAA1161	Uncharact	Homo sapi	TR4699|c0_g2_i1|m.4723	K1161_HU	35.63	3.00E-75	KIAA1161	Uncharact	Homo sapi	PF01055.2	GO:0004553^mo	Galactose metabolism`Starch and sucrose metabol	.
TR4650|c0_g2	-9.31	2.65E-14	TR4650|c0_g2_i1	FABPM_SC	47.58	7.00E-24	0	Fatty acid-l	Schistocer	TR4650|c0_g2_i1|m.4648	FABPM_SC	47.58	1.00E-32	0	Fatty acid-l	Schistocer	PF00061.1	.	PPAR signaling pathway	.
TR4954|c0_g1	-9.30	9.96E-13	TR4954|c0_g1_i1	SPRC_CAEI	46.77	2.00E-62	ost-1 sparc	SPARC (Bas	Caenorhab	TR4954|c0_g1_i1|m.5215	SPRC_CAEI	47.44	2.00E-64	ost-1 sparc	SPARC (Bas	Caenorhab	PF10591.4	GO:0005509^mo	.	.
TR3340|c1_g1	-9.30	4.75E-12	TR3340|c1_g1_i1	CTRB1_LIT	40	4.00E-30	0	Chymotryp	Litopenaeu	TR3340|c1_g1_i1|m.3149	CTRB1_LIT	40	2.00E-28	0	Chymotryp	Litopenaeu	PF00089.2	GO:0004252^mo	.	.
TR6126|c3_g1	-9.30	3.27E-13	TR6126|c3_g1_i1	PABP_DRC	51.56	3.00E-10	pAbp CG51	Polyadenyl	Drosophila	TR6126|c3_g1_i1|m.10857	PABP_DRC	52.54	4.00E-10	pAbp CG51	Polyadenyl	Drosophila	.	.	mRNA surveillance pathway`RNA degradation`RNA	.
TR5555|c0_g1	-9.30	5.80E-16	TR5555|c0_g1_i1	ALDR_RAB	61.21	6.00E-54	AKR1B1	Aldose red	Oryctolagu	TR5555|c0_g1_i1|m.6335	ALDR_RAB	60.71	2.00E-64	AKR1B1	Aldose red	Oryctolagu	PF00248.1	.	Fructose and mannose metabolism`Galactose meta	.
TR6123|c4_g1	-9.29	2.73E-12	TR6123|c4_g1_i1	GBA3_CAV	43.07	1.00E-53	Gba3 Cbg	Cytosolic b	Cavia porc	TR6123|c4_g1_i1|m.10736	GBA3_CAV	43.41	3.00E-54	Gba3 Cbg	Cytosolic b	Cavia porc	PF00232.1	GO:0004553^mo	.	.
TR3338|c0_g1	-9.29	7.85E-13	TR3338|c0_g1_i1	PRP1_MAN	61.7	8.00E-34	0	Phenoloxic	Manduca s	TR3338|c0_g1_i1|m.3147	PRP1_MAN	55.75	2.00E-35	0	Phenoloxic	Manduca s	PF03723.9	.	.	.
TR4020|c0_g2	-9.28	7.27E-14	TR4020|c0_g2_i1	.			.	.	.	TR4020|c0_g2_i1|m.3864	.			.	.	.	PF01223.1	GO:0003676^mo	.	.
TR5888|c3_g1	-9.28	6.61E-16	TR5888|c3_g1_i1	CUPP_DRC	46.32	2.00E-20	Pcp GA174	Pupal cutic	Drosophila	TR5888|c3_g1_i1|m.7373	CUPP_DRC	46.32	3.00E-23	Pcp GA174	Pupal cutic	Drosophila	PF00379.1	GO:0042302^mo	.	.
TR3469|c0_g1	-9.28	4.79E-11	TR3469|c0_g1_i1	SAHHB_XE	86.91	1.00E-174	ahcy-b ahc	Adenosylh	Xenopus la	TR3469|c0_g1_i1|m.3269	SAHHA_XE	87.27	2.00E-180	ahcy-a ahc	Adenosylh	Xenopus la	PF00670.1	GO:0004013^mo	Cysteine and methionine metabolism	.
TR6388|c2_g2	-9.25	3.49E-14	TR6388|c2_g2_i1	RS19A_DR	67.65	2.00E-50	RpS19a Rp	40S riboso	Drosophila	TR6388|c2_g2_i1|m.18786	RS19A_DR	67.65	3.00E-50	RpS19a Rp	40S riboso	Drosophila	PF01090.1	GO:0003735^mo	Ribosome	.
TR5419|c0_g1	-9.25	1.46E-20	TR5419|c0_g1_i1	.			.	.	.	TR5419|c0_g1_i1|m.6010	CTL2A_MC	36.63	6.00E-13	Ctla2a	Protein CTI	Mus muscu	PF08246.7	.	.	.
TR5236|c0_g2	-9.18	2.82E-13	TR5236|c0_g2_i1	CYP5_CAEI	75.84	3.00E-54	cyn-5 cyp-5	Peptidyl-pr	Caenorhab	TR5236|c0_g2_i1|m.5696	CYP5_CAEI	81.06	7.00E-75	cyn-5 cyp-5	Peptidyl-pr	Caenorhab	PF00160.1	GO:0003755^mo	.	.
TR2200|c1_g1	-9.18	2.28E-14	TR2200|c1_g1_i1	MPPB_RAT	75.42	1.00E-85	Pmpcb Mp	Mitochond	Rattus nor	TR2200|c1_g1_i1|m.1941	MPPB_RAT	75.42	2.00E-90	Pmpcb Mp	Mitochond	Rattus nor	PF00675.1	.	.	.
TR5476|c6_g1	-9.18	8.33E-15	TR5476|c6_g1_i1	PDI_DROM	65.2	5.00E-89	Pdi CG6988	Protein dis	Drosophila	TR5476|c6_g1_i1|m.6147	PDI_DROM	65.2	2.00E-85	Pdi CG6988	Protein dis	Drosophila	PF00085.1	GO:0045454^biol	Protein processing in endoplasmic reticulum	.
TR757|c0_g2	-9.15	6.60E-13	TR757|c0_g2_i1	PRS55_HU	34.48	1.00E-10	PRSS55 TSI	Serine prot	Homo sapi	TR757|c0_g2_i1|m.675	PRS55_HU	34.48	3.00E-11	PRSS55 TSI	Serine prot	Homo sapi	PF00089.2	GO:0004252^mo	.	.
TR8845|c0_g1	-9.15	7.84E-29	TR8845|c0_g1_i1	GST1_BLA	54.68	9.00E-67	0	Glutathion	Blattella ge	TR8845|c0_g1_i1|m.20895	GST1_BLA	54.68	2.00E-66	0	Glutathion	Blattella ge	PF00043.2	GO:0005515^mo	Arachidonic acid metabolism`Drug metabolism - cy	.
TR5814|c0_g1	-9.14	3.42E-14	TR5814|c0_g1_i1	PAXI_RAT	70.19	3.00E-49	Pxn	Paxillin	Rattus nor	TR5814|c0_g1_i1|m.7108	PAXI_RAT	70.19	1.00E-47	Pxn	Paxillin	Rattus nor	PF00412.1	GO:0008270^mo	Focal adhesion`Regulation of actin cytoskeleton	.
TR661|c0_g1	-9.13	4.89E-15	TR661|c0_g1_i1	ATPK_DRO	63.46	1.00E-48	CG4692	Putative A	Drosophila	TR661|c0_g1_i1|m.587	ATPK_DRO	62.86	6.00E-45	CG4692	Putative A	Drosophila	PF10206.4	.	Oxidative phosphorylation	.
TR5869|c1_g1	-9.12	5.98E-33	TR5869|c1_g1_i1	RL18_TIME	82.97	6.00E-106	RpL18	60S riboso	Timarcha b	TR5869|c1_g1_i1|m.7316	RL18_TIME	82.97	2.00E-107	RpL18	60S riboso	Timarcha b	PF00828.1	.	Ribosome	.
TR6342|c28_g1	-9.11	6.47E-11	TR6342|c28_g1_i1	CULP1_HEI	45.16	1.00E-11	LCP1	Larval cutic	Helicoverp	TR6342|c28_g1_i1|m.17883	CULP1_HEI	43.75	2.00E-10	LCP1	Larval cutic	Helicoverp	PF00379.1	GO:0042302^mo	.	.
TR936|c0_g1	-9.11	1.36E-14	TR936|c0_g1_i1	QCR7_BOV	44.86	3.00E-25	UQCRB	Cytochrom	Bos taurus	TR936|c0_g1_i1|m.789	QCR7_BOV	44.86	2.00E-24	UQCRB	Cytochrom	Bos taurus	PF02271.1	GO:0006122^biol	Oxidative phosphorylation	.
TR4112|c1_g1	-9.11	1.32E-12	TR4112|c1_g1_i1	ENDOU_DI	50.35	1.00E-42	CG2145	Poly(U)-sp	Drosophila	TR4112|c1_g1_i1|m.3978	ENDOU_DI	50.35	2.00E-44	CG2145	Poly(U)-sp	Drosophila	PF09412.5	GO:0016788^mo	.	.
TR68|c0_g1	-9.10	2.50E-13	TR68|c0_g1_i1	ML1P_MAI	34.62	2.00E-12	0	MD-2-relat	Manduca s	TR68|c0_g1_i1|m.63	ML1P_MAI	35.24	1.00E-11	0	MD-2-relat	Manduca s	PF02221.1	.	Lysosome	.
TR5495|c0_g2	-9.09	1.12E-11	TR5495|c0_g2_i1	TAKT_DRO	31.71	8.00E-15	to CG1185	Protein tak	Drosophila	TR5495|c0_g2_i1|m.6194	TAKT_DRO	31.25	1.00E-15	to CG1185	Protein tak	Drosophila	PF06585.6	.	.	.
TR6319|c6_g2	-9.09	1.32E-108	TR6319|c6_g2_i3	CATL_SARI	56.43	9.00E-127	0	Cathepsin	Sarcophag	TR6319|c6_g2_i1|m.16999	CATL_SARI	57.23	2.00E-127	0	Cathepsin	Sarcophag	PF00112.1	GO:0008234^mo	Apoptosis`Apoptosis`Apoptosis`Apoptosis`Autoph	.
TR3634|c0_g1	-9.08	1.89E-11	TR3634|c0_g1_i1	TAKT_DRO	27.91	6.00E-13	to CG1185	Protein tak	Drosophila	TR3634|c0_g1_i1|m.3441	TAKT_DRO	27.91	8.00E-12	to CG1185	Protein tak	Drosophila	PF06585.6	.	.	.
TR6378|c9_g2	-9.07	1.98E-17	TR6378|c9_g2_i1	TBA1_DRO	99.05	2.00E-139	alphaTub8	Tubulin alp	Drosophila	TR6378|c9_g2_i1|m.18531	TBA1_DRO	99.05	7.00E-154	alphaTub8	Tubulin alp	Drosophila	PF00091.2	.	Apoptosis`Gap junction`Phagosome`Tight junction	.
TR4572|c0_g1	-9.07	1.12E-22	TR4572|c0_g1_i1	ATP5H_DR	33.33	1.00E-21	ATPsynD A	ATP syntha	Drosophila	TR4572|c0_g1_i1|m.4528	ATP5H_DR	33.7	2.00E-25	ATPsynD A	ATP syntha	Drosophila	PF05873.7	GO:0015078^mo	Oxidative phosphorylation	.
TR5170|c1_g1	-9.05	2.78E-27	TR5170|c1_g1_i2	H33_XENT	100	6.00E-87	TGas113e2	Histone H3	Xenopus tr	TR5170|c1_g1_i1|m.5554	H33_XENT	100	1.00E-93	TGas113e2	Histone H3	Xenopus tr	PF00125.1	GO:0003677^mo	.	.
TR5894|c3_g1	-9.04	1.31E-14	TR5894|c3_g1_i1	TKTL2_MO	54.94	3.00E-79	Tktl2	Transketol	Mus muscu	TR5894|c3_g1_i1|m.7389	TKTL2_MO	54.94	3.00E-83	Tktl2	Transketol	Mus muscu	PF00456.1	.	Biosynthesis of amino acids`Carbon metabolism`Pe	.
TR8222|c0_g1	-9.04	3.74E-30	TR8222|c0_g1_i1	RS20_XENI	85.47	5.00E-63	rps20	40S riboso	Xenopus la	TR8222|c0_g1_i1|m.20529	RS20_DRO	83.33	3.00E-65	RpS20 CG1	40S riboso	Drosophila	PF00338.1	.	Ribosome	.
TR5907|c1_g1	-9.03	6.97E-31	TR5907|c1_g1_i1	RS24_SPOI	84.09	8.00E-74	RpS24	40S riboso	Spodopter	TR5907|c1_g1_i1|m.7434	RS24_SPOI	84.09	4.00E-74	RpS24	40S riboso	Spodopter	PF01282.1	GO:0003735^mo	Ribosome	.
TR4516|c0_g2	-9.03	6.00E-14	TR4516|c0_g2_i1	ENO_DROI	74.56	4.00E-51	Eno CG176	Enolase (EC	Drosophila	TR4516|c0_g2_i1|m.4437	ENO_HOM	78.38	4.00E-54	0	Enolase (EC	Homarus g	PF03952.1	GO:0000287^mo	Biosynthesis of amino acids`Carbon metabolism`Gl	.
TR6378|c9_g1	-9.03	8.14E-12	TR6378|c9_g1_i1	TBA3_DRO	100	4.00E-62	alphaTub8	Tubulin alp	Drosophila	TR6378|c9_g1_i1|m.18530	TBA1_DRO	100	2.00E-66	alphaTub8	Tubulin alp	Drosophila	PF03953.1	GO:0003924^mo	Apoptosis`Gap junction`Phagosome`Tight junction	.
TR681|c1_g1	-9.00	1.09E-13	TR681|c1_g1_i1	GRP75_CH	84.11	1.00E-117	HSPA9 RCJ	Stress-70 p	Gallus gallu	TR681|c1_g1_i1|m.604	GRP75_PO	83.33	8.00E-144	HSPA9	Stress-70 p	Pongo abe	PF00012.1	.	RNA degradation	.
TR257|c0_g1	-8.98	1.85E-13	TR257|c0_g1_i1	SSRB_CAN	57.55	5.00E-49	.	.	.	TR257|c0_g1_i1|m.223	SSRB_MOU	55.41	3.00E-50	Ssr2	Translocon	Mus muscu	PF05753.9	GO:0005783^cell	Protein processing in endoplasmic reticulum	.
TR4112|c2_g1	-8.98	4.82E-12	TR4112|c2_g1_i1	ENDOU_DI	41.06	1.00E-30	CG2145	Poly(U)-sp	Drosophila	TR4112|c2_g1_i1|m.3979	ENDOU_DI	41.06	7.00E-31	CG2145	Poly(U)-sp	Drosophila	PF09412.5	GO:0016788^mo	.	.
TR6131|c8_g1	-8.98	4.07E-28	TR6131|c8_g1_i1	HSP83_BO	86.91	0	Hsp83 Hsp	Heat shock	Bombyx m	TR6131|c8_g1_i1|m.11045	HSP83_DR	79.42	0	Hsp83 Hsp	Heat shock	Drosophila	PF00183.1	GO:0005524^mo	Protein processing in endoplasmic reticulum	.
TR7651|c0_g1	-8.97	7.24E-14	TR7651|c0_g1_i1	VA3_SOLRI	43.96	6.00E-49	0	Venom alle	Solenopsis	TR7651|c0_g1_i1|m.20182	VA3_SOLRI	45.54	4.00E-48	0	Venom alle	Solenopsis	PF00188.2	.	.	.
TR1066|c0_g1	-8.96	2.02E-14	TR1066|c0_g1_i1	ATPO_DRC	56.1	1.00E-32	ATPsynO C	ATP syntha	Drosophila	TR1066|c0_g1_i1|m.885	ATPO_DRC	56.1	2.00E-44	ATPsynO C	ATP syntha	Drosophila	PF00213.1	GO:0046933^mo	Oxidative phosphorylation	.
TR6054|c8_g1	-8.95	4.64E-14	TR6054|c8_g1_i1	ECHM_CAE	70	1.00E-70	ech-6 T05G	Probable e	Caenorhab	TR6054|c8_g1_i1|m.9044	ECHM_CAE	70	2.00E-75	ech-6 T05G	Probable e	Caenorhab	PF00378.1	GO:0003824^mo	beta-Alanine metabolism`Butanoate metabolism`C	.
TR6103|c0_g1	-8.95	1.02E-12	TR6103|c0_g1_i1	.			.	.	.	TR6103|c0_g1_i1|m.10250	.			.	.	.	.	.	.	.
TR4525|c1_g1	-8.91	1.31E-13	TR4525|c1_g1_i1	CATA_CAV	69.35	2.00E-97	CAT	Catalase (E	Cavia porc	TR4525|c1_g1_i1|m.4452	CATA_CAV	69.35	2.00E-96	CAT	Catalase (E	Cavia porc	PF00199.1	GO:0004096^mo	Carbon metabolism`FoxO signaling pathway`Glyoxy	.
TR6435|c5_g3	-8.89	3.94E-14	TR6435|c5_g3_i2	SSP1_BOM	37.7	1.00E-06	SP1	Sex-specifi	Bombyx m	TR6435|c5_g3_i2|m.19247	ARYA_MAI	31.46	7.00E-07	0	Arylphorin	Manduca s	PF03722.9	.	.	.
TR7799|c0_g1	-8.88	1.20E-10	TR7799|c0_g1_i1	SODC_CER	78.57	2.00E-79	Sod	Superoxide	Ceratitis ca	TR7799|c0_g1_i1|m.20270	SODC_CER	78.57	4.00E-75	Sod	Superoxide	Ceratitis ca	PF00080.1	GO:0046872^mo	Longevity regulating pathway - multiple species`Pe	.
TR4920|c0_g1	-8.88	8.03E-13	TR4920|c0_g1_i1	4EBP2_MC	49.09	5.00E-28	Eif4ebp2	Eukaryotic	Mus muscu	TR4920|c0_g1_i1|m.5136	4EBP2_MC	49.09	7.00E-29	Eif4ebp2	Eukaryotic	Mus muscu	PF05456.6	GO:0008190^mo	Longevity regulating pathway - multiple species`RN	.
TR1066|c0_g2	-8.87	1.67E-12	TR1066|c0_g2_i1	ATPO_DRC	53.49	3.00E-22	ATPsynO C	ATP syntha	Drosophila	TR1066|c0_g2_i1|m.886	ATPO_DRC	51.69	1.00E-22	ATPsynO C	ATP syntha	Drosophila	PF00213.1	GO:0046933^mo	Oxidative phosphorylation	.
TR6828|c0_g1	-8.86	8.59E-12	TR6828|c0_g1_i1	QCR7_BOV	46.75	3.00E-16	UQCRB	Cytochrom	Bos taurus	TR6828|c0_g1_i1|m.19750	QCR7_BOV	46.81	8.00E-21	UQCRB	Cytochrom	Bos taurus	PF02271.1	GO:0006122^biol	Oxidative phosphorylation	.
TR5775|c1_g1	-8.86	4.31E-13	TR5775|c1_g1_i1	AATM_RAI	68.12	1.00E-95	GOT2	Aspartate a	Oryctolagu	TR5775|c1_g1_i1|m.6977	AATM_RAI	68.12	7.00E-101	GOT2	Aspartate a	Oryctolagu	PF00155.1	GO:0030170^mo	2-Oxocarboxylic acid metabolism`Alanine, aspartat	.

TR6123|c9_g1	-8.85	2.09E-12	TR6123|c9_g1_i1	.			.	.	.	TR6123|c9_g1_i1|m.10754	.			.	.	.	PF01607.1	GO:0008061^mo	.	.
TR5435|c0_g1	-8.85	2.15E-13	TR5435|c0_g1_i1	ALDR_RAB	61.3	6.00E-82	AKR1B1	Aldose red	Oryctolagu	TR5435|c0_g1_i1|m.6039	A1A1A_DA	55.07	3.00E-88	akr1a1a si:	Alcohol de	Danio reric	PF00248.1	.	Fructose and mannose metabolism`Galactose meta	.
TR5435|c0_g2	-8.85	2.84E-12	TR5435|c0_g2_i1	ALDR_RAB	63.18	7.00E-81	AKR1B1	Aldose red	Oryctolagu	TR5435|c0_g2_i1|m.6040	A1A1A_DA	56.62	3.00E-88	akr1a1a si:	Alcohol de	Danio reric	PF00248.1	.	Fructose and mannose metabolism`Galactose meta	.
TR7845|c0_g1	-8.83	1.68E-05	TR7845|c0_g1_i1	.			.	.	.	TR7845|c0_g1_i1|m.20287	.			.	.	.	PF01607.1	GO:0008061^mo	.	.
TR2671|c0_g1	-8.83	1.21E-12	TR2671|c0_g1_i1	MP20_DRC	54.35	4.00E-49	Mp20 Tpn	Muscle-spe	Drosophila	TR2671|c0_g1_i1|m.2387	MP20_DRC	53.57	3.00E-50	Mp20 Tpn	Muscle-spe	Drosophila	PF00307.2	GO:0005515^mo	.	.
TR5505|c0_g1	-8.82	1.48E-19	TR5505|c0_g1_i1	LIP3_DRON	43.26	1.00E-99	Lip3 CG882	Lipase 3 (D	Drosophila	TR5505|c0_g1_i1|m.6225	LIP3_DRON	43.26	1.00E-102	Lip3 CG882	Lipase 3 (D	Drosophila	PF00561.1	GO:0006629^biol	Lysosome`Steroid biosynthesis	.
TR4541|c0_g1	-8.82	1.57E-12	TR4541|c0_g1_i1	RL14_DRO	48.33	4.00E-15	RpL14 GJ1	60S riboso	Drosophila	TR4541|c0_g1_i1|m.4479	RL14_DRO	44.44	4.00E-16	RpL14 GJ1	60S riboso	Drosophila	PF01929.1	GO:0003735^mo	Ribosome	.
TR4590|c0_g1	-8.80	3.09E-10	TR4590|c0_g1_i1	CISY_GLON	85.2	5.00E-140	0	Probable c	Glossina m	TR4590|c0_g1_i1|m.4563	CISY_GLON	85.2	7.00E-143	0	Probable c	Glossina m	PF00285.1	GO:0046912^mo	2-Oxocarboxylic acid metabolism`Biosynthesis of ai	.
TR4653|c1_g1	-8.80	1.07E-11	TR4653|c1_g1_i1	ACDSB_HU	66.67	1.00E-117	ACADSB	Short/bran	Homo sapi	TR4653|c1_g1_i1|m.4654	ACDSB_HU	66.4	5.00E-123	ACADSB	Short/bran	Homo sapi	PF00441.1	GO:0003995^mo	Fatty acid degradation`Fatty acid metabolism`Valin	.
TR4914|c0_g1	-8.79	1.05E-13	TR4914|c0_g1_i1	FRI_AEDAE	44.83	8.00E-47	FERH AAEL	Ferritin sub	Aedes aegy	TR4914|c0_g1_i1|m.5128	FRI_AEDAE	44.61	8.00E-49	FERH AAEL	Ferritin sub	Aedes aegy	PF00210.1	GO:0008199^mo	.	.
TR4586|c1_g1	-8.79	3.35E-10	TR4586|c1_g1_i1	.			.	.	.	TR4586|c1_g1_i1|m.4553	.			.	.	.	.	.	.	.
TR6353|c12_g1	-8.79	1.60E-14	TR6353|c12_g1_i1	EF1A2_DR	91.09	3.00E-58	Ef1alpha10	Elongation	Drosophila	TR6353|c12_g1_i1|m.18158	EF1A1_DR	86.84	1.00E-65	Ef1alpha48	Elongation	Drosophila	PF03143.1	GO:0005525^mo	RNA transport	.
TR6212|c1_g1	-8.78	4.69E-44	TR6212|c1_g1_i2	RL11_DRO	89.01	8.00E-114	RpL11 RPL	60S riboso	Drosophila	TR6212|c1_g1_i2|m.13544	RL11_DRO	89.01	1.00E-116	RpL11 RPL	60S riboso	Drosophila	PF00281.1	GO:0003735^mo	Ribosome`Ribosome	.
TR5670|c1_g1	-8.77	6.19E-12	TR5670|c1_g1_i1	NP1L4_MC	47.9	4.00E-25	Nap1l4	Nucleosom	Mus muscu	TR5670|c1_g1_i1|m.6685	NP1L4_MC	48.72	2.00E-25	Nap1l4	Nucleosom	Mus muscu	PF00956.1	GO:0006334^biol	.	.
TR8603|c0_g1	-8.77	1.87E-28	TR8603|c0_g1_i1	RS30_RAT	83.05	2.00E-19	Fau	40S riboso	Rattus nor	TR8603|c0_g1_i1|m.20731	RS30_ORYI	71.19	2.00E-20	fau rps30	40S riboso	Oryzias lati	PF00240.1	GO:0005515^mo	Ribosome	.
TR4598|c0_g1	-8.75	1.85E-12	TR4598|c0_g1_i1	.			.	.	.	TR4598|c0_g1_i1|m.4569	.			.	.	.	.	.	.	.
TR5602|c0_g1	-8.74	2.86E-11	TR5602|c0_g1_i1	ACO11_SP	38.32	2.00E-53	0	Acyl-CoA D	Spodopter	TR5602|c0_g1_i1|m.6447	ACO11_SP	37.97	4.00E-58	0	Acyl-CoA D	Spodopter	.	.	Biosynthesis of unsaturated fatty acids`Fatty acid n	.
TR6307|c21_g1	-8.73	4.16E-12	TR6307|c21_g1_i1	ATC1_ANC	88.21	2.00E-155	Ca-P60A A	Calcium-tra	Anopheles	TR6307|c21_g1_i1|m.16638	ATC1_ANC	88.21	3.00E-162	Ca-P60A A	Calcium-tra	Anopheles	PF00702.2	.	Calcium signaling pathway	.
TR5228|c2_g1	-8.73	5.40E-12	TR5228|c2_g1_i1	MAL1_DRC	49.85	1.00E-114	Mal-A1 Lvp	Maltase A1	Drosophila	TR5228|c2_g1_i1|m.5679	MAL1_DRC	50.15	7.00E-111	Mal-A1 Lvp	Maltase A1	Drosophila	PF00128.1	GO:0003824^mo	Galactose metabolism`Starch and sucrose metabol	.
TR8940|c0_g1	-8.73	4.81E-12	TR8940|c0_g1_i1	TNNC_TAC	60.14	9.00E-48	0	Troponin C	Tachypleus	TR8940|c0_g1_i1|m.20929	TNNC1_DR	62.76	1.00E-55	TpnC41C T	Troponin C	Drosophila	PF00036.2	GO:0005509^mo	.	.
TR5897|c0_g1	-8.72	1.27E-12	TR5897|c0_g1_i1	PRDX1_DR	79.66	3.00E-63	Jafrac1 TP	Peroxiredo	Drosophila	TR5897|c0_g1_i1|m.7403	PRDX1_DR	77.69	3.00E-66	Jafrac1 TP	Peroxiredo	Drosophila	PF00578.1	GO:0016209^mo	Peroxisome	.
TR4710|c0_g1	-8.72	4.95E-12	TR4710|c0_g1_i1	DCOR_CHI	50.98	6.00E-10	ODC1 ODC	Ornithine c	Gallus gallu	TR4710|c0_g1_i1|m.4746	DCOR_CHI	50.98	2.00E-11	ODC1 ODC	Ornithine c	Gallus gallu	PF00278.1	GO:0003824^mo	Arginine and proline metabolism`Glutathione meta	.
TR4914|c0_g2	-8.72	4.88E-12	TR4914|c0_g2_i1	FRI_AEDAE	44.83	8.00E-47	FERH AAEL	Ferritin sub	Aedes aegy	TR4914|c0_g2_i1|m.5129	FRI_AEDAE	44.61	8.00E-49	FERH AAEL	Ferritin sub	Aedes aegy	PF00210.1	GO:0008199^mo	.	.
TR4520|c0_g1	-8.70	7.46E-13	TR4520|c0_g1_i1	TSPO_RAT	45.75	1.00E-48	Tspo Bzrp	Translocat	Rattus nor	TR4520|c0_g1_i1|m.4440	TSPO_RAT	45.16	8.00E-46	Tspo Bzrp	Translocat	Rattus nor	PF03073.1	GO:0016021^cell	Apoptosis - fly`Neuroactive ligand-receptor interac	.
TR6226|c5_g1	-8.69	2.78E-28	TR6226|c5_g1_i1	.			.	.	.	TR6226|c5_g1_i1|m.14034	.			.	.	.	PF03103.1	.	.	.
TR4611|c0_g1	-8.69	8.55E-13	TR4611|c0_g1_i1	TCPE_MAC	78.28	6.00E-103	CCT5 QtsA	T-complex	Macaca fas	TR4611|c0_g1_i1|m.4591	TCPE_MAC	78.28	9.00E-124	CCT5 QtsA	T-complex	Macaca fas	PF00118.1	GO:0005524^mo	.	.
TR3856|c0_g1	-8.68	9.01E-12	TR3856|c0_g1_i1	NCPR_DRC	68.38	1.00E-120	Cpr CG115	NADPH--cy	Drosophila	TR3856|c0_g1_i1|m.3677	NCPR_DRC	68.38	3.00E-131	Cpr CG115	NADPH--cy	Drosophila	PF00175.1	GO:0016491^mo	.	.
TR3844|c1_g1	-8.67	8.49E-14	TR3844|c1_g1_i1	GPX_PROC	48.91	9.00E-34	GPx	Glutathion	Procambar	TR3844|c1_g1_i1|m.3669	GPX_PROC	48.91	6.00E-35	GPx	Glutathion	Procambar	PF00255.1	GO:0004602^mo	Arachidonic acid metabolism`Glutathione metaboli	.
TR6342|c27_g1	-8.66	2.26E-08	TR6342|c27_g1_i1	CUD2_SCH	66.67	1.00E-09	0	Endocuticl	Schistocer	TR6342|c27_g1_i1|m.17882	CUD2_SCH	67.57	9.00E-10	0	Endocuticl	Schistocer	.	.	.	.
TR2916|c0_g1	-8.66	4.63E-12	TR2916|c0_g1_i1	COX5A_DR	52.63	1.00E-36	COX5A Co	Cytochrom	Drosophila	TR2916|c0_g1_i1|m.2686	COX5A_DR	52.63	1.00E-48	COX5A Co	Cytochrom	Drosophila	PF02284.1	GO:0004129^mo	Oxidative phosphorylation	.
TR3411|c0_g1	-8.66	4.35E-10	TR3411|c0_g1_i1	ELOV4_MC	37.12	9.00E-42	Elovl4	Elongation	Mus muscu	TR3411|c0_g1_i1|m.3217	ELOV4_MC	37.02	1.00E-43	Elovl4	Elongation	Mus muscu	PF01151.1	GO:0016021^cell	.	.
TR5994|c0_g4	-8.65	5.24E-11	TR5994|c0_g4_i1	CRYL1_HU	52.17	3.00E-51	CRYL1 CRY	Lambda-cr	Homo sapi	TR5994|c0_g4_i1|m.8238	CRYL1_HU	52.17	4.00E-53	CRYL1 CRY	Lambda-cr	Homo sapi	PF00725.1	GO:0003857^mo	Pentose and glucuronate interconversions	.
TR2522|c0_g1	-8.64	1.70E-13	TR2522|c0_g1_i1	IM23_SCHI	36.52	8.00E-13	0	23 kDa inte	Schistoson	TR2522|c0_g1_i1|m.2233	CD9_BOVI	30.22	6.00E-20	CD9	CD9 antige	Bos taurus	PF00335.1	GO:0016021^cell	Lysosome	.
TR8766|c0_g1	-8.63	3.24E-12	TR8766|c0_g1_i1	RPAB3_MC	74.8	6.00E-61	Polr2h	DNA-direct	Mus muscu	TR8766|c0_g1_i1|m.20856	RPAB3_MC	74.8	2.00E-62	Polr2h	DNA-direct	Mus muscu	PF03870.1	GO:0006351^biol	Cytosolic DNA-sensing pathway`Purine metabolism	.
TR4309|c1_g1	-8.59	9.92E-11	TR4309|c1_g1_i1	TALDO_HU	74	5.00E-102	TALDO1 TA	Transaldol	Homo sapi	TR4309|c1_g1_i1|m.4191	TALDO_HU	74	2.00E-108	TALDO1 TA	Transaldol	Homo sapi	PF00923.1	GO:0005975^biol	Biosynthesis of amino acids`Carbon metabolism`Pe	.
TR3654|c0_g1	-8.59	1.83E-09	TR3654|c0_g1_i1	CUD8_SCH	44	2.00E-22	0	Endocuticl	Schistocer	TR3654|c0_g1_i1|m.3467	CUD2_SCH	50	5.00E-21	0	Endocuticl	Schistocer	PF00379.1	GO:0042302^mo	.	.
TR5702|c2_g1	-8.58	6.35E-13	TR5702|c2_g1_i1	QCR2_HUN	38.83	1.00E-33	UQCRC2	Cytochrom	Homo sapi	TR5702|c2_g1_i1|m.6761	QCR2_HUN	39.08	8.00E-35	UQCRC2	Cytochrom	Homo sapi	PF00675.1	.	Oxidative phosphorylation	.
TR1115|c0_g1	-8.57	2.06E-08	TR1115|c0_g1_i1	LEG8_RAT	31.94	5.00E-17	Lgals8	Galectin-8	Rattus nor	TR1115|c0_g1_i1|m.931	LEG8_RAT	31.94	7.00E-17	Lgals8	Galectin-8	Rattus nor	PF00337.1	GO:0030246^mo	.	.
TR4799|c0_g1	-8.55	1.15E-11	TR4799|c0_g1_i1	COGS_UCA	25.24	3.00E-12	0	Brachyurin	Uca pugilat	TR4799|c0_g1_i1|m.4920	COGS_UCA	27.78	6.00E-17	0	Brachyurin	Uca pugilat	PF00089.2	GO:0004252^mo	.	.
TR5994|c0_g2	-8.55	3.61E-11	TR5994|c0_g2_i1	CRYL1_HU	51.55	1.00E-50	CRYL1 CRY	Lambda-cr	Homo sapi	TR5994|c0_g2_i1|m.8236	CRYL1_HU	51.55	2.00E-52	CRYL1 CRY	Lambda-cr	Homo sapi	PF00725.1	GO:0003857^mo	Pentose and glucuronate interconversions	.
TR6131|c13_g1	-8.54	8.23E-12	TR6131|c13_g1_i1	HSP83_DR	97.44	8.00E-74	Hsp83 Hsp	Heat shock	Drosophila	TR6131|c13_g1_i1|m.11054	HSP83_DR	87.33	1.00E-81	Hsp83 Hsp	Heat shock	Drosophila	PF00183.1	GO:0005524^mo	Protein processing in endoplasmic reticulum	.
TR6054|c2_g1	-8.53	2.10E-11	TR6054|c2_g1_i1	.			.	.	.	TR6054|c2_g1_i1|m.9032	.			.	.	.	.	.	.	.
TR5698|c1_g1	-8.52	2.17E-12	TR5698|c1_g1_i1	SQD_DRON	61.88	2.00E-59	sqd hrp40	RNA-bindir	Drosophila	TR5698|c1_g1_i1|m.6743	SQD_DRON	61.88	8.00E-58	sqd hrp40	RNA-bindir	Drosophila	PF00076.1	GO:0003676^mo	Dorso-ventral axis formation	.
TR5861|c0_g1	-8.52	7.08E-11	TR5861|c0_g1_i1	.			.	.	.	TR5861|c0_g1_i1|m.7303	.			.	.	.	PF01223.1	GO:0003676^mo	.	.
TR6322|c22_g1	-8.51	2.10E-10	TR6322|c22_g1_i1	PPB_BOMI	45.64	5.00E-77	Alp-m	Membrane	Bombyx m	TR6322|c22_g1_i1|m.17125	PPB_BOMI	44.95	2.00E-78	Alp-m	Membrane	Bombyx m	PF00245.1	GO:0016791^mo	Folate biosynthesis`Thiamine metabolism	.
TR3449|c0_g1	-8.50	2.41E-13	TR3449|c0_g1_i1	ASPP_AED	75.16	4.00E-78	AAEL0061	Lysosomal	Aedes aegy	TR3449|c0_g1_i1|m.3250	ASPP_AED	75.16	9.00E-79	AAEL0061	Lysosomal	Aedes aegy	PF00026.1	GO:0004190^mo	Apoptosis`Autophagy - animal`Lysosome`Sphingoli	.
TR6123|c6_g1	-8.50	8.20E-35	TR6123|c6_g1_i1	MDHM_RA	69.23	5.00E-161	Mdh2 Mor	Malate deh	Rattus nor	TR6123|c6_g1_i1|m.10739	MDHM_HU	68.64	1.00E-169	MDH2	Malate deh	Homo sapi	PF00056.1	GO:0016491^mo	Carbon metabolism`Carbon metabolism`Citrate cyc	.
TR3469|c1_g2	-8.50	2.21E-10	TR3469|c1_g2_i1	SAHH_ANC	81.69	1.00E-79	Ahcy13 AG	Adenosylh	Anopheles	TR3469|c1_g2_i1|m.3270	SAHH_ANC	81.69	2.00E-81	Ahcy13 AG	Adenosylh	Anopheles	PF00670.1	GO:0004013^mo	Cysteine and methionine metabolism	.
TR1911|c0_g1	-8.48	1.16E-17	TR1911|c0_g1_i1	COX42_TH	33.93	7.00E-18	0	Cytochrom	Thunnus o	TR1911|c0_g1_i1|m.1626	COX42_TH	33.93	2.00E-17	0	Cytochrom	Thunnus o	PF02936.9	GO:0004129^mo	Oxidative phosphorylation	.
TR6069|c7_g1	-8.46	5.15E-11	TR6069|c7_g1_i1	TALDO_HU	69.63	1.00E-55	TALDO1 TA	Transaldol	Homo sapi	TR6069|c7_g1_i1|m.9361	TALDO_HU	69.63	2.00E-63	TALDO1 TA	Transaldol	Homo sapi	PF00923.1	GO:0005975^biol	Biosynthesis of amino acids`Carbon metabolism`Pe	.
TR618|c0_g1	-8.45	4.93E-11	TR618|c0_g1_i1	STUB_DRO	33.04	7.00E-35	Sb Sb-sbd	Serine prot	Drosophila	TR618|c0_g1_i1|m.545	STUB_DRO	32.89	1.00E-34	Sb Sb-sbd	Serine prot	Drosophila	PF00089.2	GO:0004252^mo	.	.
TR4894|c2_g1	-8.43	1.04E-10	TR4894|c2_g1_i1	TSSP_MOU	36.27	2.00E-15	Prss16 Tss	Thymus-sp	Mus muscu	TR4894|c2_g1_i1|m.5091	TSSP_MOU	36.27	3.00E-16	Prss16 Tss	Thymus-sp	Mus muscu	PF05577.7	GO:0008236^mo	.	.
TR6033|c1_g1	-8.43	2.22E-21	TR6033|c1_g1_i1	CATB_BOV	55.87	1.00E-120	CTSB	Cathepsin	Bos taurus	TR6033|c1_g1_i1|m.8477	CATB_RAT	54.84	3.00E-132	Ctsb	Cathepsin	Rattus nor	PF00112.1	GO:0004197^mo	Apoptosis`Autophagy - animal`Lysosome	.
TR1494|c1_g1	-8.42	2.56E-11	TR1494|c1_g1_i1	NDUB5_PA	40.34	1.00E-21	NDUFB5	NADH deh	Pan troglo	TR1494|c1_g1_i1|m.1256	NDUB5_PA	39.34	2.00E-20	NDUFB5	NADH deh	Pan troglo	PF09781.4	.	Oxidative phosphorylation	.
TR370|c1_g1	-8.42	1.61E-11	TR370|c1_g1_i1	GPX3_CAE	42.98	4.00E-26	gpx-3 C11E	Glutathion	Caenorhab	TR370|c1_g1_i1|m.347	GPX3_CAE	42.98	3.00E-25	gpx-3 C11E	Glutathion	Caenorhab	PF00255.1	GO:0004602^mo	Arachidonic acid metabolism`Glutathione metaboli	.
TR5838|c3_g1	-8.42	2.44E-22	TR5838|c3_g1_i1	MP20_DRC	73.51	2.00E-94	Mp20 Tpn	Muscle-spe	Drosophila	TR5838|c3_g1_i1|m.7196	MP20_DRC	73.51	1.00E-98	Mp20 Tpn	Muscle-spe	Drosophila	PF00307.2	GO:0005515^mo	.	.
TR6258|c1_g1	-8.42	1.12E-47	TR6258|c1_g1_i1	G3P2_DRO	87.95	0	Gapdh2 GA	Glyceralde	Drosophila	TR6258|c1_g1_i1|m.15172	G3P2_DRO	87.95	0	Gapdh2 GA	Glyceraldel	Drosophila	PF00044.1	GO:0016620^mo	Biosynthesis of amino acids`Carbon metabolism`Gl	.
TR916|c0_g1	-8.41	3.12E-10	TR916|c0_g1_i1	VATE_MAN	70.98	4.00E-72	VHA26	V-type pro	Manduca s	TR916|c0_g1_i1|m.781	VATE_MAN	70.98	2.00E-95	VHA26	V-type pro	Manduca s	PF01991.1	GO:0046961^mo	mTOR signaling pathway`Oxidative phosphorylatior	.
TR4113|c0_g1	-8.40	3.11E-11	TR4113|c0_g1_i1	MPPB_RAT	70.39	1.00E-153	Pmpcb Mp	Mitochond	Rattus nor	TR4113|c0_g1_i1|m.3980	MPPB_HU	70.39	2.00E-166	PMPCB MF	Mitochond	Homo sapi	PF00675.1	.	.	.
TR5565|c0_g1	-8.39	2.90E-10	TR5565|c0_g1_i1	.			.	.	.	TR5565|c0_g1_i1|m.6363	.			.	.	.	.	.	.	.
TR2673|c0_g1	-8.38	9.55E-18	TR2673|c0_g1_i1	IDHC_MICI	77.89	0	IDH1 IDP2	Isocitrate c	Microtus n	TR2673|c0_g1_i1|m.2390	IDHC_MICI	77.89	0	IDH1 IDP2	Isocitrate c	Microtus n	PF00180.1	GO:0016616^mo	2-Oxocarboxylic acid metabolism`Biosynthesis of ai	.
TR6044|c28_g1	-8.36	5.00E-21	TR6044|c28_g1_i1	RS5_HUMA	97.39	3.00E-71	RPS5	40S riboso	Homo sapi	TR6044|c28_g1_i1|m.8782	RS5_HUMA	97.39	8.00E-75	RPS5	40S riboso	Homo sapi	PF00177.1	.	Ribosome	.
TR5994|c0_g1	-8.36	5.57E-11	TR5994|c0_g1_i1	CRYL1_HU	53.06	2.00E-48	CRYL1 CRY	Lambda-cr	Homo sapi	TR5994|c0_g1_i1|m.8235	CRYL1_HU	53.06	1.00E-50	CRYL1 CRY	Lambda-cr	Homo sapi	PF00725.1	GO:0003857^mo	Pentose and glucuronate interconversions	.
TR9388|c0_g1	-8.36	1.25E-09	TR9388|c0_g1_i1	AL7A1_CAI	72.85	2.00E-110	alh-9 F01F	Putative al	Caenorhab	TR9388|c0_g1_i1|m.21193	AL7A1_CAI	72.85	2.00E-113	alh-9 F01F	Putative al	Caenorhab	PF00171.1	GO:0016491^mo	Arginine and proline metabolism`Ascorbate and alc	.
TR5640|c3_g1	-8.34	5.14E-11	TR5640|c3_g1_i1	TBA1_DRO	97.59	1.00E-113	alphaTub8	Tubulin alp	Drosophila	TR5640|c3_g1_i1|m.6559	TBA1_DRO	97.59	7.00E-117	alphaTub8	Tubulin alp	Drosophila	PF00091.2	GO:0003924^mo	Apoptosis`Gap junction`Phagosome`Tight junction	.
TR6353|c20_g1	-8.34	3.77E-09	TR6353|c20_g1_i1	EF1A_BOM	93.03	1.00E-132	0	Elongation	Bombyx m	TR6353|c20_g1_i1|m.18162	EF1A_BOM	93.03	4.00E-136	0	Elongation	Bombyx m	PF03143.1	GO:0005525^mo	RNA transport	.
TR3190|c0_g1	-8.33	3.05E-21	TR3190|c0_g1_i1	TAKT_DRO	35.71	3.00E-35	to CG1185	Protein tak	Drosophila	TR3190|c0_g1_i1|m.3011	TAKT_DRO	33.2	1.00E-35	to CG1185	Protein tak	Drosophila	PF06585.6	.	.	.
TR4658|c0_g1	-8.32	3.66E-09	TR4658|c0_g1_i1	XYL2_EME	41.84	2.00E-27	xdhA AN9	Probable D	Emericella	TR4658|c0_g1_i1|m.4663	ARPD_ENT	34.78	4.00E-30	0	D-arabitol-	Enterococ	PF08240.7	GO:0016491^mo	.	.
TR3749|c0_g1	-8.31	5.84E-09	TR3749|c0_g1_i1	CBPB_AST	45.56	2.00E-80	0	Carboxype	Astacus as	TR3749|c0_g1_i1|m.3574	CBPB_AST	45.39	1.00E-79	0	Carboxype	Astacus as	PF00246.1	GO:0004181^mo	.	.
TR9531|c0_g1	-8.31	1.76E-10	TR9531|c0_g1_i1	SSRD_PON	45.07	5.00E-37	SSR4	Translocon	Pongo abe	TR9531|c0_g1_i1|m.21244	SSRD_MOU	45.21	6.00E-40	Ssr4	Translocon	Mus muscu	PF05404.7	GO:0005783^cell	Protein processing in endoplasmic reticulum	.
TR4647|c0_g1	-8.31	1.80E-09	TR4647|c0_g1_i1	ACO11_TR	56.23	2.00E-111	D11DS PGI	Acyl-CoA D	Trichoplusi	TR4647|c0_g1_i1|m.4645	ACO11_TR	54.74	4.00E-108	D11DS PGI	Acyl-CoA D	Trichoplusi	PF00487.1	GO:0006629^biol	Biosynthesis of unsaturated fatty acids`Fatty acid n	.
TR5238|c0_g1	-8.31	1.05E-17	TR5238|c0_g1_i1	PEB3_DRO	57.8	1.00E-43	EbpIII PebI	Ejaculatory	Drosophila	TR5238|c0_g1_i1|m.5698	PEB3_DRO	57.8	2.00E-42	EbpIII PebI	Ejaculatory	Drosophila	PF03392.8	.	.	.
TR6012|c1_g1	-8.30	1.38E-09	TR6012|c1_g1_i1	IDGF4_DR	56.13	1.00E-44	Idgf4 CG17	Chitinase-l	Drosophila	TR6012|c1_g1_i1|m.8309	IDGF4_DR	56.13	3.00E-44	Idgf4 CG17	Chitinase-li	Drosophila	PF00704.2	GO:0004553^mo	.	.
TR4500|c0_g1	-8.30	2.99E-10	TR4500|c0_g1_i1	CRYL1_HU	52.59	5.00E-35	CRYL1 CRY	Lambda-cr	Homo sapi	TR4500|c0_g1_i1|m.4415	CRYL1_HU	52.59	2.00E-36	CRYL1 CRY	Lambda-cr	Homo sapi	PF00725.1	GO:0003857^mo	Pentose and glucuronate interconversions	.
TR5479|c2_g1	-8.29	3.18E-09	TR5479|c2_g1_i1	PPO2_DRC	38.56	3.00E-46	PPO2 proP	Phenoloxic	Drosophila	TR5479|c2_g1_i1|m.6158	PPO2_DRC	38.56	7.00E-45	PPO2 proP	Phenoloxic	Drosophila	PF00372.1	.	.	.
TR4195|c0_g1	-8.29	3.33E-26	TR4195|c0_g1_i1	RS17_SPOI	90.4	2.00E-77	RpS17	40S riboso	Spodopter	TR4195|c0_g1_i1|m.4074	RS17_SPOI	87.88	3.00E-81	RpS17	40S riboso	Spodopter	PF00833.1	GO:0003735^mo	Ribosome	.
TR1866|c0_g1	-8.29	1.28E-10	TR1866|c0_g1_i1	GST2_MAN	26.8	2.00E-07	GST2	Glutathion	Manduca s	TR1866|c0_g1_i1|m.1592	GSTA4_DIC	33.33	2.00E-08	gsta4 DDB	Putative gl	Dictyosteli	PF00043.2	.	Arachidonic acid metabolism`Drug metabolism - cy	.
TR5945|c2_g1	-8.28	1.12E-43	TR5945|c2_g1_i2	RS2_DRON	90.54	8.00E-130	RpS2 sop C	40S riboso	Drosophila	TR5945|c2_g1_i1|m.7572	RS2_DRON	90.54	1.00E-144	RpS2 sop C	40S riboso	Drosophila	PF00333.1	GO:0003723^mo	Ribosome`Ribosome	.
TR4312|c0_g1	-8.27	3.02E-11	TR4312|c0_g1_i1	SPRC_CAEI	50.98	1.00E-27	ost-1 sparc	SPARC (Bas	Caenorhab	TR4312|c0_g1_i1|m.4193	SPRC_CAEI	50.86	5.00E-33	ost-1 sparc	SPARC (Bas	Caenorhab	PF10591.4	GO:0005509^mo	.	.
TR1531|c0_g1	-8.27	8.37E-10	TR1531|c0_g1_i1	NDUAD_PA	39	3.00E-12	NDUFA13	NADH deh	Pan troglo	TR1531|c0_g1_i1|m.1290	NDUAD_PA	39	5.00E-13	NDUFA13	NADH deh	Pan troglo	PF06212.7	.	Oxidative phosphorylation	.
TR3331|c0_g1	-8.27	2.05E-10	TR3331|c0_g1_i1	COGS_HYP	33.95	2.00E-16	0	Collagenas	Hypoderm	TR3331|c0_g1_i1|m.3144	COGS_HYP	33.95	5.00E-17	0	Collagenas	Hypoderm	PF00089.2	GO:0004252^mo	.	.
TR3630|c0_g2	-8.25	1.40E-09	TR3630|c0_g2_i1	GPMA_BDI	61.64	8.00E-24	gpmA Bd2	2,3-bispho	Bdellovibri	TR3630|c0_g2_i1|m.3439	GPMA_BDI	61.64	1.00E-24	gpmA Bd2	2,3-bispho	Bdellovibri	PF00300.1	.	Biosynthesis of amino acids`Carbon metabolism`Gl	.
TR4763|c0_g1	-8.25	1.96E-09	TR4763|c0_g1_i1	ELVL1_AED	38.33	2.00E-32	AAEL0080	Elongation	Aedes aegy	TR4763|c0_g1_i1|m.4836	ELVL1_AED	38.33	2.00E-26	AAEL0080	Elongation	Aedes aegy	PF01151.1	GO:0016021^cell	.	.
TR4586|c1_g2	-8.24	1.99E-09	TR4586|c1_g2_i1	.			.	.	.	TR4586|c1_g2_i1|m.4555	.			.	.	.	.	.	.	.
TR202|c0_g1	-8.23	3.16E-10	TR202|c0_g1_i1	RLP24_DR	61.11	9.00E-30	RpL24-like	Probable ri	Drosophila	TR202|c0_g1_i1|m.183	RLP24_DR	67.11	4.00E-28	RpL24-like	Probable ri	Drosophila	.	.	Ribosome	.
TR767|c0_g1	-8.23	5.80E-09	TR767|c0_g1_i1	THIO2_DR	60.78	3.00E-38	Trx-2	Thioredoxi	Drosophila	TR767|c0_g1_i1|m.681	THIO2_DR	62	3.00E-40	Trx-2	Thioredoxi	Drosophila	PF00085.1	GO:0016209^mo	.	.
TR6124|c0_g1	-8.22	7.05E-25	TR6124|c0_g1_i1	RL6_PIG^^	49.15	1.00E-47	RPL6	60S riboso	Sus scrofa	TR6124|c0_g1_i1|m.10768	RL6_PIG^^	49.15	1.00E-62	RPL6	60S riboso	Sus scrofa	PF01159.1	GO:0003735^mo	Ribosome	.
TR1863|c0_g1	-8.22	1.50E-14	TR1863|c0_g1_i1	CUD2_SCH	52.73	4.00E-34	0	Endocuticl	Schistocer	TR1863|c0_g1_i1|m.1590	CUD2_SCH	55.45	4.00E-31	0	Endocuticl	Schistocer	PF00379.1	GO:0042302^mo	.	.
TR6165|c34_g1	-8.21	1.58E-10	TR6165|c34_g1_i1	IDHC_MOU	79.71	2.00E-75	Idh1	Isocitrate c	Mus muscu	TR6165|c34_g1_i1|m.12303	IDHC_MOU	79.71	9.00E-78	Idh1	Isocitrate c	Mus muscu	PF00180.1	GO:0016616^mo	2-Oxocarboxylic acid metabolism`Biosynthesis of ai	.
TR2003|c0_g1	-8.21	5.84E-18	TR2003|c0_g1_i1	CATA_HUN	72.81	0	CAT	Catalase (E	Homo sapi	TR2003|c0_g1_i1|m.1731	CATA_HUN	70.59	0	CAT	Catalase (E	Homo sapi	PF00199.1	GO:0004096^mo	Carbon metabolism`FoxO signaling pathway`Glyoxy	.
TR5897|c1_g2	-8.21	1.18E-09	TR5897|c1_g2_i1	PRDX1_DR	76.47	9.00E-81	Jafrac1 TP	Peroxiredo	Drosophila	TR5897|c1_g2_i1|m.7405	PRDX1_DR	76.47	2.00E-83	Jafrac1 TP	Peroxiredo	Drosophila	PF00578.1	GO:0016209^mo	Peroxisome	.
TR772|c0_g1	-8.20	1.34E-09	TR772|c0_g1_i1	NDUBA_BC	61.72	1.00E-49	0	NADH deh	Bombyx m	TR772|c0_g1_i1|m.685	NDUBA_BC	59.85	5.00E-48	0	NADH deh	Bombyx m	PF10249.4	.	Oxidative phosphorylation	.
TR6063|c19_g1	-8.20	1.68E-09	TR6063|c19_g1_i1	D1_ONCVC	48.59	1.00E-38	D1	Protein D1	Onchocerc	TR6063|c19_g1_i1|m.9286	D1_ONCVC	48.59	8.00E-39	D1	Protein D1	Onchocerc	PF01161.1	.	.	.
TR6355|c3_g1	-8.20	1.56E-19	TR6355|c3_g1_i1	ATPA_DRC	86.78	3.00E-96	blw ATPSY	ATP syntha	Drosophila	TR6355|c3_g1_i1|m.18204	ATPA_DRC	86.63	1.00E-98	blw ATPSY	ATP syntha	Drosophila	PF02874.1	GO:0015992^biol	Oxidative phosphorylation	.
TR7664|c0_g1	-8.20	3.98E-10	TR7664|c0_g1_i1	ML1P_MAI	33.33	1.00E-14	0	MD-2-relat	Manduca s	TR7664|c0_g1_i1|m.20194	ML1P_MAI	34.15	9.00E-14	0	MD-2-relat	Manduca s	PF02221.1	.	Lysosome	.
TR6307|c38_g1	-8.19	1.32E-09	TR6307|c38_g1_i1	ATC1_DRO	86.96	6.00E-76	Ca-P60A C	Calcium-tra	Drosophila	TR6307|c38_g1_i1|m.16654	ATC1_DRO	86.96	5.00E-79	Ca-P60A C	Calcium-tra	Drosophila	PF13246.1	.	Calcium signaling pathway	.
TR6135|c38_g1	-8.19	1.13E-09	TR6135|c38_g1_i1	QCR6_RAT	47.83	3.00E-19	Uqcrh	Cytochrom	Rattus nor	TR6135|c38_g1_i1|m.11183	QCR6_RAT	49.21	1.00E-15	Uqcrh	Cytochrom	Rattus nor	PF02320.1	.	Oxidative phosphorylation	.
TR5875|c1_g1	-8.19	9.00E-18	TR5875|c1_g1_i1	RS9_DRON	92.41	8.00E-45	RpS9 CG33	40S riboso	Drosophila	TR5875|c1_g1_i1|m.7331	RS9_DRON	92.41	1.00E-45	RpS9 CG33	40S riboso	Drosophila	PF00163.1	GO:0019843^mo	Ribosome	.
TR5702|c3_g1	-8.19	1.06E-09	TR5702|c3_g1_i1	QCR2_MO	40.31	5.00E-16	Uqcrc2	Cytochrom	Mus muscu	TR5702|c3_g1_i1|m.6762	QCR2_RAT	41.86	6.00E-18	Uqcrc2	Cytochrom	Rattus nor	PF05193.1	.	Oxidative phosphorylation	.
TR2891|c0_g1	-8.18	6.49E-11	TR2891|c0_g1_i1	TAKT_DRO	21.6	3.00E-07	to CG1185	Protein tak	Drosophila	TR2891|c0_g1_i1|m.2627	TAKT_DRO	22.22	3.00E-07	to CG1185	Protein tak	Drosophila	PF06585.6	.	.	.
TR2200|c2_g1	-8.18	4.35E-10	TR2200|c2_g1_i1	MPPB_RAT	66.23	1.00E-24	Pmpcb Mp	Mitochond	Rattus nor	TR2200|c2_g1_i1|m.1942	MPPB_RAT	66.23	8.00E-26	Pmpcb Mp	Mitochond	Rattus nor	PF00675.1	.	.	.
TR5789|c0_g1	-8.17	1.80E-17	TR5789|c0_g1_i1	ELA1_SALS	39.37	6.00E-39	0	Elastase-1	Salmo sala	TR5789|c0_g1_i1|m.7024	ELA1_SALS	39.76	1.00E-38	0	Elastase-1	Salmo sala	PF00089.2	GO:0004252^mo	.	.
TR5586|c1_g1	-8.17	1.45E-10	TR5586|c1_g1_i1	NDUB3_M	37.21	8.00E-10	Ndufb3	NADH deh	Mus muscu	TR5586|c1_g1_i1|m.6425	NDUB3_M	37.08	4.00E-09	Ndufb3	NADH deh	Mus muscu	PF08122.7	GO:0022900^biol	Oxidative phosphorylation	.
TR5702|c4_g1	-8.16	1.13E-10	TR5702|c4_g1_i1	QCR2_HUN	37.34	1.00E-20	UQCRC2	Cytochrom	Homo sapi	TR5702|c4_g1_i1|m.6763	QCR2_HUN	36.96	3.00E-28	UQCRC2	Cytochrom	Homo sapi	PF05193.1	.	Oxidative phosphorylation	.
TR5950|c3_g2	-8.15	1.56E-10	TR5950|c3_g2_i1	GPX7_ARA	57.05	5.00E-56	GPX7 At4g	Putative gl	Arabidopsi	TR5950|c3_g2_i1|m.7657	GPX7_ARA	57.05	2.00E-57	GPX7 At4g	Putative gl	Arabidopsi	PF00255.1	GO:0004602^mo	Arachidonic acid metabolism`Glutathione metaboli	.
TR4955|c0_g1	-8.15	8.52E-10	TR4955|c0_g1_i1	CAH13_HU	41.46	6.00E-42	CA13	Carbonic a	Homo sapi	TR4955|c0_g1_i1|m.5217	CAH13_HU	40.98	7.00E-42	CA13	Carbonic a	Homo sapi	PF00194.1	.	Nitrogen metabolism	.
TR3569|c0_g1	-8.14	1.12E-09	TR3569|c0_g1_i1	GRXC4_AR	54.41	1.00E-16	GRXC4 GLL	Glutaredox	Arabidopsi	TR3569|c0_g1_i1|m.3362	GRXC4_AR	54.41	1.00E-16	GRXC4 GLL	Glutaredox	Arabidopsi	PF00462.1	GO:0009055^mo	.	.
TR2736|c0_g1	-8.14	8.84E-09	TR2736|c0_g1_i1	VATE_DRO	62.99	9.00E-54	Vha26 CG1	V-type pro	Drosophila	TR2736|c0_g1_i1|m.2435	VATE_DRO	62.99	5.00E-65	Vha26 CG1	V-type pro	Drosophila	PF01991.1	GO:0046961^mo	mTOR signaling pathway`Oxidative phosphorylatior	.
TR5435|c1_g1	-8.12	1.67E-10	TR5435|c1_g1_i1	ALDR_HUN	67.57	7.00E-27	AKR1B1 AL	Aldose red	Homo sapi	TR5435|c1_g1_i1|m.6041	ALDR_HUN	67.57	5.00E-28	AKR1B1 AL	Aldose red	Homo sapi	PF00248.1	.	Fructose and mannose metabolism`Galactose meta	.
TR5555|c2_g1	-8.11	1.26E-08	TR5555|c2_g1_i1	ALDR_RAT	52.63	1.00E-36	Akr1b1 Ak	Aldose red	Rattus nor	TR5555|c2_g1_i1|m.6337	AKCL2_PIG	54.39	5.00E-37	AKR1E2 AK	1,5-anhydr	Sus scrofa	PF00248.1	.	Fructose and mannose metabolism`Galactose meta	.
TR8936|c0_g1	-8.10	1.30E-09	TR8936|c0_g1_i1	VATG_MAI	77.32	4.00E-20	0	V-type pro	Manduca s	TR8936|c0_g1_i1|m.20928	VATG_MAI	77.32	4.00E-48	0	V-type pro	Manduca s	PF01442.1	GO:0008289^mo	mTOR signaling pathway`Oxidative phosphorylatior	.
TR2693|c0_g1	-8.10	3.13E-10	TR2693|c0_g1_i1	IAP3_NPV	51.72	3.00E-34	IAP3 IAP O	E3 ubiquiti	Orgyia pse	TR2693|c0_g1_i1|m.2408	IAP1_DROI	40.21	3.00E-38	.	.	.	PF00653.1	.	Apoptosis - multiple species`Ubiquitin mediated pr	.
TR81|c0_g1	-8.10	3.59E-16	TR81|c0_g1_i1	COX5A_MA	55.13	1.00E-45	COX5A	Cytochrom	Macropus	TR81|c0_g1_i1|m.74	COX5A_PA	57.14	3.00E-46	COX5A	Cytochrom	Papio anub	PF02284.1	GO:0004129^mo	Oxidative phosphorylation	.
TR482|c0_g1	-8.09	6.66E-09	TR482|c0_g1_i1	GLYC_CAEI	64.1	1.00E-87	mel-32 CB	Serine hyd	Caenorhab	TR482|c0_g1_i1|m.439	GLYC_CAEI	64.1	8.00E-91	mel-32 CB	Serine hyd	Caenorhab	PF00464.1	GO:0004372^mo	Biosynthesis of amino acids`Carbon metabolism`Gl	.
TR1828|c1_g1	-8.09	4.59E-10	TR1828|c1_g1_i1	GLYC_CAEI	69.84	3.00E-58	mel-32 CB	Serine hyd	Caenorhab	TR1828|c1_g1_i1|m.1568	GLYC_CAEI	69.84	4.00E-61	mel-32 CB	Serine hyd	Caenorhab	PF00464.1	GO:0004372^mo	Biosynthesis of amino acids`Carbon metabolism`Gl	.
TR1284|c0_g1	-8.08	1.34E-09	TR1284|c0_g1_i1	PGK_DRON	75.36	3.00E-51	Pgk CG312	Phosphogl	Drosophila	TR1284|c0_g1_i1|m.1086	PGK_DRON	75.36	2.00E-66	Pgk CG312	Phosphogl	Drosophila	PF00162.1	GO:0004618^mo	Biosynthesis of amino acids`Carbon metabolism`Gl	.
TR4515|c0_g1	-8.08	2.28E-27	TR4515|c0_g1_i1	ENO_DRON	83.22	0	Eno CG176	Enolase (E	Drosophila	TR4515|c0_g1_i1|m.4435	ENO_DRON	83.8	0	Eno CG176	Enolase (E	Drosophila	PF00113.1	GO:0000287^mo	Biosynthesis of amino acids`Carbon metabolism`Gl	.
TR6000|c2_g1	-8.07	1.03E-18	TR6000|c2_g1_i1	MYSP1_DR	69.48	5.00E-92	Prm CG59	Paramyosi	Drosophila	TR6000|c2_g1_i1|m.8267	MYSP_RHII	67.76	6.00E-88	PRM	Paramyosi	Rhipicepha	PF01576.1	GO:0003774^mo	.	.
TR2521|c0_g1	-8.07	6.01E-09	TR2521|c0_g1_i1	PPAP_MOU	31.25	5.00E-15	Acpp	Prostatic a	Mus muscu	TR2521|c0_g1_i1|m.2232	PPAP_MOU	31.25	3.00E-15	Acpp	Prostatic a	Mus muscu	PF00328.1	GO:0003993^mo	.	.
TR5762|c0_g1	-8.07	1.11E-29	TR5762|c0_g1_i1	RL19_DROI	84.26	1.00E-97	RpL19 M(2	60S riboso	Drosophila	TR5762|c0_g1_i1|m.6928	RL19_DROI	85.35	3.00E-105	RpL19 M(2	60S riboso	Drosophila	PF01280.1	GO:0003735^mo	Ribosome	.
TR5230|c1_g1	-8.06	1.14E-09	TR5230|c1_g1_i1	KPYK_DRO	70.63	4.00E-55	PyK CG707	Pyruvate k	Drosophila	TR5230|c1_g1_i1|m.5683	KPYK_DRO	70.91	1.00E-50	PyK CG707	Pyruvate ki	Drosophila	PF02887.1	.	Biosynthesis of amino acids`Carbon metabolism`Gl	.
TR3344|c3_g1	-8.06	8.39E-10	TR3344|c3_g1_i1	.			.	.	.	TR3344|c3_g1_i1|m.3153	.			.	.	.	.	.	.	.
TR3323|c0_g1	-8.06	1.28E-08	TR3323|c0_g1_i1	OAT_DRON	73.65	1.00E-71	Oat CG878	Ornithine a	Drosophila	TR3323|c0_g1_i1|m.3131	OAT_DRON	73.65	1.00E-75	Oat CG878	Ornithine a	Drosophila	PF00202.1	GO:0008483^mo	Arginine and proline metabolism	.
TR3701|c0_g1	-8.06	3.21E-09	TR3701|c0_g1_i1	NOG1_DR	50.41	1.00E-25	Non1 CG8	Nucleolar (	Drosophila	TR3701|c0_g1_i1|m.3522	NOG1_DR	50.41	1.00E-28	Non1 CG8	Nucleolar (	Drosophila	PF08155.6	.	Ribosome biogenesis in eukaryotes	.
TR4598|c0_g2	-8.05	4.71E-09	TR4598|c0_g2_i1	.			.	.	.	TR4598|c0_g2_i1|m.4571	.			.	.	.	.	.	.	.
TR1331|c1_g1	-8.05	2.69E-08	TR1331|c1_g1_i1	NDUS3_PC	81.06	1.00E-76	NDUFS3	NADH deh	Pongo pyg	TR1331|c1_g1_i1|m.1126	NDUS3_PA	81.06	2.00E-75	NDUFS3	NADH deh	Pan troglo	PF00329.1	GO:0008137^mo	Oxidative phosphorylation	.
TR6435|c5_g1	-8.04	9.18E-10	TR6435|c5_g1_i1	CRPI_PERA	64.71	1.00E-07	0	Allergen Cr	Periplaneta	TR6435|c5_g1_i1|m.19233	CRPI_PERA	64.71	2.00E-07	0	Allergen Cr	Periplaneta	PF03723.9	.	.	.
TR5775|c0_g1	-8.03	1.81E-09	TR5775|c0_g1_i1	AATM_RAI	68.99	8.00E-74	GOT2	Aspartate a	Oryctolagu	TR5775|c0_g1_i1|m.6976	AATM_RAI	68.99	2.00E-75	GOT2	Aspartate a	Oryctolagu	PF00155.1	GO:0030170^mo	2-Oxocarboxylic acid metabolism`Alanine, aspartat	.
TR6322|c4_g1	-8.03	2.87E-26	TR6322|c4_g1_i2	MYSA_DRC	78.49	0	Mhc CG17	Myosin hea	Drosophila	TR6322|c4_g1_i2|m.17095	MYSA_DRC	78.49	0	Mhc CG17	Myosin hea	Drosophila	PF00063.1	GO:0003774^mo	.	.
TR2916|c0_g2	-7.99	4.65E-09	TR2916|c0_g2_i1	COX5A_DR	52.67	1.00E-36	COX5A Co	Cytochrom	Drosophila	TR2916|c0_g2_i1|m.2687	COX5A_DR	52.67	3.00E-48	COX5A Co	Cytochrom	Drosophila	PF02284.1	GO:0004129^mo	Oxidative phosphorylation	.
TR108|c0_g1	-7.99	4.34E-08	TR108|c0_g1_i1	SLMO_DRC	50.47	4.00E-26	slmo kisir (	Protein slo	Drosophila	TR108|c0_g1_i1|m.103	SLMO_DRC	50.47	6.00E-28	slmo kisir (	Protein slo	Drosophila	PF04707.9	.	.	.
TR1395|c0_g1	-7.98	4.97E-08	TR1395|c0_g1_i1	.			.	.	.	TR1395|c0_g1_i1|m.1173	.			.	.	.	PF07225.7	GO:0008137^mo	.	.
TR767|c0_g2	-7.98	1.10E-07	TR767|c0_g2_i1	THIO2_DR	60.78	3.00E-38	Trx-2	Thioredoxi	Drosophila	TR767|c0_g2_i1|m.682	THIO2_DR	62	3.00E-40	Trx-2	Thioredoxi	Drosophila	PF00085.1	GO:0016209^mo	.	.
TR5230|c0_g1	-7.97	9.53E-09	TR5230|c0_g1_i1	KPYK_DRO	86.05	7.00E-71	PyK CG707	Pyruvate k	Drosophila	TR5230|c0_g1_i1|m.5682	KPYK_DRO	86.05	2.00E-74	PyK CG707	Pyruvate ki	Drosophila	PF00224.1	GO:0000287^mo	Biosynthesis of amino acids`Carbon metabolism`Gl	.
TR5102|c1_g1	-7.97	1.55E-08	TR5102|c1_g1_i1	ACLY_BOV	78.61	4.00E-106	ACLY	ATP-citrate	Bos taurus	TR5102|c1_g1_i1|m.5469	ACLY_BOV	78.61	7.00E-110	ACLY	ATP-citrate	Bos taurus	PF00285.1	GO:0046912^mo	Citrate cycle (TCA cycle)	.

TR4920|c2_g1	-7.96	8.34E-09	TR4920|c2_g1_i1	4EBP2_HU	59.46	5.00E-26	EIF4EBP2	Eukaryotic	Homo sapi	TR4920|c2_g1_i1|m.5137	4EBP2_MC	65.15	2.00E-26	Eif4ebp2	Eukaryotic	Mus musc	PF05456.6	GO:0008190^mo	Longevity regulating pathway - multiple species`RN	.
TR5079|c4_g1	-7.96	8.47E-08	TR5079|c4_g1_i1	AMPN_PLL	31.82	2.00E-10	APN1	Aminopept	Plutella xyl	TR5079|c4_g1_i1|m.5434	AMPN_PLL	31.82	1.00E-10	APN1	Aminopept	Plutella xyl	PF11838.3	.	.	.
TR3356|c0_g1	-7.96	5.88E-10	TR3356|c0_g1_i1	ANXB9_DR	62.8	3.00E-56	AnxB9 Ann	Annexin B9	Drosophila	TR3356|c0_g1_i1|m.3164	ANXB9_DR	62.8	1.00E-61	AnxB9 Ann	Annexin B9	Drosophila	PF00191.1	GO:0005509^mo	.	.
TR4385|c1_g1	-7.95	2.53E-08	TR4385|c1_g1_i1	PRDX6_CH	53.28	6.00E-36	PRDX6 RCJ	Peroxiredo	Gallus gallu	TR4385|c1_g1_i1|m.4275	PRDX6_RA	52.46	1.00E-35	Prdx6 Aipla	Peroxiredo	Rattus nor	PF10417.4	GO:0051920^mo	.	.
TR5894|c0_g1	-7.95	5.58E-10	TR5894|c0_g1_i1	TKTL2_HUI	45.16	3.00E-42	TKTL2	Transketol	Homo sapi	TR5894|c0_g1_i1|m.7383	TKT_BOVIN	46.79	8.00E-43	TKT TKT1	Transketol	Bos taurus	PF00456.1	.	Biosynthesis of amino acids`Carbon metabolism`Pe	.
TR4040|c0_g1	-7.95	4.65E-16	TR4040|c0_g1_i1	TPIS_CULT	72.87	2.00E-128	Tpi	Triosephos	Culex tarsa	TR4040|c0_g1_i1|m.3890	TPIS_CULT	72.87	6.00E-134	Tpi	Triosephos	Culex tarsa	PF00121.1	GO:0004807^mo	Biosynthesis of amino acids`Carbon metabolism`Fr	.
TR5756|c5_g1	-7.95	1.00E-07	TR5756|c5_g1_i1	.			.	.	.	TR5756|c5_g1_i1|m.6912	.			.	.	.	PF01607.1	GO:0008061^mo	.	.
TR2891|c0_g2	-7.93	8.52E-10	TR2891|c0_g2_i1	TAKT_DRO	21.6	3.00E-07	to CG1185	Protein tak	Drosophila	TR2891|c0_g2_i1|m.2628	TAKT_DRO	22.22	3.00E-07	to CG1185	Protein tak	Drosophila	PF06585.6	.	.	.
TR679|c0_g1	-7.91	6.99E-09	TR679|c0_g1_i1	NDUB7_BC	43.48	2.00E-19	NDUFB7	NADH deh	Bos taurus	TR679|c0_g1_i1|m.603	NDUB7_CA	41.51	9.00E-18	D2030.4	NADH deh	Caenorhab	PF05676.8	GO:0003954^mo	Oxidative phosphorylation	.
TR2882|c0_g2	-7.88	5.16E-25	TR2882|c0_g2_i1	CATB_MAC	52.31	7.00E-119	CTSB QccE	Cathepsin	Macaca fas	TR2882|c0_g2_i1|m.2614	CATB_MAC	51.5	1.00E-114	CTSB QccE	Cathepsin	Macaca fas	PF00112.1	GO:0004197^mo	Apoptosis`Autophagy - animal`Lysosome	.
TR5874|c2_g1	-7.88	5.96E-09	TR5874|c2_g1_i1	PPIA_DROI	91.67	5.00E-43	Cyp1 Cyp-1	Peptidyl-pr	Drosophila	TR5874|c2_g1_i1|m.7329	PPIA_DROI	80.23	7.00E-45	Cyp1 Cyp-1	Peptidyl-pr	Drosophila	PF00160.1	GO:0003755^mo	Calcium signaling pathway	.
TR5894|c1_g2	-7.88	9.76E-09	TR5894|c1_g2_i1	TKTL2_HUI	65.81	4.00E-59	TKTL2	Transketol	Homo sapi	TR5894|c1_g2_i1|m.7388	TKTL2_HUI	65.81	4.00E-66	TKTL2	Transketol	Homo sapi	PF02779.1	GO:0003824^mo	Biosynthesis of amino acids`Carbon metabolism`Pe	.
TR5956|c6_g2	-7.87	1.96E-08	TR5956|c6_g2_i1	.			.	.	.	TR5956|c6_g2_i1|m.7749	.			.	.	.	.	.	.	.
TR4715|c0_g1	-7.87	3.51E-09	TR4715|c0_g1_i1	.			.	.	.	TR4715|c0_g1_i1|m.4755	.			.	.	.	PF08212.7	.	.	.
TR5621|c0_g1	-7.87	2.69E-15	TR5621|c0_g1_i1	CUD3_SCH	45.69	1.00E-25	0	Endocuticl	Schistocer	TR5621|c0_g1_i1|m.6507	CUD3_SCH	45.69	4.00E-26	0	Endocuticl	Schistocer	PF00379.1	GO:0042302^mo	.	.
TR6322|c2_g2	-7.86	1.01E-09	TR6322|c2_g2_i1	MYSA_DRC	77.62	8.00E-53	Mhc CG179	Myosin hea	Drosophila	TR6322|c2_g2_i1|m.17091	MYSA_DRC	77.08	2.00E-66	Mhc CG179	Myosin hea	Drosophila	PF00612.2	GO:0005515^mo	.	.
TR4821|c1_g1	-7.86	8.94E-05	TR4821|c1_g1_i1	PR5_ARAT	55.97	4.00E-50	At1g75040	Pathogene	Arabidopsi	TR4821|c1_g1_i1|m.4954	PR5_ARAT	55.97	2.00E-46	At1g75040	Pathogene	Arabidopsi	PF00314.1	.	.	.
TR4735|c1_g1	-7.85	5.72E-10	TR4735|c1_g1_i1	GLYM_HUI	59.23	3.00E-46	SHMT2	Serine hyd	Homo sapi	TR4735|c1_g1_i1|m.4787	GLYM_HUI	59.23	4.00E-49	SHMT2	Serine hyd	Homo sapi	PF00464.1	GO:0004372^mo	Biosynthesis of amino acids`Carbon metabolism`Gl	.
TR5250|c0_g1	-7.82	1.27E-07	TR5250|c0_g1_i1	S61A2_MC	90.11	1.00E-112	Sec61a2	Protein tra	Mus musc	TR5250|c0_g1_i1|m.5731	S61A2_MC	90.11	3.00E-116	Sec61a2	Protein tra	Mus musc	PF00344.1	GO:0015031^biol	Phagosome`Protein export`Protein processing in e	.
TR3813|c0_g1	-7.81	1.27E-14	TR3813|c0_g1_i1	COX5B_BO	40	1.00E-18	COX5B	Cytochrom	Bos taurus	TR3813|c0_g1_i1|m.3625	COX5B_MC	36.44	7.00E-20	Cox5b	Cytochrom	Mus musc	PF01215.1	GO:0004129^mo	Oxidative phosphorylation	.
TR5925|c0_g2	-7.81	4.09E-07	TR5925|c0_g2_i1	CUD1_SCH	42.73	3.00E-14	0	Endocuticl	Schistocer	TR5925|c0_g2_i1|m.7493	CUD1_SCH	45.63	7.00E-20	0	Endocuticl	Schistocer	PF00379.1	GO:0042302^mo	.	.
TR4020|c0_g1	-7.79	3.26E-08	TR4020|c0_g1_i1	.			.	.	.	TR4020|c0_g1_i1|m.3863	.			.	.	.	PF01223.1	GO:0003676^mo	.	.
TR3647|c1_g1	-7.78	1.55E-09	TR3647|c1_g1_i1	CATL_DRO	69.03	3.00E-54	Cp1 fs(2)5	Cathepsin	Drosophila	TR3647|c1_g1_i1|m.3463	CATL_DRO	66.95	6.00E-55	Cp1 fs(2)5	Cathepsin	Drosophila	PF00112.1	GO:0008234^mo	Apoptosis`Autophagy - animal`Lysosome`Phagosor	.
TR5804|c1_g1	-7.78	9.84E-25	TR5804|c1_g1_i1	RL44_OCH	92.41	4.00E-48	RpL44	60S riboso	Ochlerotat	TR5804|c1_g1_i1|m.7080	RL44_OCH	89.42	1.00E-60	RpL44	60S riboso	Ochlerotat	PF00935.1	GO:0003735^mo	Ribosome	.
TR6047|c2_g1	-7.77	2.08E-15	TR6047|c2_g1_i1	PTGR1_BO	53.23	2.00E-69	PTGR1 LTB	Prostaglan	Bos taurus	TR6047|c2_g1_i1|m.8896	PTGR1_BO	53.61	1.00E-82	PTGR1 LTB	Prostaglan	Bos taurus	PF00107.2	GO:0008270^mo	.	.
TR6087|c2_g1	-7.75	3.55E-08	TR6087|c2_g1_i1	.			.	.	.	TR6087|c2_g1_i1|m.9855	MRJP3_AP	33.33	2.00E-06	MRJP3	Major roya	Apis mellif	.	.	.	.
TR5479|c0_g1	-7.75	2.20E-07	TR5479|c0_g1_i1	PPO3_DRC	41.45	1.00E-31	PPO3 Dox-	Phenoloxic	Drosophila	TR5479|c0_g1_i1|m.6154	PPO3_DRC	41.18	5.00E-31	PPO3 Dox-	Phenoloxic	Drosophila	PF03723.9	.	.	.
TR4712|c0_g1	-7.74	2.21E-28	TR4712|c0_g1_i2	RL10A_SPC	88.94	2.00E-124	RpL10A	60S riboso	Spodopter	TR4712|c0_g1_i2|m.4749	RL10A_SPC	88.94	7.00E-129	RpL10A	60S riboso	Spodopter	PF00687.1	.	Ribosome`Ribosome	.
TR6390|c4_g1	-7.72	2.20E-44	TR6390|c4_g1_i1	RLA0_DRO	79.55	3.00E-152	RpLP0 AP3	60S acidic	Drosophila	TR6390|c4_g1_i1|m.18873	RLA0_CER	75.71	7.00E-166	RpLP0 RpP	60S acidic	Ceratitis ca	PF00428.1	GO:0042254^biol	Ribosome	.
TR3665|c0_g1	-7.71	5.00E-07	TR3665|c0_g1_i1	IPYR_DROI	68.99	6.00E-77	Nurf-38 CG	Inorganic p	Drosophila	TR3665|c0_g1_i1|m.3486	IPYR_DROI	68.99	1.00E-76	Nurf-38 CG	Inorganic p	Drosophila	PF00719.1	GO:0000287^mo	Oxidative phosphorylation	.
TR6307|c28_g1	-7.70	2.64E-16	TR6307|c28_g1_i1	ATC1_DRO	87.23	1.00E-153	Ca-P60A C	Calcium-tra	Drosophila	TR6307|c28_g1_i1|m.16645	ATC1_ANC	85.61	2.00E-168	Ca-P60A A	Calcium-tra	Anopheles	PF00689.1	.	Calcium signaling pathway	.
TR5115|c1_g1	-7.69	7.54E-08	TR5115|c1_g1_i1	MKNK1_XE	56.95	2.00E-51	mknk1	MAP kinas	Xenopus tr	TR5115|c1_g1_i1|m.5479	MKNK1_XE	61.07	1.00E-52	mknk1	MAP kinas	Xenopus tr	PF00069.2	GO:0004672^mo	MAPK signaling pathway	.
TR8826|c0_g1	-7.68	1.19E-04	TR8826|c0_g1_i1	ALL2_LEPD	47.58	4.00E-34	0	Mite group	Lepidoglyp	TR8826|c0_g1_i1|m.20887	ALL2_LEPD	47.58	5.00E-37	0	Mite group	Lepidoglyp	PF02221.1	.	Lysosome	.
TR866|c0_g1	-7.67	1.06E-26	TR866|c0_g1_i1	CP6K1_BL	38.98	2.00E-121	CYP6K1	Cytochrom	Blattella ge	TR866|c0_g1_i1|m.746	CP6K1_BL	39.17	5.00E-126	CYP6K1	Cytochrom	Blattella ge	PF00067.1	GO:0005506^mo	.	.
TR187|c0_g1	-7.67	3.63E-05	TR187|c0_g1_i1	LSD2_DRO	28.96	7.00E-21	Lsd-2 CG9	Lipid stora	Drosophila	TR187|c0_g1_i1|m.173	LSD2_DRO	29.48	9.00E-20	Lsd-2 CG9	Lipid stora	Drosophila	PF03036.1	.	PPAR signaling pathway	.
TR9559|c0_g1	-7.66	6.87E-08	TR9559|c0_g1_i1	NDUA6_PC	44.35	6.00E-30	NDUFA6	NADH deh	Pongo pyg	TR9559|c0_g1_i1|m.21249	NDUA6_PC	44.35	3.00E-30	NDUFA6	NADH deh	Pongo pyg	PF05347.1	.	Oxidative phosphorylation	.
TR9346|c0_g1	-7.63	1.28E-07	TR9346|c0_g1_i1	CRYAA_CH	42.73	2.00E-17	CRYAA	Alpha-crys	Choloepus	TR9346|c0_g1_i1|m.21171	CRYAA_ER	42.48	2.00E-18	CRYAA	Alpha-crys	Erinaceus	PF00011.1	.	Longevity regulating pathway - multiple species`Pro	.
TR6054|c6_g1	-7.62	1.64E-08	TR6054|c6_g1_i1	ECHM_BOV	57.02	6.00E-39	ECHS1	Enoyl-CoA	Bos taurus	TR6054|c6_g1_i1|m.9042	ECHM_BOV	55.28	2.00E-40	ECHS1	Enoyl-CoA	Bos taurus	PF00378.1	GO:0003824^mo	beta-Alanine metabolism`Butanoate metabolism`C	.
TR5786|c1_g1	-7.62	1.74E-27	TR5786|c1_g1_i1	EF1G_ART	72.75	0	0	Elongation	Artemia sa	TR5786|c1_g1_i1|m.7011	EF1G_ART	73.71	0	0	Elongation	Artemia sa	PF00043.2	GO:0005515^mo	.	.
TR5962|c0_g1	-7.62	2.48E-07	TR5962|c0_g1_i1	APLP_LOCI	43.58	2.00E-59	0	Apolipoph	Locusta mi	TR5962|c0_g1_i1|m.7857	APLP_LOCI	43.58	5.00E-60	0	Apolipoph	Locusta mi	.	.	.	.
TR6008|c2_g1	-7.61	9.53E-09	TR6008|c2_g1_i1	ALF_DROM	70.3	3.00E-36	Ald CG605	Fructose-b	Drosophila	TR6008|c2_g1_i1|m.8298	ALDOA_M	65.35	3.00E-36	Aldoa Aldo	Fructose-b	Mus musc	PF00274.1	GO:0004332^mo	Biosynthesis of amino acids`Carbon metabolism`Fr	.
TR4516|c0_g1	-7.61	3.97E-21	TR4516|c0_g1_i1	ENO_DROI	87.12	0	Eno CG176	Enolase (E	Drosophila	TR4516|c0_g1_i1|m.4436	ENO_DROI	87.12	0	Eno CG176	Enolase (E	Drosophila	PF00113.1	GO:0000287^mo	Biosynthesis of amino acids`Carbon metabolism`Gl	.
TR5856|c0_g1	-7.59	3.00E-08	TR5856|c0_g1_i1	CBPZ_SIM	50	2.00E-20	0	Zinc carbo	Simulium v	TR5856|c0_g1_i1|m.7276	CBPZ_SIM	48.98	4.00E-20	0	Zinc carbo	Simulium v	PF00246.1	GO:0004181^mo	.	.
TR6126|c0_g1	-7.58	6.57E-57	TR6126|c0_g1_i1	PABPA_XE	65.57	0	pabpc1-a p	Polyadenyl	Xenopus la	TR6126|c0_g1_i1|m.10853	PABP1_HU	66.51	0	PABPC1 PA	Polyadenyl	Homo sapi	PF00076.1	GO:0003676^mo	mRNA surveillance pathway`mRNA surveillance pat	.
TR5875|c0_g1	-7.58	3.75E-30	TR5875|c0_g1_i1	RS9_DROM	96.13	4.00E-119	RpS9 CG33	40S riboso	Drosophila	TR5875|c0_g1_i1|m.7330	RS9_DROM	96.13	5.00E-121	RpS9 CG33	40S riboso	Drosophila	PF00163.1	GO:0019843^mo	Ribosome	.
TR5715|c0_g1	-7.57	7.69E-28	TR5715|c0_g1_i1	RS27A_DR	78.21	9.00E-54	RpS27A UE	Ubiquitin-4	Drosophila	TR5715|c0_g1_i1|m.6794	RS27A_DR	78.21	3.00E-71	RpS27A UE	Ubiquitin-4	Drosophila	PF00240.1	GO:0005515^mo	Ribosome	.
TR5937|c0_g1	-7.55	9.50E-09	TR5937|c0_g1_i1	PNPH_HUI	64.75	1.00E-50	PNP NP	Purine nuc	Homo sapi	TR5937|c0_g1_i1|m.7538	PNPH_HUI	64.75	3.00E-50	PNP NP	Purine nuc	Homo sapi	PF01048.1	GO:0003824^mo	Nicotinate and nicotinamide metabolism`Purine m	.
TR7480|c0_g1	-7.51	1.81E-17	TR7480|c0_g1_i1	UCRI_BOVI	58.39	1.00E-109	UQCRFS1	Cytochrom	Bos taurus	TR7480|c0_g1_i1|m.20051	UCRI_COLF	60.87	2.00E-112	UQCRFS1	Cytochrom	Colobus pc	PF00355.2	GO:0008121^mo	Oxidative phosphorylation	.
TR2145|c0_g1	-7.51	1.24E-18	TR2145|c0_g1_i1	TRAM1_BC	49.24	1.00E-99	TRAM1 TR	Translocati	Bos taurus	TR2145|c0_g1_i1|m.1885	TR1L1_XEN	45.43	7.00E-111	tram1l1	Translocati	Xenopus la	PF03798.1	GO:0016021^cell	Protein processing in endoplasmic reticulum	.
TR4305|c0_g1	-7.50	1.97E-06	TR4305|c0_g1_i1	CY1_MOUS	66.92	6.00E-38	Cyc1	Cytochrom	Mus musc	TR4305|c0_g1_i1|m.4187	CY1_BOVIN	66.14	4.00E-57	CYC1	Cytochrom	Bos taurus	PF02167.1	GO:0005506^mo	Oxidative phosphorylation	.
TR3962|c0_g1	-7.49	9.28E-07	TR3962|c0_g1_i1	GRP75_CH	76.98	6.00E-65	HSPA9 RCJ	Stress-70 p	Gallus gallu	TR3962|c0_g1_i1|m.3784	GRP75_PO	69.94	6.00E-69	HSPA9	Stress-70 p	Pongo abe	PF00012.1	.	RNA degradation	.
TR8215|c0_g1	-7.48	1.28E-15	TR8215|c0_g1_i1	ATIF2_CAE	46.43	9.00E-07	mai-2 B054	ATPase inh	Caenorhab	TR8215|c0_g1_i1|m.20522	ATIF2_CAE	49.23	6.00E-16	mai-2 B054	ATPase inh	Caenorhab	PF04568.7	GO:0004857^mo	.	.
TR5962|c0_g2	-7.47	3.60E-06	TR5962|c0_g2_i1	APLP_LOCI	42.75	3.00E-58	0	Apolipoph	Locusta mi	TR5962|c0_g2_i1|m.7859	APLP_LOCI	42.75	1.00E-58	0	Apolipoph	Locusta mi	.	.	.	.
TR4182|c0_g1	-7.47	9.91E-08	TR4182|c0_g1_i1	3HIDH_BO	57.86	4.00E-59	HIBADH	3-hydroxyi	Bos taurus	TR4182|c0_g1_i1|m.4059	3HIDH_BO	57.86	3.00E-61	HIBADH	3-hydroxyi	Bos taurus	PF03446.1	GO:0004616^mo	Valine, leucine and isoleucine degradation	.
TR3433|c0_g1	-7.47	7.14E-08	TR3433|c0_g1_i1	MPCP_CHC	83.82	7.00E-58	0	Phosphate	Choristone	TR3433|c0_g1_i1|m.3240	MPCP_CHC	83.82	4.00E-78	0	Phosphate	Choristone	PF00153.2	.	.	.
TR2431|c0_g1	-7.46	1.14E-05	TR2431|c0_g1_i1	INO1A_XEI	64.66	1.00E-43	isyna1-a in	Inositol-3-p	Xenopus la	TR2431|c0_g1_i1|m.2164	INO1A_XEI	60	7.00E-46	isyna1-a in	Inositol-3-p	Xenopus la	PF01658.1	GO:0004512^mo	Inositol phosphate metabolism	.
TR320|c0_g1	-7.42	4.19E-21	TR320|c0_g1_i1	ATPG_DRC	76.19	3.00E-139	ATPsyngan	ATP syntha	Drosophila	TR320|c0_g1_i1|m.303	ATPG_DRC	72.2	1.00E-151	ATPsyngan	ATP syntha	Drosophila	PF00231.1	GO:0046933^mo	Oxidative phosphorylation	.
TR4983|c1_g1	-7.42	4.07E-07	TR4983|c1_g1_i1	APOD_MA	37.74	7.00E-16	APOD QccI	Apolipopro	Macaca fas	TR4983|c1_g1_i1|m.5277	APOD_MA	37.74	4.00E-17	APOD QccI	Apolipopro	Macaca fas	PF00061.1	.	.	.
TR4937|c0_g1	-7.42	1.66E-18	TR4937|c0_g1_i1	MPCP_RAT	69.6	3.00E-157	Slc25a3 Ph	Phosphate	Rattus nor	TR4937|c0_g1_i1|m.5180	MPCP_CHC	71.59	8.00E-173	0	Phosphate	Choristone	PF00153.2	.	.	.
TR2882|c0_g1	-7.42	2.85E-18	TR2882|c0_g1_i1	CATB_RAT	48.13	1.00E-79	Ctsb	Cathepsin	Rattus nor	TR2882|c0_g1_i1|m.2613	CATB_RAT	47.79	2.00E-78	Ctsb	Cathepsin	Rattus nor	PF00112.1	GO:0004197^mo	Apoptosis`Autophagy - animal`Lysosome	.
TR2829|c0_g2	-7.41	2.88E-07	TR2829|c0_g2_i1	GPX2_ARA	70	2.00E-23	GPX2 At2g	Probable g	Arabidopsi	TR2829|c0_g2_i1|m.2544	GPX2_ARA	70	2.00E-25	GPX2 At2g	Probable g	Arabidopsi	PF00255.1	GO:0004602^mo	Arachidonic acid metabolism`Glutathione metaboli	.
TR5564|c1_g1	-7.39	9.17E-32	TR5564|c1_g1_i2	RSSA_MAC	85.99	4.00E-117	0	40S riboso	Maconellic	TR5564|c1_g1_i2|m.6361	RSSA_DIAC	78.31	5.00E-138	0	40S riboso	Diaphorina	PF00318.1	GO:0003735^mo	Ribosome`Ribosome	.
TR6173|c7_g2	-7.38	3.02E-19	TR6173|c7_g2_i1	CUD2_SCH	48.62	2.00E-26	0	Endocuticl	Schistocer	TR6173|c7_g2_i1|m.12488	CUD2_SCH	48.45	2.00E-25	0	Endocuticl	Schistocer	PF00379.1	GO:0042302^mo	.	.
TR6164|c11_g2	-7.37	5.49E-20	TR6164|c11_g2_i1	HSP7D_MA	84.09	2.00E-71	0	Heat shock	Manduca s	TR6164|c11_g2_i1|m.12225	HSP7D_MA	84.09	6.00E-73	0	Heat shock	Manduca s	PF00012.1	.	Endocytosis`Longevity regulating pathway - multipl	.
TR6298|c14_g3	-7.37	1.83E-17	TR6298|c14_g3_i1	TBB_STRPU	98.11	0	0	Tubulin be	Strongyloc	TR6298|c14_g3_i1|m.16242	TBB1_MAN	99.64	0	0	Tubulin be	Manduca s	PF00091.2	GO:0003924^mo	Gap junction`Phagosome	.
TR6145|c12_g1	-7.35	3.43E-52	TR6145|c12_g1_i1	AT5G_MAI	83.33	1.00E-19	0	ATP syntha	Manduca s	TR6145|c12_g1_i1|m.11675	AT5G_MAI	78.57	3.00E-60	0	ATP syntha	Manduca s	PF00137.1	GO:0015078^mo	Oxidative phosphorylation`Oxidative phosphorylati	.
TR4757|c2_g1	-7.35	1.38E-06	TR4757|c2_g1_i1	GLNA_PAN	78.38	7.00E-54	0	Glutamine	Panulirus a	TR4757|c2_g1_i1|m.4827	GLNA_PAN	78.38	4.00E-55	0	Glutamine	Panulirus a	PF00120.1	GO:0004356^mo	Alanine, aspartate and glutamate metabolism`Argi	.
TR919|c0_g1	-7.33	2.03E-04	TR919|c0_g1_i1	PN16_PHC	33.94	1.00E-13	0	U24-ctenit	Phoneutria	TR919|c0_g1_i1|m.782	PN16_PHC	34.78	8.00E-12	0	U24-ctenit	Phoneutria	PF00086.1	.	.	.
TR5774|c4_g1	-7.32	5.50E-07	TR5774|c4_g1_i1	PAIRB_RAT	55.81	3.00E-06	Serbp1 Pai	Plasminoge	Rattus nor	TR5774|c4_g1_i1|m.6972	PAIRB_RAT	40.51	9.00E-09	Serbp1 Pai	Plasminoge	Rattus nor	PF04774.1	.	.	.
TR5998|c0_g1	-7.32	1.25E-30	TR5998|c0_g1_i2	RL30_SPOI	87.16	4.00E-62	RpL30	60S riboso	Spodopter	TR5998|c0_g1_i2|m.8256	RL30_SPOI	87.16	2.00E-65	RpL30	60S riboso	Spodopter	PF01248.2	.	Ribosome`Ribosome	.
TR528|c0_g1	-7.30	6.40E-07	TR528|c0_g1_i1	FABP_LEPI	47.62	4.00E-27	0	Fatty acid-l	Lepidoglyp	TR528|c0_g1_i1|m.467	FABP_LEPI	47.62	4.00E-26	0	Fatty acid-l	Lepidoglyp	PF00061.1	.	.	.
TR5804|c1_g2	-7.30	5.91E-17	TR5804|c1_g2_i1	RL44_OCH	92.41	4.00E-48	RpL44	60S riboso	Ochlerotat	TR5804|c1_g2_i1|m.7081	RL44_OCH	89.42	1.00E-60	RpL44	60S riboso	Ochlerotat	PF00935.1	GO:0003735^mo	Ribosome	.
TR6089|c3_g2	-7.25	6.53E-17	TR6089|c3_g2_i1	VDAC_DRC	57.71	2.00E-108	porin POR-	Voltage-de	Drosophila	TR6089|c3_g2_i1|m.9948	VDAC_DRC	57.5	9.00E-118	porin POR-	Voltage-de	Drosophila	PF01459.1	GO:0055085^biol	Calcium signaling pathway	.
TR5765|c0_g1	-7.22	8.57E-36	TR5765|c0_g1_i1	TNNT_PER	81.88	5.00E-137	TNT	Troponin T	Periplaneta	TR5765|c0_g1_i1|m.6949	TNNT_PER	80.95	5.00E-166	TNT	Troponin T	Periplaneta	PF00992.1	GO:0005861^cell	.	.
TR3750|c0_g2	-7.22	9.63E-12	TR3750|c0_g2_i1	GST1D_AN	69.87	4.00E-77	GstD1 GST	Glutathion	Anopheles	TR3750|c0_g2_i1|m.3576	GST1D_AN	69.87	2.00E-78	GstD1 GST	Glutathion	Anopheles	PF02798.1	GO:0005515^mo	Drug metabolism - cytochrome P450`Glutathione n	.
TR6205|c7_g1	-7.19	4.30E-35	TR6205|c7_g1_i2	RS7_MANS	87.7	6.00E-94	RpS7	40S riboso	Manduca s	TR6205|c7_g1_i2|m.13339	RS7_MANS	86.77	2.00E-115	RpS7	40S riboso	Manduca s	PF01251.1	GO:0003735^mo	Ribosome`Ribosome	.
TR6378|c6_g1	-7.19	5.59E-14	TR6378|c6_g1_i1	TBA_LYTPI	98.88	2.00E-57	0	Tubulin alp	Lytechinus	TR6378|c6_g1_i1|m.18525	TBA_BOMI	98.99	2.00E-63	0	Tubulin alp	Bombyx m	PF03953.1	GO:0003924^mo	Apoptosis`Gap junction`Phagosome`Tight junction	.
TR6032|c2_g1	-7.19	3.60E-41	TR6032|c2_g1_i1	RL8_SPOFF	89.17	5.00E-159	RpL8	60S riboso	Spodopter	TR6032|c2_g1_i1|m.8469	RL8_SPOFF	89.8	2.00E-167	RpL8	60S riboso	Spodopter	PF00181.1	GO:0003735^mo	Ribosome`Ribosome	.
TR6010|c0_g1	-7.19	9.12E-31	TR6010|c0_g1_i1	TNNC3_DR	85.33	7.00E-84	TpnC73F T	Troponin C	Drosophila	TR6010|c0_g1_i1|m.8304	TNNC3_DR	85.33	4.00E-88	TpnC73F T	Troponin C	Drosophila	PF00036.2	GO:0005509^mo	.	.
TR6259|c11_g1	-7.17	4.48E-48	TR6259|c11_g1_i1	KARG_PLO	88.73	0	ARGK	Arginine ki	Plodia inte	TR6259|c11_g1_i1|m.15205	KARG_PLO	88.73	0	ARGK	Arginine ki	Plodia inte	PF00217.1	GO:0016301^mo	Arginine and proline metabolism`Arginine and prol	.
TR5545|c1_g1	-7.16	1.46E-18	TR5545|c1_g1_i1	RS6_MANS	80.86	7.00E-67	RpS6	40S riboso	Manduca s	TR5545|c1_g1_i1|m.6309	RS6_MANS	80.86	7.00E-76	RpS6	40S riboso	Manduca s	PF01092.1	GO:0003735^mo	mTOR signaling pathway`Ribosome	.
TR6322|c3_g1	-7.15	7.27E-14	TR6322|c3_g1_i2	MYSA_DRC	86.36	6.00E-64	Mhc CG179	Myosin hea	Drosophila	TR6322|c3_g1_i1|m.17092	MYSA_DRC	88.31	9.00E-69	Mhc CG179	Myosin hea	Drosophila	PF00063.1	GO:0003774^mo	.	.
TR6199|c10_g1	-7.15	1.21E-21	TR6199|c10_g1_i1	RL9_DROM	82.01	2.00E-104	RpL9 M(2):	60S riboso	Drosophila	TR6199|c10_g1_i1|m.13196	RL9_DROM	82.01	8.00E-110	RpL9 M(2):	60S riboso	Drosophila	PF00347.1	GO:0003735^mo	Ribosome	.
TR7873|c0_g1	-7.15	7.17E-19	TR7873|c0_g1_i1	NACA_DRC	76.25	5.00E-54	Nacalpha a	Nascent pc	Drosophila	TR7873|c0_g1_i1|m.20305	NACA_DRC	75.46	2.00E-71	Nacalpha a	Nascent pc	Drosophila	PF01849.1	.	.	.
TR4480|c1_g1	-7.14	5.26E-10	TR4480|c1_g1_i1	VATL_MAN	81.33	8.00E-64	VHA16	V-type pro	Manduca s	TR4480|c1_g1_i1|m.4386	VATL_MAN	79.74	1.00E-80	VHA16	V-type pro	Manduca s	PF00137.1	GO:0015078^mo	Lysosome`Oxidative phosphorylation`Phagosome`S	.
TR6232|c1_g1	-6.99	5.77E-21	TR6232|c1_g1_i1	TPM1_BON	85.65	3.00E-120	0	Tropomyos	Bombyx m	TR6232|c1_g1_i1|m.14199	TPM1_BON	85.65	7.00E-118	0	Tropomyos	Bombyx m	PF00261.1	GO:0007155^biol	.	.
TR5729|c0_g1	-6.99	1.46E-16	TR5729|c0_g1_i1	UBB_PONF	98.73	1.00E-104	UBB	Polyubiqui	Pongo pyg	TR5729|c0_g1_i1|m.6817	UBB_PONF	98.73	1.00E-107	UBB	Polyubiqui	Pongo pyg	PF00240.1	GO:0005515^mo	PPAR signaling pathway	.
TR6114|c1_g1	-6.98	1.78E-35	TR6114|c1_g1_i1	TNNI_DRO	84.36	1.00E-63	wupA HDP	Troponin I	Drosophila	TR6114|c1_g1_i1|m.10546	TNNI_DRO	82.44	8.00E-82	wupA HDP	Troponin I	Drosophila	PF00992.1	GO:0005861^cell	.	.
TR6274|c1_g1	-6.97	3.47E-38	TR6274|c1_g1_i2	C4G15_DR	63.67	0	Cyp4g15 C	Cytochrom	Drosophila	TR6274|c1_g1_i2|m.15611	C4G15_DR	64.73	0	Cyp4g15 C	Cytochrom	Drosophila	PF00067.1	GO:0005506^mo	.	.
TR6322|c6_g1	-6.97	1.09E-38	TR6322|c6_g1_i2	MYSA_DRC	94.38	0	Mhc CG179	Myosin hea	Drosophila	TR6322|c6_g1_i1|m.17103	MYSA_DRC	95.17	0	Mhc CG179	Myosin hea	Drosophila	PF01576.1	GO:0003774^mo	.	.
TR1935|c0_g1	-6.96	1.50E-12	TR1935|c0_g1_i1	PROF_APIN	92.8	2.00E-75	0	Profilin	Apis mellif	TR1935|c0_g1_i1|m.1642	PROF_APIN	92.8	8.00E-81	0	Profilin	Apis mellif	PF00235.1	GO:0003779^mo	MAPK signaling pathway - fly`Rap1 signaling pathw	.
TR6298|c14_g2	-6.94	5.67E-15	TR6298|c14_g2_i1	TBB_STRPU	98.11	0	0	Tubulin be	Strongyloc	TR6298|c14_g2_i1|m.16241	TBB1_MAN	99.64	0	0	Tubulin be	Manduca s	PF00091.2	GO:0003924^mo	Gap junction`Phagosome	.
TR8001|c0_g1	-6.94	3.12E-20	TR8001|c0_g1_i1	AT5F1_DR	51.31	6.00E-51	ATPsynB A	ATP syntha	Drosophila	TR8001|c0_g1_i1|m.20353	AT5F1_DR	50.75	1.00E-66	ATPsynB A	ATP syntha	Drosophila	PF05405.9	GO:0015078^mo	Oxidative phosphorylation	.
TR4650|c0_g1	-6.90	4.31E-16	TR4650|c0_g1_i1	FABPM_SC	47.37	2.00E-27	0	Fatty acid-l	Schistocer	TR4650|c0_g1_i1|m.4647	FABPM_SC	47.37	4.00E-36	0	Fatty acid-l	Schistocer	PF00061.1	.	PPAR signaling pathway	.
TR4113|c0_g2	-6.84	4.16E-18	TR4113|c0_g2_i1	MPPB_BOV	69.87	0	PMPCB	Mitochond	Bos taurus	TR4113|c0_g2_i1|m.3981	MPPB_HUI	69.49	0	PMPCB MF	Mitochond	Homo sapi	PF00675.1	.	.	.
TR5993|c0_g1	-6.83	1.59E-34	TR5993|c0_g1_i1	RS31_XENI	88.79	9.00E-145	rps3-a	40S riboso	Xenopus la	TR5993|c0_g1_i1|m.8232	RS3_ICTPU	86.97	8.00E-150	rps3	40S riboso	Ictalurus p	PF00189.1	GO:0003723^mo	Ribosome`Ribosome	.
TR5941|c1_g1	-6.82	1.14E-20	TR5941|c1_g1_i1	.			.	.	.	TR5941|c1_g1_i1|m.7549	.			.	.	.	PF15430.1	.	.	.
TR5572|c0_g2	-6.80	2.96E-18	TR5572|c0_g2_i1	RL23A_RA	65.13	1.00E-60	Rpl23a	60S riboso	Rattus nor	TR5572|c0_g2_i1|m.6386	RL23A_RA	71.31	7.00E-53	Rpl23a	60S riboso	Rattus nor	PF00276.1	GO:0003735^mo	Ribosome	.
TR6121|c8_g1	-6.75	4.24E-49	TR6121|c8_g1_i1	MLC1_DRC	63.51	2.00E-48	Mlc1	Myosin ligh	Drosophila	TR6121|c8_g1_i1|m.10696	MLC1_DRC	64.19	1.00E-61	Mlc1 MLC-	Myosin ligh	Drosophila	PF13202.1	GO:0005509^mo	.	.
TR866|c0_g2	-6.69	2.33E-12	TR866|c0_g2_i1	CP6K1_BL	42.42	2.00E-31	CYP6K1	Cytochrom	Blattella ge	TR866|c0_g2_i1|m.747	CP6K1_BL	42.42	4.00E-32	CYP6K1	Cytochrom	Blattella ge	PF00067.1	GO:0005506^mo	.	.
TR2145|c1_g1	-6.65	7.99E-10	TR2145|c1_g1_i1	TRAM1_RA	47.02	5.00E-44	Tram1	Translocati	Rattus nor	TR2145|c1_g1_i1|m.1886	TR1L1_XEN	40	1.00E-44	tram1l1	Translocati	Xenopus la	PF03798.1	GO:0016021^cell	Protein processing in endoplasmic reticulum	.
TR6322|c0_g2	-6.64	1.86E-10	TR6322|c0_g2_i1	MYSA_DRC	77.86	9.00E-71	Mhc CG179	Myosin hea	Drosophila	TR6322|c0_g2_i1|m.17088	MYSA_DRC	78.1	3.00E-74	Mhc CG179	Myosin hea	Drosophila	PF00063.1	GO:0003774^mo	.	.
TR5917|c0_g2	-6.64	9.95E-19	TR5917|c0_g2_i1	RL22_PIG	74.26	3.00E-30	RPL22	60S riboso	Sus scrofa	TR5917|c0_g2_i1|m.7472	RL22_DROI	69.35	6.00E-48	RpL22 CG7	60S riboso	Drosophila	PF01776.1	GO:0003735^mo	Ribosome	.
TR6220|c9_g1	-6.63	1.24E-29	TR6220|c9_g1_i1	RL10_BOM	88.58	3.00E-137	RpL10	60S riboso	Bombyx m	TR6220|c9_g1_i1|m.13843	RL10_BOM	88.58	3.00E-145	RpL10	60S riboso	Bombyx m	PF00252.1	GO:0003735^mo	Ribosome	.
TR6180|c2_g1	-6.63	1.64E-14	TR6180|c2_g1_i1	ISCU_MOU	82.64	4.00E-80	Iscu Nifun	Iron-sulfur	Mus musc	TR6180|c2_g1_i1|m.12631	ISCU_MOU	82.64	7.00E-84	Iscu Nifun	Iron-sulfur	Mus musc	PF01592.1	GO:0005506^mo	.	.
TR6318|c2_g1	-6.62	8.46E-56	TR6318|c2_g1_i3	ATPB_DRO	94.32	0	ATPsynbet	ATP syntha	Drosophila	TR6318|c2_g1_i3|m.16985	ATPB_DRO	93.59	0	ATPsynbet	ATP syntha	Drosophila	PF00006.2	GO:0015992^biol	Oxidative phosphorylation`Oxidative phosphorylati	.
TR6112|c9_g1	-6.59	1.70E-16	TR6112|c9_g1_i1	CUD1_SCH	51.4	1.00E-28	0	Endocuticl	Schistocer	TR6112|c9_g1_i1|m.10512	CUD1_SCH	51.4	2.00E-28	0	Endocuticl	Schistocer	PF00379.1	GO:0042302^mo	.	.
TR6164|c13_g1	-6.59	1.20E-33	TR6164|c13_g1_i1	HSP7D_MA	93.35	0	0	Heat shock	Manduca s	TR6164|c13_g1_i1|m.12232	HSP7D_MA	93.35	0	0	Heat shock	Manduca s	PF00012.1	GO:0000902^biol	Endocytosis`Endocytosis`Longevity regulating path	.
TR5846|c1_g1	-6.58	1.05E-14	TR5846|c1_g1_i1	BT3L4_XEN	73.47	6.00E-54	btf3l4 TNe	Transcripti	Xenopus tr	TR5846|c1_g1_i1|m.7237	BTF3_CAEI	71.03	5.00E-67	icd-1 C56C	Transcripti	Caenorhab	PF01849.1	.	Apoptosis - fly	.
TR1313|c0_g2	-6.58	2.14E-16	TR1313|c0_g2_i1	RL21_HUM	61.88	6.00E-69	RPL21	60S riboso	Homo sapi	TR1313|c0_g2_i1|m.1111	RL21_HUM	61.88	2.00E-67	RPL21	60S riboso	Homo sapi	PF01157.1	GO:0003735^mo	Ribosome	.
TR5832|c1_g1	-6.57	6.15E-19	TR5832|c1_g1_i1	RS10_RAT	70.27	2.00E-67	Rps10	40S riboso	Rattus nor	TR5832|c1_g1_i1|m.7167	RS10B_DR	73.46	7.00E-74	RpS10b Rp	40S riboso	Drosophila	PF03501.1	.	Ribosome	.
TR6164|c22_g1	-6.57	4.33E-17	TR6164|c22_g1_i1	HSP7C_CH	88.34	1.00E-97	HSPA8 HSC	Heat shock	Gallus gallu	TR6164|c22_g1_i1|m.12245	HSP7C_CH	87.8	2.00E-103	HSPA8 HSC	Heat shock	Gallus gallu	PF00012.1	.	Endocytosis`Longevity regulating pathway - multipl	.
TR6344|c9_g1	-6.56	5.46E-19	TR6344|c9_g1_i1	RS14_DRO	95	1.00E-68	.	.	.	TR6344|c9_g1_i1|m.17943	RS14_DRO	95	2.00E-93	.	.	.	PF00411.1	GO:0003735^mo	Ribosome`Ribosome	.
TR1935|c0_g2	-6.55	9.79E-10	TR1935|c0_g2_i1	PROF_APIN	92.8	2.00E-75	0	Profilin	Apis mellif	TR1935|c0_g2_i1|m.1643	PROF_APIN	92.8	8.00E-81	0	Profilin	Apis mellif	PF00235.1	GO:0003779^mo	MAPK signaling pathway - fly`Rap1 signaling pathw	.
TR5811|c0_g1	-6.51	3.61E-17	TR5811|c0_g1_i1	.			.	.	.	TR5811|c0_g1_i1|m.7097	.			.	.	.	.	.	.	.
TR6251|c9_g1	-6.51	8.98E-39	TR6251|c9_g1_i2	GBLP_DRO	86.03	0	Rack1 CG7	Guanine nu	Drosophila	TR6251|c9_g1_i1|m.14977	GBLP_DRO	85.76	0	Rack1 CG7	Guanine nu	Drosophila	PF00400.2	GO:0005515^mo	.	.
TR5936|c0_g1	-6.51	1.49E-09	TR5936|c0_g1_i1	.			.	.	.	TR5936|c0_g1_i1|m.7534	.			.	.	.	.	.	Steroid biosynthesis	.
TR6793|c0_g1	-6.50	1.29E-20	TR6793|c0_g1_i1	RS26_DRO	83.65	4.00E-58	RpS26 CG1	40S riboso	Drosophila	TR6793|c0_g1_i1|m.19741	RS26_DRO	85.29	2.00E-56	RpS26 CG1	40S riboso	Drosophila	PF01283.1	GO:0003735^mo	Ribosome	.
TR5767|c0_g2	-6.50	1.47E-14	TR5767|c0_g2_i1	UBCD1_DR	98.64	3.00E-106	eff UbcD1	Ubiquitin-c	Drosophila	TR5767|c0_g2_i1|m.6953	UBCD1_DR	98.64	2.00E-105	eff UbcD1	Ubiquitin-c	Drosophila	PF00179.2	GO:0016881^mo	MAPK signaling pathway - fly`Protein processing in	.
TR6298|c14_g1	-6.48	5.17E-13	TR6298|c14_g1_i1	TBB1_MAN	98.2	4.00E-99	0	Tubulin be	Manduca s	TR6298|c14_g1_i1|m.16240	TBB1_MAN	98.2	8.00E-119	0	Tubulin be	Manduca s	PF00091.2	.	Gap junction`Phagosome	.
TR8403|c0_g1	-6.48	1.88E-13	TR8403|c0_g1_i1	ACBP_CHI	65.12	1.00E-34	DBI	Acyl-CoA-b	Gallus gallu	TR8403|c0_g1_i1|m.20619	ACBP_HYP	63.64	2.00E-34	0	Putative ac	Hypsibius	PF00887.1	GO:0000062^mo	PPAR signaling pathway	.
TR5877|c2_g1	-6.47	4.37E-09	TR5877|c2_g1_i1	RTN1A_XE	49.11	9.00E-55	rtn1-a	Reticulon-	Xenopus la	TR5877|c2_g1_i1|m.7338	RTN3B_XEI	50.3	6.00E-54	rtn3-b	Reticulon-	Xenopus la	PF02453.1	.	.	.
TR7810|c0_g1	-6.46	8.64E-17	TR7810|c0_g1_i1	RS12_PIG	77.87	7.00E-64	RPS12	40S riboso	Sus scrofa	TR7810|c0_g1_i1|m.20273	RS12_PIG	77.24	6.00E-63	RPS12	40S riboso	Sus scrofa	PF01248.2	.	Ribosome	.
TR1718|c0_g1	-6.44	6.18E-17	TR1718|c0_g1_i1	RS16_DRO	87.07	4.00E-91	RpS16 CG4	40S riboso	Drosophila	TR1718|c0_g1_i1|m.1477	RS16_DRO	87.07	1.00E-91	RpS16 CG4	40S riboso	Drosophila	PF00380.1	GO:0003735^mo	Ribosome	.
TR6089|c3_g1	-6.44	3.89E-12	TR6089|c3_g1_i1	VDAC_DRC	57.71	9.00E-109	porin POR-	Voltage-de	Drosophila	TR6089|c3_g1_i1|m.9947	VDAC_DRC	57.5	9.00E-118	porin POR-	Voltage-de	Drosophila	PF01459.1	GO:0055085^biol	Calcium signaling pathway	.
TR5925|c1_g1	-6.43	7.11E-12	TR5925|c1_g1_i1	CUD2_SCH	44.94	1.00E-16	0	Endocuticl	Schistocer	TR5925|c1_g1_i1|m.7494	CUD2_SCH	44.94	3.00E-16	0	Endocuticl	Schistocer	PF00379.1	GO:0042302^mo	.	.
TR4718|c0_g1	-6.42	4.26E-18	TR4718|c0_g1_i1	RL12_MOU	78.26	9.00E-90	Rpl12	60S riboso	Mus musc	TR4718|c0_g1_i1|m.4758	RL12_MOU	78.26	4.00E-92	Rpl12	60S riboso	Mus musc	PF00298.1	GO:0003735^mo	Ribosome	.
TR6252|c4_g1	-6.42	3.43E-13	TR6252|c4_g1_i1	ATPD_MOI	63.04	8.00E-11	Atp5d	ATP syntha	Mus musc	TR6252|c4_g1_i1|m.15009	ATPD_MOI	51.52	1.00E-26	Atp5d	ATP syntha	Mus musc	PF02823.1	GO:0046933^mo	Oxidative phosphorylation	.
TR1158|c0_g1	-6.41	2.43E-08	TR1158|c0_g1_i1	VATG_MAI	77.59	3.00E-29	0	V-type pro	Manduca s	TR1158|c0_g1_i1|m.963	VATG_MAI	77.59	8.00E-59	0	V-type pro	Manduca s	PF03179.1	.	mTOR signaling pathway`Oxidative phosphorylatior	.
TR6388|c2_g1	-6.41	5.99E-18	TR6388|c2_g1_i1	RS19A_DR	66.67	9.00E-65	RpS19a Rp	40S riboso	Drosophila	TR6388|c2_g1_i1|m.18785	RS19A_DR	60.76	2.00E-66	RpS19a Rp	40S riboso	Drosophila	PF01090.1	GO:0003735^mo	Ribosome	.
TR6347|c1_g1	-6.40	1.26E-08	TR6347|c1_g1_i1	GST1C_AN	62.64	1.00E-74	GstD1 GST	Glutathion	Anopheles	TR6347|c1_g1_i1|m.18077	GST1C_AN	62.29	2.00E-77	GstD1 GST	Glutathion	Anopheles	PF00043.2	GO:0005515^mo	Drug metabolism - cytochrome P450`Glutathione n	.
TR8895|c0_g1	-6.35	1.69E-11	TR8895|c0_g1_i1	SSRB_CAN	56.69	5.00E-58	.	.	.	TR8895|c0_g1_i1|m.20915	SSRB_BOVI	52.84	2.00E-61	SSR2	Translocon	Bos taurus	PF05753.9	GO:0005783^cell	Protein processing in endoplasmic reticulum	.
TR5752|c0_g2	-6.34	4.06E-16	TR5752|c0_g2_i1	EF1D_XEN	51.75	9.00E-62	eef1d	Elongation	Xenopus la	TR5752|c0_g2_i1|m.6899	EF1D_XEN	50.38	8.00E-78	eef1d	Elongation	Xenopus la	PF00736.1	GO:0003746^mo	.	.
TR123|c0_g1	-6.33	1.61E-08	TR123|c0_g1_i1	TOM20_RA	70.77	4.00E-50	Tomm20	Mitochond	Rattus nor	TR123|c0_g1_i1|m.113	TOM20_RA	70.23	3.00E-52	Tomm20	Mitochond	Rattus nor	PF02064.1	GO:0006605^biol	.	.
TR5566|c2_g1	-6.33	1.63E-09	TR5566|c2_g1_i1	KPYK_DRO	82.44	2.00E-112	PyK CG707	Pyruvate k	Drosophila	TR5566|c2_g1_i1|m.6365	KPYK_DRO	82.04	2.00E-116	PyK CG707	Pyruvate k	Drosophila	PF00224.1	GO:0000287^mo	Biosynthesis of amino acids`Carbon metabolism`Gl	.

TR6205|c10_g1	0.66	3.72E-03	TR6205|c10_g1_i1	.			.	.	.	TR6205|c10_g1_i1|m.13343	.			.	.	.	PF00100.1	.	.	.
TR6243|c9_g1	0.65	2.74E-02	TR6243|c9_g1_i1	DERP3_DE	35.07	5.00E-38	DERP3	Mite allerg	Dermatopl	TR6243|c9_g1_i1|m.14670	DERP3_DE	35.07	7.00E-39	DERP3	Mite allerg	Dermatopl	PF00089.2	GO:0004252^mo	.	.
TR264|c0_g1	0.65	1.79E-03	TR264|c0_g1_i1	HSP11_CAI	40.43	1.00E-10	hsp-16.1 h	Heat shock	Caenorhab	TR264|c0_g1_i1|m.230	HSP11_CAI	39.33	1.00E-11	hsp-16.1 h	Heat shock	Caenorhab	PF00011.1	.	Longevity regulating pathway - multiple species`Prc	.
TR6075|c11_g1	0.64	2.38E-05	TR6075|c11_g1_i1	TENS3_MC	53.69	5.00E-34	Tns3 Tens1	Tensin-3 (T	Mus muscu	TR6075|c11_g1_i1|m.9538	TENS3_MC	53.33	9.00E-37	Tns3 Tens1	Tensin-3 (T	Mus muscu	PF00017.1	GO:0005515^mo	.	.
TR3688|c0_g1	0.64	1.56E-02	TR3688|c0_g1_i1	.			.	.	.	TR3688|c0_g1_i1|m.3509	.			.	.	.	.	.	.	.
TR6131|c3_g2	0.64	1.31E-02	TR6131|c3_g2_i1	TITIN_DRO	26.3	1.00E-22	sls titin CG	Titin (D-Tit	Drosophila	TR6131|c3_g2_i1|m.11036	TITIN_HUN	25.17	2.00E-26	TTN	Titin (EC 2.	Homo sapi	PF00047.2	.	.	.
TR6344|c2_g1	0.64	2.79E-03	TR6344|c2_g1_i1	CP9C1_DR	29.03	4.00E-22	Cyp9c1 CG	Cytochrom	Drosophila	TR6344|c2_g1_i1|m.17929	C356_FUN	30.34	1.00E-30	cyp3a56	Cytochrom	Fundulus h	PF00067.1	GO:0005506^mo	.	.
TR6050|c12_g1	0.64	7.01E-04	TR6050|c12_g1_i1	.			.	.	.	TR6050|c12_g1_i1|m.8951	.			.	.	.	PF01607.1	GO:0008061^mo	.	.
TR6190|c0_g1	0.63	1.67E-02	TR6190|c0_g1_i1	CLCN2_CA	59.21	3.00E-20	CLCN2	Chloride ch	Cavia porce	TR6190|c0_g1_i1|m.12894	CLCN2_DR	50.86	1.00E-26	ClC-a CG31	Chloride ch	Drosophila	PF00571.2	GO:0030554^mo	.	.
TR6190|c0_g2	0.61	2.57E-02	TR6190|c0_g2_i1	CLCN2_CA	59.21	3.00E-20	CLCN2	Chloride ch	Cavia porce	TR6190|c0_g2_i1|m.12895	CLCN2_DR	50.86	1.00E-26	ClC-a CG31	Chloride ch	Drosophila	PF00571.2	GO:0030554^mo	.	.
TR6285|c3_g1	0.61	5.97E-03	TR6285|c3_g1_i1	.			.	.	.	TR6285|c3_g1_i1|m.15864	.			.	.	.	.	.	.	.
TR6315|c3_g1	0.61	4.06E-04	TR6315|c3_g1_i1	LIN10_CAE	58.79	2.00E-129	lin-10 C09H	Protein lin-	Caenorhab	TR6315|c3_g1_i1|m.16856	LIN10_CAE	53.51	2.00E-143	lin-10 C09H	Protein lin-	Caenorhab	PF00595.1	GO:0005515^mo	.	.
TR6344|c4_g2	0.61	1.55E-04	TR6344|c4_g2_i1	.			.	.	.	TR6344|c4_g2_i1|m.17934	.			.	.	.	.	.	.	.
TR6206|c27_g1	0.61	2.10E-03	TR6206|c27_g1_i1	TGFR1_BO	41.56	7.00E-15	TGFBR1	TGF-beta r	Bos taurus	TR6206|c27_g1_i1|m.13407	TGFR1_RA	41.56	6.00E-17	Tgfbr1	TGF-beta r	Rattus nor	.	.	Adherens junction`Endocytosis`FoxO signaling path	.
TR6315|c3_g2	0.60	3.41E-03	TR6315|c3_g2_i1	LIN10_CAE	58.03	2.00E-130	lin-10 C09H	Protein lin-	Caenorhab	TR6315|c3_g2_i1|m.16857	LIN10_CAE	58.03	4.00E-143	lin-10 C09H	Protein lin-	Caenorhab	PF00595.1	GO:0005515^mo	.	.
TR6277|c4_g1	0.60	1.18E-04	TR6277|c4_g1_i1	.			.	.	.	TR6277|c4_g1_i1|m.15730	.			.	.	.	PF02995.1	.	.	.
TR4323|c1_g1	0.60	4.17E-02	TR4323|c1_g1_i1	CBPB_AST	39.87	2.00E-64	0	Carboxype	Astacus as	TR4323|c1_g1_i1|m.4211	CBPB_AST	39.87	6.00E-70	0	Carboxype	Astacus as	PF00246.1	GO:0004180^mo	.	.
TR6147|c7_g1	0.60	1.15E-03	TR6147|c7_g1_i1	NRF6_CAE	22.31	4.00E-13	nrf-6 C08B	Nose resist	Caenorhab	TR6147|c7_g1_i1|m.11769	NRF6_CAE	21.26	6.00E-16	nrf-6 C08B	Nose resist	Caenorhab	.	.	.	.
TR6416|c17_g1	0.60	4.62E-05	TR6416|c17_g1_i1	F214A_XEI	35	7.00E-32	fam214a T	Protein FA	Xenopus tr	TR6416|c17_g1_i1|m.19077	F214A_DA	35	1.00E-36	fam214a si	Protein FA	Danio reric	PF13889.1	.	.	.
TR6180|c40_g1	0.60	4.63E-06	TR6180|c40_g1_i1	UBQL1_RA	81.82	4.00E-12	Ubqln1 Da	Ubiquilin-1	Rattus nor	TR6180|c40_g1_i1|m.12663	UBQL1_RA	74	1.00E-13	Ubqln1 Da	Ubiquilin-1	Rattus nor	PF00627.2	GO:0005515^mo	Protein processing in endoplasmic reticulum	.
TR1217|c0_g1	0.60	1.74E-05	TR1217|c0_g1_i1	CATS_CAN	33.66	5.00E-31	.	.	.	TR1217|c0_g1_i1|m.1028	CATH_MO	33.18	9.00E-38	Ctsh	Pro-cathep	Mus muscu	PF00112.1	GO:0008234^mo	Apoptosis`Autophagy - animal`Lysosome`Phagosor	.
TR6131|c4_g1	0.60	7.98E-05	TR6131|c4_g1_i1	.			.	.	.	TR6131|c4_g1_i1|m.11037	.			.	.	.	.	.	.	.
TR6155|c1_g2	0.59	3.10E-03	TR6155|c1_g2_i1	LIPE_MOU	27.3	2.00E-19	Lipg	Endothelia	Mus muscu	TR6155|c1_g2_i1|m.12030	LIPL_CAVP	28.74	6.00E-19	LPL	Lipoprotei	Cavia porce	PF00151.1	.	Glycerolipid metabolism`Glycerolipid metabolism	.
TR6145|c7_g2	0.59	8.56E-05	TR6145|c7_g2_i1	MFD6A_D	24.57	5.00E-16	mfsd6a mf	Major facil	Danio reric	TR6145|c7_g2_i1|m.11667	MFSD6_M	22.9	3.00E-28	Mfsd6 Mm	Major facil	Mus muscu	PF12832.2	.	.	.
TR2592|c0_g2	0.59	2.95E-02	TR2592|c0_g2_i1	ENTK_HUN	28.97	3.00E-18	TMPRSS15	Enteropep	Homo sapi	TR2592|c0_g2_i1|m.2292	ENTK_HUN	29.37	1.00E-18	TMPRSS15	Enteropep	Homo sapi	PF00089.2	GO:0004252^mo	.	.
TR6222|c5_g1	0.59	3.87E-06	TR6222|c5_g1_i1	SCD5_BOV	54.36	3.00E-103	SCD5	Stearoyl-C	Bos taurus	TR6222|c5_g1_i1|m.13929	SCD5_BOV	54.36	2.00E-109	SCD5	Stearoyl-C	Bos taurus	PF00487.1	GO:0006629^biol	Biosynthesis of unsaturated fatty acids`Fatty acid n	.
TR6301|c6_g1	0.58	1.68E-04	TR6301|c6_g1_i1	.			.	.	.	TR6301|c6_g1_i1|m.16390	.			.	.	.	PF05497.7	GO:0003796^mo	.	.
TR6235|c7_g2	0.58	8.73E-05	TR6235|c7_g2_i1	HDAC4_CH	47.28	4.00E-126	HDAC4	Histone de	Gallus gallu	TR6235|c7_g2_i1|m.14308	HDAC4_CH	47.28	9.00E-134	HDAC4	Histone de	Gallus gallu	PF00850.1	.	.	.
TR6385|c8_g1	0.58	1.89E-04	TR6385|c8_g1_i1	LIPJ_HUM	29.15	2.00E-12	LIPJ LIPL1	Lipase mer	Homo sapi	TR6385|c8_g1_i1|m.18702	LIPJ_HUM	29	2.00E-12	LIPJ LIPL1	Lipase mer	Homo sapi	PF04083.1	GO:0006629^biol	Lysosome`Steroid biosynthesis	.
TR6301|c28_g1	0.58	2.63E-04	TR6301|c28_g1_i1	SOX14_DA	87.18	7.00E-41	sox14 zgc:	Transcripti	Danio reric	TR6301|c28_g1_i1|m.16424	SOX14_DA	83.95	5.00E-47	sox14 zgc:	Transcripti	Danio reric	PF00505.1	.	.	.
TR6139|c13_g1	0.57	3.65E-05	TR6139|c13_g1_i1	LIMD_DICD	35.63	4.00E-07	limD limD1	LIM domai	Dictyosteli	TR6139|c13_g1_i1|m.11380	LIMD_DICD	38.36	4.00E-08	limD limD1	LIM domai	Dictyosteli	PF00412.1	GO:0008270^mo	.	.
TR6344|c4_g1	0.57	8.33E-05	TR6344|c4_g1_i1	.			.	.	.	TR6344|c4_g1_i1|m.17932	.			.	.	.	.	.	.	.
TR6385|c4_g1	0.57	1.35E-05	TR6385|c4_g1_i1	NCAH_DRO	85.48	4.00E-107	Nca CG764	Neurocalci	Drosophila	TR6385|c4_g1_i1|m.18692	NCAH_DRO	85.48	3.00E-122	Nca CG764	Neurocalci	Drosophila	PF00036.2	GO:0005506^mo	.	.
TR6416|c13_g1	0.57	6.03E-04	TR6416|c13_g1_i1	SWS_DROI	58.11	2.00E-156	sws CG221	Neuropath	Drosophila	TR6416|c13_g1_i1|m.19073	PLPL6_HUI	52.59	0	PNPLA6 NT	Neuropath	Homo sapi	PF01734.1	GO:0006629^biol	Glycerophospholipid metabolism	.
TR5990|c1_g2	0.57	4.56E-04	TR5990|c1_g2_i1	.			.	.	.	TR5990|c1_g2_i1|m.8144	RN19A_MC	31.62	1.00E-07	Rnf19a Ge	E3 ubiquiti	Mus muscu	.	.	.	.
TR6324|c8_g1	0.57	5.86E-06	TR6324|c8_g1_i1	RPTOR_MC	37.74	5.00E-43	Rptor Rapt	Regulatory	Mus muscu	TR6324|c8_g1_i1|m.17175	RPTOR_MC	36.43	4.00E-50	Rptor Rapt	Regulatory	Mus muscu	PF00400.2	GO:0005515^mo	Autophagy - animal`Longevity regulating pathway`L	.
TR9193|c0_g1	0.56	6.65E-03	TR9193|c0_g1_i1	.			.	.	.	TR9193|c0_g1_i1|m.21066	.			.	.	.	.	.	.	.
TR6138|c17_g1	0.56	3.33E-05	TR6138|c17_g1_i1	MLR_BOM	51.97	1.00E-46	0	Myosin reg	Bombyx m	TR6138|c17_g1_i1|m.11331	MLR_BOM	51.97	9.00E-52	0	Myosin reg	Bombyx m	PF13202.1	GO:0005509^mo	Focal adhesion`Regulation of actin cytoskeleton`Tig	.
TR6343|c20_g1	0.56	7.15E-04	TR6343|c20_g1_i1	KCC1A_HU	71.79	4.00E-10	CAMK1	Calcium/ca	Homo sapi	TR6343|c20_g1_i1|m.17920	KCC1A_HU	71.79	5.00E-12	CAMK1	Calcium/ca	Homo sapi	.	.	.	.
TR5487|c1_g1	0.56	3.67E-03	TR5487|c1_g1_i1	ACYP2_HU	40	3.00E-19	ACYP2 ACY	Acylphospl	Homo sapi	TR5487|c1_g1_i1|m.6180	ACYP2_HU	40	5.00E-20	ACYP2 ACY	Acylphospl	Homo sapi	PF00708.1	.	Pyruvate metabolism	.
TR6248|c11_g1	0.56	1.61E-04	TR6248|c11_g1_i1	RDHE2_HU	44.73	1.00E-77	SDR16C5 R	Epidermal	Homo sapi	TR6248|c11_g1_i1|m.14882	RDHE2_HU	44.51	7.00E-85	SDR16C5 R	Epidermal	Homo sapi	PF00106.2	GO:0016491^mo	Retinol metabolism	.
TR6192|c4_g1	0.56	3.62E-04	TR6192|c4_g1_i2	ASTE1_MC	24.56	1.00E-14	Aste1	Protein ast	Mus muscu	TR6192|c4_g1_i2|m.12970	ASTE1_POI	26.74	1.00E-16	ASTE1	Protein ast	Pongo abe	PF12813.2	.	.	.
TR5418|c0_g2	0.55	6.35E-05	TR5418|c0_g2_i1	TM163_HU	33.92	1.00E-22	TMEM163	Transmem	Homo sapi	TR5418|c0_g2_i1|m.6009	TM163_BC	31.58	2.00E-26	TMEM163	Transmem	Bos taurus	.	.	.	.
TR5418|c0_g1	0.55	8.29E-05	TR5418|c0_g1_i1	TM163_HU	33.92	1.00E-22	TMEM163	Transmem	Homo sapi	TR5418|c0_g1_i1|m.6008	TM163_BC	31.58	2.00E-26	TMEM163	Transmem	Bos taurus	.	.	.	.
TR6343|c9_g2	0.55	8.75E-04	TR6343|c9_g2_i1	CMK1_CAE	68.61	8.00E-152	cmk-1 CBG	Calcium/ca	Caenorhab	TR6343|c9_g2_i1|m.17906	CMK1_CAE	68.49	5.00E-162	cmk-1 CBG	Calcium/ca	Caenorhab	PF00069.2	GO:0004672^mo	.	.
TR92|c0_g1	0.55	7.93E-03	TR92|c0_g1_i1	.			.	.	.	TR92|c0_g1_i1|m.81	.			.	.	.	.	.	.	.
TR6298|c3_g1	0.55	3.71E-02	TR6298|c3_g1_i1	ELF1_DROI	49.45	7.00E-19	grh elf1 CG	Protein gra	Drosophila	TR6298|c3_g1_i1|m.16224	ELF1_DROI	48.51	2.00E-24	grh elf1 CG	Protein gra	Drosophila	.	.	.	.
TR6071|c4_g2	0.55	6.02E-05	TR6071|c4_g2_i1	CAH14_MC	31.29	9.00E-35	Ca14 Car14	Carbonic a	Mus muscu	TR6071|c4_g2_i1|m.9385	CAH14_MC	31.29	3.00E-34	Ca14 Car14	Carbonic a	Mus muscu	PF00194.1	.	Nitrogen metabolism	.
TR6286|c9_g2	0.55	6.64E-03	TR6286|c9_g2_i1	GSC1L_MC	38.14	5.00E-15	Gltscr1l Kia	GLTSCR1-li	Mus muscu	TR6286|c9_g2_i1|m.15909	GSC1L_MC	38.14	3.00E-16	Gltscr1l Kia	GLTSCR1-li	Mus muscu	PF15249.1	.	.	.
TR6286|c9_g1	0.55	1.82E-04	TR6286|c9_g1_i1	GSC1L_MC	38.14	7.00E-15	Gltscr1l Kia	GLTSCR1-li	Mus muscu	TR6286|c9_g1_i1|m.15906	GSC1L_MC	36.15	3.00E-17	Gltscr1l Kia	GLTSCR1-li	Mus muscu	PF15249.1	.	.	.
TR6145|c7_g3	0.54	2.08E-04	TR6145|c7_g3_i1	MFD6A_D	24.57	6.00E-16	mfsd6a mf	Major facil	Danio reric	TR6145|c7_g3_i1|m.11668	MFSD6_M	22.9	3.00E-28	Mfsd6 Mm	Major facil	Mus muscu	PF12832.2	.	.	.
TR6080|c3_g1	0.54	1.82E-02	TR6080|c3_g1_i1	CMTA1_HU	45.61	1.00E-08	CAMTA1 K	Calmodulir	Homo sapi	TR6080|c3_g1_i1|m.9663	CMTA1_HU	45.61	5.00E-10	CAMTA1 K	Calmodulir	Homo sapi	.	.	.	.
TR6324|c28_g1	0.54	8.45E-04	TR6324|c28_g1_i1	DORS_DRC	53.82	4.00E-108	dl CG6667	Embryonic	Drosophila	TR6324|c28_g1_i1|m.17205	DORS_DRC	54.66	3.00E-115	dl CG6667	Embryonic	Drosophila	PF00554.1	GO:0003700^mo	Ras signaling pathway	.
TR5904|c0_g2	0.53	4.17E-02	TR5904|c0_g2_i1	CALCR_RAI	33.59	1.00E-09	CALCR	Calcitonin	Oryctolagu	TR5904|c0_g2_i1|m.7421	CALCR_RAI	32.59	2.00E-09	CALCR	Calcitonin	Oryctolagu	PF00002.1	GO:0004930^mo	Neuroactive ligand-receptor interaction	.
TR6150|c5_g1	0.53	1.27E-04	TR6150|c5_g1_i1	ZASP_DRO	32.89	5.00E-22	Zasp52 Zas	PDZ and LI	Drosophila	TR6150|c5_g1_i1|m.11891	ZASP_DRO	50	1.00E-15	Zasp52 Zas	PDZ and LI	Drosophila	PF00412.1	GO:0008270^mo	.	.
TR6242|c2_g1	0.53	7.72E-03	TR6242|c2_g1_i1	SMC6_MO	41.58	3.00E-16	Smc6 Kiaa4	Structural	Mus muscu	TR6242|c2_g1_i1|m.14590	SMC6_MO	41.58	1.00E-18	Smc6 Kiaa4	Structural	Mus muscu	PF01442.1	GO:0008289^mo	.	.
TR6292|c6_g2	0.53	3.04E-03	TR6292|c6_g2_i1	.			.	.	.	TR6292|c6_g2_i2|m.16017	DFP_MANS	29.1	1.00E-05	0	Putative de	Manduca s	PF02014.1	.	.	.
TR6238|c15_g1	0.53	2.49E-03	TR6238|c15_g1_i1	S16C6_BO	38.6	2.00E-53	SDR16C6	Short-chai	Bos taurus	TR6238|c15_g1_i1|m.14407	RDH10_XE	37.06	2.00E-59	rdh10	Retinol del	Xenopus tr	PF00106.2	GO:0016491^mo	Retinol metabolism	.
TR3322|c1_g1	0.53	6.02E-05	TR3322|c1_g1_i1	AQP9_MO	31.73	3.00E-29	Aqp9	Aquaporin	Mus muscu	TR3322|c1_g1_i1|m.3129	AQP9_RAT	31.61	4.00E-36	Aqp9	Aquaporin	Rattus nor	PF00230.1	GO:0005215^mo	.	.
TR5969|c7_g1	0.53	1.56E-04	TR5969|c7_g1_i1	HSPB1_CH	47.67	2.00E-16	HSPB1	Heat shock	Gallus gallu	TR5969|c7_g1_i1|m.7925	HSPB1_CH	47.67	1.00E-18	HSPB1	Heat shock	Gallus gallu	PF00011.1	.	.	.
TR6222|c11_g2	0.53	7.32E-04	TR6222|c11_g2_i1	FA63A_DA	45.81	3.00E-97	.	.	.	TR6222|c11_g2_i1|m.13949	FA63A_DA	48	3.00E-99	.	.	.	PF04424.8	.	.	.
TR6378|c4_g1	0.52	1.97E-02	TR6378|c4_g1_i1	LIPN_HUM	23.91	9.00E-15	LIPN LIPL4	Lipase mer	Homo sapi	TR6378|c4_g1_i1|m.18523	LIPN_HUM	23.97	2.00E-14	LIPN LIPL4	Lipase mer	Homo sapi	PF04083.1	GO:0006629^biol	Lysosome`Steroid biosynthesis	.
TR4871|c0_g1	0.52	1.82E-03	TR4871|c0_g1_i1	PAHX_HUN	25.42	3.00E-17	PHYH PAH	Phytanoyl-	Homo sapi	TR4871|c0_g1_i1|m.5051	PAHX_HUN	25.45	1.00E-19	PHYH PAH	Phytanoyl-	Homo sapi	PF05721.8	.	Peroxisome	.
TR5969|c6_g1	0.52	4.04E-02	TR5969|c6_g1_i1	NFIL_PIG^	78.95	6.00E-84	NFI	Nuclear fa	Sus scrofa	TR5969|c6_g1_i1|m.7923	NFIC_MOU	77.59	2.00E-91	Nfic	Nuclear fa	Mus muscu	PF03165.1	GO:0006355^biol	.	.
TR5954|c2_g2	0.52	8.57E-05	TR5954|c2_g2_i1	CBPM_MO	48.91	2.00E-107	Cpm	Carboxype	Mus muscu	TR5954|c2_g2_i1|m.7718	CBPM_MO	48.92	2.00E-118	Cpm	Carboxype	Mus muscu	PF00246.1	GO:0004181^mo	.	.
TR6244|c2_g2	0.52	4.64E-04	TR6244|c2_g2_i1	ABCGK_DI	30.08	3.00E-51	abcG20 DD	ABC transp	Dictyosteli	TR6244|c2_g2_i1|m.14711	ABCGK_DI	29.72	2.00E-52	abcG20 DD	ABC transp	Dictyosteli	PF01061.1	GO:0016020^cell	.	.
TR6181|c0_g1	0.52	1.61E-04	TR6181|c0_g1_i1	.			.	.	.	TR6181|c0_g1_i1|m.12664	COLL1_DR	42.62	1.00E-10	CG42342	Collagen al	Drosophila	PF01391.1	.	.	.
TR6085|c18_g1	0.52	5.17E-05	TR6085|c18_g1_i1	.			.	.	.	TR6085|c18_g1_i1|m.9822	.			.	.	.	PF00089.2	GO:0004252^mo	.	.
TR6297|c23_g1	0.51	4.51E-04	TR6297|c23_g1_i1	MTG1_ICT	39.34	3.00E-57	mtg1	Mitochond	Ictalurus p	TR6297|c23_g1_i1|m.16199	MTG1_MO	41.81	6.00E-62	Mtg1 Gm1	Mitochond	Mus muscu	PF01926.1	GO:0005525^mo	.	.
TR6228|c7_g1	0.51	2.17E-03	TR6228|c7_g1_i1	PERC_ANC	36.75	4.00E-97	pxt AGAP0	Chorion pe	Anopheles	TR6228|c7_g1_i1|m.14082	PERC_ANC	37.07	1.00E-102	pxt AGAP0	Chorion pe	Anopheles	PF03098.1	.	.	.
TR1101|c0_g1	0.51	1.14E-02	TR1101|c0_g1_i1	ALKMO_RA	45.48	1.00E-123	Agmo Tme	Alkylglycer	Rattus nor	TR1101|c0_g1_i1|m.918	ALKMO_RA	45	1.00E-122	Agmo Tme	Alkylglycer	Rattus nor	PF04116.8	GO:0005506^mo	.	.
TR6068|c0_g2	0.51	1.83E-04	TR6068|c0_g2_i1	LIPH_DANI	24.76	7.00E-14	liph zgc:91	Lipase mer	Danio reric	TR6068|c0_g2_i1|m.9317	LIPR1_MO	34.75	1.00E-14	Pnliprp1	Inactive pa	Mus muscu	PF00151.1	.	Glycerolipid metabolism	.
TR5954|c2_g1	0.51	1.07E-04	TR5954|c2_g1_i1	CBPM_MO	48.91	2.00E-107	Cpm	Carboxype	Mus muscu	TR5954|c2_g1_i1|m.7717	CBPM_MO	48.92	2.00E-118	Cpm	Carboxype	Mus muscu	PF00246.1	GO:0004181^mo	.	.
TR6163|c12_g1	0.50	1.02E-02	TR6163|c12_g1_i1	MLXPL_RA	41.79	3.00E-42	Mlxipl Wbs	Carbohydr	Rattus nor	TR6163|c12_g1_i1|m.12192	MLXPL_MC	36.68	5.00E-43	Mlxipl Mio	Carbohydr	Mus muscu	PF00010.2	GO:0046983^mo	.	.
TR6139|c4_g3	0.50	9.06E-03	TR6139|c4_g3_i1	.			.	.	.	TR6139|c4_g3_i1|m.11358	.			.	.	.	PF01607.1	GO:0008061^mo	.	.
TR5455|c1_g1	0.50	6.34E-04	TR5455|c1_g1_i1	CP3AC_CA	26.89	3.00E-34	.	.	.	TR5455|c1_g1_i1|m.6086	CP3AC_CA	27.27	1.00E-33	.	.	.	PF00067.1	GO:0005506^mo	.	.
TR6137|c15_g1	0.50	1.22E-04	TR6137|c15_g1_i1	PERC_ANC	34.68	3.00E-92	pxt AGAP0	Chorion pe	Anopheles	TR6137|c15_g1_i1|m.11271	PERC_ANC	35.02	3.00E-96	pxt AGAP0	Chorion pe	Anopheles	PF03098.1	.	.	.
TR6286|c8_g2	0.50	1.65E-02	TR6286|c8_g2_i1	SCRT1_HU	62.16	2.00E-60	SCRT1	Transcripti	Danio reric	TR6286|c8_g2_i1|m.15904	SCRT1_HU	61.49	2.00E-61	Scrt1	Transcripti	Mus muscu	PF00096.2	GO:0046872^mo	.	.
TR6191|c7_g1	0.50	3.72E-03	TR6191|c7_g1_i1	MACF1_RA	31.98	1.00E-136	Macf1 Acf7	Microtubu	Rattus nor	TR6191|c7_g1_i1|m.12926	MACF1_RA	35.42	3.00E-152	Macf1 Acf7	Microtubu	Rattus nor	PF00307.2	GO:0005515^mo	.	.